









A New Functional Renormalization Group Study of Universality Classes with O(N) Symmetry

Tesis de Maestría **Piero Beretta**

Programa de Posgrado de Pedeciba Física Facultad de Ciencias Universidad de la República Montevideo-Uruguay











A New Functional Renormalization Group Study of Universality Classes with O(N) Symmetry

Master's Thesis **Piero Beretta**

Physics Postgraduate Program
Faculty of Sciences
University of the Republic

Supervisor:

Dr. Alessandro Codello

Montevideo-Uruguay

MEMBERS OF THE DEFENSE TRIBUNAL MIEMBROS DEL TRIBUNAL DE DEFENSA

Dr. Gonzalo De Polsi Universidad de la República

Dr. Guzmán Hernández-Chifflet *Universidad de la República*

> Dr. Kevin Falls Universidad de la República

> Dra. Julia Alonso Universidad de la República

> Dr. Alessandro Codello *Universidad de la República*

Substitute / Suplente:

Dra. Marcela Peláez Universidad de la República

Date / Fecha: 28th of March, 2025

Agradecimientos

En primer lugar quiero agradecer a mi tutor Alessandro Codello, no solo por haber aceptado trabajar conmigo sino también por todos los conocimientos transmitidos y guiarme en mis primeros pasos en la investigación.

A mis compañeros de maestría, Marina, Carlos, Nico Horvath, Adrian, gracias por las tardes de estudios de física.

A los miembros del tribunal por tomarse su tiempo y haber aceptado leer esta tesis.

A mis padres por el apoyo infinito y a mis hermanos por estar siempre presentes. A los amigos de la vida, Vero, Pablo, Rodri, Letu y Holy por bancar siempre.

A PEDECIBA, en especial a Jimena por atender con rapidez los asuntos administrativos.

A la Facultad de Ingeniería y al IFFI por brindarme un cálido lugar de trabajo.

A la CSIC por el apoyo financiero.

Abstract

The functional renormalization group (FRG) is a powerful tool that has facilitated the investigation of various strongly interacting theories, encompassing systems characterized by both bosonic and fermionic variables. Specifically, this project focuses on the analysis of theories with O(N) symmetry with bosonic scalar fields. These theories are of particular interest due to their broad applicability in real physical systems. For example, \mathbb{Z}_2 symmetry (the O(1) model) describes the well-known Ising universality class, which in turn models the liquid-gas transition. On the other hand, the O(2) model belongs to the universality class of the XY model, used to describe the transition from fluid to superfluid in 4He , while the O(3) model, known as the Heisenberg model, describes the ferromagnetic transition in isotropic materials. Finally the O(0) model is related to the self-avoiding walk (SAW).

To characterize these theories, various methods have been implemented within the framework of the renormalization group. Perturbation theory has been applied since the early days of the subject, specifically in the form of the ε -expansion, which has reached high loop order in recent years. Alternatively, a non-perturbative approach can be chosen, which is known as the non-perturbative renormalization group (NPRG). Within the NPRG, there are several approximation schemes, with the derivative expansion being particularly noteworthy. The ultimate goal of these efforts is to calculate the critical exponents, which define the given universality class. The standard non-perturbative method involves solving an equation that depends on a regulator or cut-off, which represents one of the main challenges of this approach. Although the regulators are designed so that the theory does not depend on them at the scales of interest, the results for the critical exponents can vary depending on the regulator used once approximations are made.

In this project, we propose an approach that eliminates the need for an explicit mass cut-off significantly simplifying the calculation of critical exponents while mitigating the regulator dependence of the results. In particular, we show that it is possible to use dimensional regularization (DR) beyond the ε -expansion in the context of RG calculations of critical properties.

Based on this we propose a new functional RG scheme called *Functional Dimensional Regularization* (FDR) and apply it to the O(N) model in three dimension, finding excellent agreement with state-of-the-art computations.

Keywords: Non-perturbative renormalization group, universality, critical phenomena.

Resumen

El grupo de renormalización funcional (FRG, por sus siglas en inglés) es una herramienta poderosa que ha facilitado la investigación de diversas teorías fuertemente correlacionadas, abarcando sistemas caracterizados tanto por variables bosónicas como fermiónicas. En particular, este proyecto se centra en el análisis de teorías con simetría O(N) conformadas por campos escalares bosónicos. Estas teorías son de interés particular debido a su amplia aplicabilidad en sistemas físicos reales. Por ejemplo, la simetría \mathbb{Z}_2 (el modelo O(1)) describe la bien conocida clase de universalidad de Ising, que a su vez modela la transición líquido-gas. Por otro lado, el modelo O(2) pertenece a la clase de universalidad del modelo XY, empleado para describir la transición de fluido a superfluido en 4 He, mientras que el modelo O(3), conocido como el modelo de Heisenberg, describe la transición ferromagnética en materiales isotrópicos. Finalmente, el modelo O(0) está relacionado con la caminata autoevitante (SAW, por sus siglas en inglés).

Para caracterizar estas teorías, se han implementado diversos métodos dentro del marco del grupo de renormalización. La teoría de perturbaciones se ha aplicado desde los inicios de este campo, concretamente en la forma de la expansión en ε , la cual ha alcanzado altos órdenes de bucle en los últimos años. Alternativamente, se puede optar por un enfoque no perturbativo, conocido como grupo de renormalización no perturbativo (NPRG). Dentro del NPRG existen varios esquemas de aproximación, siendo la expansión en derivadas particularmente destacable. El objetivo final de estos esfuerzos es calcular los exponentes críticos, que definen una clase de universalidad dada. El método no perturbativo estándar implica resolver una ecuación que depende de un regulador o corte, lo que representa uno de los principales desafíos de este enfoque. Aunque los reguladores están diseñados de manera tal que la teoría no dependa de ellos en las escalas de interés, los resultados para los exponentes críticos pueden variar según el regulador utilizado.

En este proyecto, proponemos un enfoque que elimina la necesidad de un corte de masa explícito, lo que simplifica significativamente el cálculo de los exponentes críticos y, al mismo tiempo, reduce la dependencia de los resultados respecto al regulador. En particular, demostramos que es posible usar la regularización dimensional (DR) más allá de la expansión en ε en el contexto del RG en el cálculo de propiedades críticas.

Basándonos en esto, proponemos un nuevo esquema de renormalización funcional llamado *Functional Dimensional Regularization* (FDR) y lo aplicamos al modelo O(N) en tres dimensiones, encontrando una excelente concordancia con los cálculos del estado del arte.

Palabras clave: Grupo de renormalización no perturbativo, universalidad, fenómenos criticos.

Contents

List of Figures List of Tables				X		
				xiii		
1	Intr	oductio	on	1		
2	Pha	se Tran	nsitions and Critical Phenomena	4		
	2.1	Phase	e Transitions	4		
		2.1.1	Types of Phase Transitions	5		
		2.1.2	Liquid-gas Phase Transition	5		
		2.1.3	Magnetic Phase Transitions	10		
	2.2	Landa	au's theory of phase transitions	16		
		2.2.1	Mean Field Theory	16		
		2.2.2	The Ginzburg-Landau criterion	18		
	2.3	Renor	rmalization Group and Universality	20		
		2.3.1	Renormalization Group	20		
		2.3.2	Critical Surface and Fixed Points	24		
		2.3.3	Universality	28		
	2.4 Universality Classes with $O(N)$ Symmetry					
		2.4.1	N=2 XY	30		
		2.4.2	N=3 Heisenberg	31		
		2.4.3	$N=0 exttt{SAW}$	31		
		2.4.4	N=-2 Lerw	32		
		2.4.5	Large- <i>N</i>	32		
		2.4.6	State of the Art data for Critical Exponents	33		
3	Fun	ctional	Renormalization Groups	38		
	3.1	Effect	ive Action	38		

ibliography 10		
Con	clusions and Perspectives	103
	4.2.8 Comparison with State-of-the-Art of the critical exponents	99
	4.2.7 Results	94
	4.2.6 Fixed Points and Critical Exponents	93
	4.2.5 Beta Functionals	92
	4.2.4 Diagrams and Propagator	87
	4.2.3 Feynman Rules	83
	4.2.2 β_U in presence of Z and Y	
	4.2.1 Action	80
4.2	O(N) Derivative Expansion	80
	4.1.4 Comparison with NPRG-Litim	76
	4.1.3 Fixed Points and Critical Exponents	
	4.1.2 NPRG-LPA	71
2.2	4.1.1 FDR-LPA	68
4.1	O(N) Local Potential Approximation	68
Fun	ctional Dimensional Regularization for the $O(N)$ Model	68
	3.5.3 Fixed Points and Critical Exponents in $d = 3$ at FDR-LPA	63
	3.5.2 Fixed Points and Critical Exponents in $d = 4 - \varepsilon$	
	3.5.1 Dimensionless Flow Equation for $\beta_V \& \beta_Z \dots \dots$	
3.5	Fixed Point Analysis (FPRG vs NPRG vs FDR)	61
	3.4.4 Local Potential Approximation (LPA') in FDR	60
	3.4.3 Calculation of the a_n and c_n coefficients	57
	3.4.2 Dimensional Analysis	55
	3.4.1 Beta Functionals	52
3.4	Functional Dimensional Regularization (FDR)	52
	3.3.3 Local Potential Approximation (LPA') in NPRG	50
	3.3.2 Approximation Schemes	49
	3.3.1 EAA and the Wetterich-Morris Equation	46
3.3	Functional Non-Perturbative RG (NPRG)	45
	3.2.3 Local Potential Approximation (LPA') in FRPG	
	3.2.2 Perturbative Regularization and Renormalization	
	3.2.1 Loop Expansion	40

Appendices		113
Α	Derivation of the Wetterich's equation	113
В	The Feynman rules for the derivative expansion at order two .	114
C	Strict, Light and Strict-light beta functions	119

List of Figures

2.2	Isotherms of a van der Waals system (taken from [7])	8
2.3	Formation of blocks of spins and rescaling [9]	22
2.4	Lines of flow about the three types of fixed points: (a) attractive, (b)	
	repulsive and (c) mixed [16]	24
2.5	Representation of the critical surface. Black dot represent an attractive	
	(stable) fixed point while the white represent an unstable fixed point	25
3.1	Diagrammatic representation of the RG equation. The line represent the prop-	
	agator and the cross is $\partial_t R_k$, the closed loop means integration over q	48
3.2	Diagrammatic representation of $\partial_t \Gamma_k^{(1)}$	49
3.3	Diagrammatic representation of $\partial_t \Gamma_k^{(2)}$	49
3.4	Top: Poles of the Gamma function $\Gamma(-\frac{d}{2})$ in the complex plane. Mid-	
	dle: Poles of the Gamma function with $d=4$ pole regularized. Bottom:	
	Gamma function in the complex plane with all poles regularized	53
3.5	Feynman diagram for the $\beta_Z^{\rm DR}$ at 1 loop	56
3.6	Flow in the (λ_2, λ_4) plane in $d = 3$. The Gaussian (red) and Wilson-	
	Fisher (green) fixed point	64
3.7	Comparison of the convergence of the critical exponent ν in $d=3$	
	among the FDR-LPA, NPRG-LPA + Litim cutoff and FPRG	66
3.8	Convergence of the critical exponent ω in the FDR-LPA approximation	
	in $d = 3$. Comparison is shown against the state-of-the-art Bootstrap	
	value, the NPRG-LPA + Litim cutoff and FPRG	67
4.1	Convergence of the critical exponent ν in the FDR-LPA applied to $O(N)$	
	models. Comparison is made with state-of-the-art estimates (CB)	74
4.2	Convergence of the critical exponent ω in the FDR-LPA applied to $O(N)$	
	models. Comparison is made with state-of-the-art estimates DE at $\mathcal{O}(\partial^4)$	
	[39]	74

LIST OF FIGURES ix

4.3	Convergence of the critical exponent ν in the FDR-LPA around the minima	
	applied to $O(N)$ models. Comparison is made with state-of-the-art estimates	
	(CB) dashed lines	76
4.4	Convergence of the critical exponent ω in the FDR-LPA around the minima	
	applied to $O(N)$ models. Comparison is made with state-of-the-art estimates	
	DE at $\mathcal{O}(\partial^4)$ [39]	76
4.5	Comparison of the critical exponent ω_3 and ω_4 computed from the	
	Litim equations and the FDR at the LPA around zero	78
4.6	Comparison of the critical exponent ω_3 and ω_4 computed from the	
	Litim equations and the FDR at the LPA around the minima	79
4.7	Estimate of the critical exponent ν as a function of N at $d=3$ at order	
	LPA (black), order $\mathcal{O}(\partial^2)$ (red), order $\mathcal{O}(\partial^4)$ (green), FDR(blue)	79
4.8	Estimate of the critical exponent ω as a function of N at $d=3$ at order	
	LPA (black), order $\mathcal{O}(\partial^2)$ (red), order $\mathcal{O}(\partial^4)$ (green), FDR at LPA (blue).	80
4.9	Feynman diagrams contributions to the one loop two point function	87
4.10	Convergence of the critical exponent ν in the DE FDR- $\mathcal{O}(\partial^2)$ around	
	zero applied to O(N) models. Comparison is made with state-of-the-	
	art estimates (CB) dashed lines	95
4.11	Convergence of the critical exponent ω in the DE FDR- $\mathcal{O}(\partial^2)$ around	
	zero applied to $O(N)$ models. Comparison is made with final estimate	
	DE2 (dashed) and DE4 (continuous)	96
4.12	Convergence of the critical exponent η in the DE FDR- $\mathcal{O}(\partial^2)$ around	
	zero applied to $O(N)$ models. Comparison is made with state-of-the-	
	art estimates	96
4.13	Convergence of the critical exponent ν in the DE FDR- $\mathcal{O}(\partial^2)$ around	
	the minima applied to $O(N)$ models. Comparison is made with state-	
	of-the-art estimates (CB).	98
4.14	Convergence of the critical exponent ω in the DE FDR- $\mathcal{O}(\partial^2)$ around	
	the minima applied to $O(N)$ models. Comparison is made with DE2	
	(dashed) and DE4 (continuous)	98
4.15	Estimate of the critical exponent η as a function of N in $d=3$ at or-	
	der NPRG-DE2 (red-square final and red-dot raw), order NPRG-DE4	
	(green-square final and green-dot) and at order NPDR-DE2 blue $n=$	
	11, large- N magenta and conformal bootstrap black stars	99

LIST OF FIGURES x

4.16 Estimate of the critical exponent v as a function of N in d = 3 at order NPRG-DE2 (red square final and red-dotted raw), order NPRG-DE4 (green-square final and green-dotted raw) and at order NPDR-DE2 blue n = 11, large-N magenta and conformal bootstrap black stars.
4.17 Estimate of the critical exponent w as a function of N in d = 3 at or-

4.17 Estimate of the critical exponent ω as a function of N in d=3 at order NPRG-DE2 (red-square final and red-dotted raw), order NPRG-DE4 (green-square final and green-dotted raw) and at order NPDR-DE2 blue n=11, large-N magenta and conformal bootstrap black stars. 100

List of Tables

2.1	Characteristic behaviour of ferromagnetic quantities close to criticality.	15
2.2	Comparison of the critical exponent predicted by the mean field (MF) theory	
	and the exact result from Onsager	18
2.3	Critical exponent for the $O(0)$ symmetric scalar model in $d=3$. DE at	
	LPA, $\mathcal{O}(\partial^2)$ and $\mathcal{O}(\partial^4)$ [39], Monte-Carlo simulation, six-loop pertur-	
	bation theory at fixed $d=3$ [40] , $d=4-\epsilon$ at ϵ^6 [41], the conformal	
	bootstrap and the large- N expansion [42, 43, 44]	33
2.4	Critical exponent for the $O(1)$ symmetric scalar model in $d=3$. DE	
	at LPA, $\mathcal{O}(\partial^2)$, $\mathcal{O}(\partial^4)$ improved and raw with exponential cut-off from	
	[45], Monte-Carlo simulation [46, 47], six-loop perturbation theory at	
	fixed $d=3$ [40], $d=4-\epsilon$ expansion at ϵ^6 [41], the conformal bootstrap	
	[33, 48].	34
2.5	Critical exponent for the $O(2)$ symmetric scalar model in $d=3$. DE	
	at LPA, $\mathcal{O}(\partial^2)$ and $\mathcal{O}(\partial^4)$ (raw computed with exponential regulator)	
	[39], Monte-Carlo simulation, six-loop perturbation theory at fixed $d =$	
	3[40], $d=4-\epsilon$ at ϵ^6 [41], the conformal bootstrap	34
2.6	Critical exponent for the $O(3)$ symmetric scalar model in $d=3$. DE at	
	LPA, $\mathcal{O}(\partial^2)$ and $\mathcal{O}(\partial^4)$ (raw computed with exponential regulator) [39],	
	Monte-Carlo simulation, six-loop perturbation theory at fixed $d=3$	
	[40], $d = 4 - \epsilon$ at ϵ^6 [41], the conformal bootstrap	35
2.7	Critical exponent for the $O(4)$ symmetric scalar model in $d=3$. DE	
	at LPA, $\mathcal{O}(\partial^2)$ and $\mathcal{O}(\partial^4)$ (raw computed with exponential regulator)	
	[39], Monte-Carlo simulation, six-loop perturbation theory at fixed $d =$	
	3 [40], $d=4-\epsilon$ at ϵ^6 [41], the conformal bootstrap and the large-N	
	expansion [42, 43, 44]	35

LIST OF TABLES xii

2.8	Critical exponent ν , ω and η of the $O(5)$ symmetric scalar model in	
	d=3. DE results are final estimate from [45], six-loop [56] and the	
	large- <i>N</i> expansion [42, 43, 44]	36
2.9	Critical exponent ν , ω and η of the $O(10)$ symmetric scalar model in	
	d = 3. DE results are final estimate from [45] (raw computed with	
	exponential regulator), six-loop [56] and the large-N expansion [42, 43,	
	44]	36
2.10	Critical exponent ν , ω and η of the $O(20)$ symmetric scalar model in	
	d = 3. DE results are final estimate from [45], conformal bootstrap [32],	
	six-loop [56] and the large- <i>N</i> expansion [42, 43, 44]	36
2.11	Critical exponent ν , ω and η of the $O(100)$ symmetric scalar model in	
	d=3. DE results are final estimate from [45] and the large- N expansion	
	[42, 43, 44]	37
2.12	Critical exponent ν , ω and η of the $O(-2)$ symmetric scalar model in	
	d=3. DE results are final estimate from [45] and perturbative results	
	can be found in [25, 26]	37
3.1	Comparison of the ν and ω critical exponents against the differents	
0.1	methods	67
4.1	FDR-LPA with expansion around zero (4 significant digits). The first	
	column shows in bold face those two significant digits for the exponent	
	ν which match state-of-the-art estimates	73
4.2	FDR-LPA with expansion around the minima (4 significant digits)	75
4.3	Comparision between the critical exponent ν and ω for the NPRG and	
	FDR at LPA level	77
4.4	Comparision of the sub-leading critical exponent within the NPRG and	
	FDR	77
4.5	Convergence of critical exponents for expansion around zero	97
4.6	Final values of critical exponents for expansion around zero for large N .	97
4.7	Convergence of critical exponents for expansion around the minima	99
4.8	Comparison of the critical exponent with the state-of-the-art. The NPRG	1.01
4.0	results (raw) are taken from [45], and CB values from Tables 2.4 and 2.5	101
4.9	Comparison of the critical exponent with the state-of-the-art. The NPRG	101
1 10	results (raw) are taken from [45], and CB values from Tables 2.6 and 2.7	101
4.10	Final results for the $N=5$ universality class for different methods	102
4.11	Final results for the $N=0$ universality class for different methods	102

LIST OF TABLES	xiii
4.12 Comparison of the critical exponent with the state-of-the-art. The NPRG	
results (raw) are taken from [45], six-loop and CB values from Tables 2.3	
and 2.8	102

Chapter 1

Introduction

In thermodynamics, systems can exist in different states or phases which, when in equilibrium, are characterized by a set of parameters known as thermodynamic variables. One of the main objectives of thermodynamics is to properly define the physical quantities (or state variables) that describe the macroscopic properties of matter—known as macrostates—and to relate these quantities through valid universal equations, namely equations of state and thermodynamic laws. Many systems experience changes in the macroscopic behavior of their properties when some control parameter is varied, typically the temperature. These changes in macroscopic behavior are called phase transitions. The order parameter is a property of the system which tells the degree of order on the two sides of the transition. Sometimes the order parameter varies continuously during the transition and there is no latent heat associated; therefore, this kind of transition is denominated as "continuous phase transition".

Almost every day we witness a phase transition, such as water boiling in a kettle. Another example one can find in nature, though only observable in colder climates, is a lake freezing over. The state, of water in this case, is physically described¹ by a set of macroscopic parameters such as pressure and temperature, for instance. Another example of a phase transition took place in the early universe [1]. Shortly after the Big Bang it is thought that the three fundamental forces of the Standard Model² (which manifest independently nowadays) were unified at the high temperatures of the early universe [2, 3]. At this same stage the Quark-Hadron transition is another example of phase transition, where quarks and gluons were free³ and as the universe cooled

¹This is when the substance to describe is in equilibrium.

²Weak, strong and electromagnetic forces.

³This state is known as the quark-gluon plasma.

they combined to form hadrons. As seen, phase transitions are central not only to our daily lives but also in understanding the universe.

In physics, when we want to describe or characterize a system (from a thermodynamic point of view), we appeal to the statistical mechanics formalism. It is known that the vast majority of these systems fall into one of the following two categories. On one side, the microscopic constituent of the system can be treated as nearly non-interacting, which leads to smooth and continuous thermodynamic functions. Normally the solution to the problems is straightforward, for example, it is possible to solve it with a perturbative approach. On the other side, system which are strongly correlated (like a second-order phase transition) presents analytic discontinuities or singularities in the thermodynamic functions which give rise to the phase transition. Materials that undergo a second-order phase transition are those whose second derivatives of the free energy, like the specific heat or the magnetic susceptibility, show a divergence while the first derivative – such as the entropy or the magnetization –are continuous functions.

Critical phenomena is characterized by *universality*, which – broadly speaking – means that systems which are completely unalike at the microscopic level present the same power law behavior, of their macroscopic thermodynamical quantities, when criticality is approached. Later we will see that a set of *critical exponents* characterize a universality class – among other quantities; then we say that two systems belong to the same universality class if they share the same critical exponents. Among the extensive list of universality classes, we will focus on those characterized by O(N)-symmetry. It is important to say that in order to characterize a universality class we need two parameters, the order parameter itself and also the dimension, for instance. As an example, the O(2) universality class differs in the critical exponents as well as the symmetry displayed, when d=2 or d=3.

Since the solutions to problems like these are hard to handle, due to the great number of degrees of freedom involved, it was proposed by Wilson a framework to deal with this kind of system which is known as the *renormalization group* (RG). This approach not only gives us a way to treat critical systems but also explains the phenomena of universality. The renormalization group consist in formulating effective theories where the main ingredient is the effective action, a functional that encapsulates the coarse-grained physics at different scales. The renormalization group has two branches, either one can formulate it perturbativly or non-perturbativly. In the latter way, together with the path integral formalism, we can derive an exact equa-

tion⁴ describing how the effective action changes when the scale changes. The problem is that this functional partial differential equation has no analytic solution and thus approximation are required. Among several approaches, the one most used in the literature is the derivative expansion. This methods consist in an ansatz for the effective action which includes up to a certain degree of derivatives of the field.

This thesis is organized as follows. In Chapter 2 we give the basic notions of phase transitions and critical phenomena, we also present an introduction to the Wilson's renormalization group and to universality classes. At the end of this chapter we briefly indicate which are the universality classes of interest and explain how they manifest in nature giving real life examples. In Chapter 3 we introduce the two different approaches to the renormalization group well known in the literature, the functional perturbative renormalization group (FPRG) and the non-perturbative renormalization group (NPRG), to this we add our new approach baptized as *Functional Dimensional Regularization* (FDR). Moreover, we apply our new approach to one component scalar fields and give a connection between the FDR and the NPRG.

Later, on Chapter 4 we generalize our theory and analyze the multi-component case where we study O(N) models for certain values of N by means of the derivative expansion up to order $O(\partial^2)$ with the FDR. We also compare our results with the state of the art corresponding to the conformal bootstrap and $O(\partial^4)$ NPRG calculations when available . Finally, we present our conclusion and discuss which improvements are possible.

⁴Sometimes called the Wetterich/Morris equation.

Chapter 2

Phase Transitions and Critical Phenomena

One of the main goals of statistical mechanics is the computation of macroscopic properties of systems composed by a large number of particles from the knowledge of the microscopic interactions between the constituents. In particular, one is interested in the study of the phenomena of phase transitions; in this thesis we focus on second order phase transitions that constitute the main subject in the theory of critical phenomena.

In this chapter, basic concepts of phase transitions are introduced with the aim of preparing the reader for subsequent chapters. We introduce a few toy models in order to fix ideas – in particular the Ising model – which will serve us as an example when defining Wilson's renormalization group [4], one of the main pillars of the theory of critical phenomena; after this is settled up, we explain the phenomena of universality, another key point of this project. Then we explain what are O(N) models and briefly describe the different universality classes arising from it. Finally, we summarize the most recent results for the critical exponents of O(N) models calculated using the different known methods available.

2.1 Phase Transitions

In this section, we will define what a phase transition is and present examples of first- and second-order phase transitions. In particular, we are interested in second-order transitions, since they allow us to define very interesting properties, such as universality.

2.1.1 Types of Phase Transitions

In general, it is understood that a phase transition is produced when some property of a system changes abruptly by fine-tuning a parameter. As an example, this it what happens in the case of the liquid-steam or paramagnetic-ferromagnetic transition. Formally, we say that phase transitions occur when some thermodynamic function presents a non-analytic point. This is because the equation of state arises from derivatives of the free energy, therefore a discontinuity on the derivative implies the equations of state of the two phases be different. One way to classify a phase transitions is to use the Ehrenfest's classification which says that the transition is of order-n if the n-derivative of the free energy is singular. The most extensively studied types of transitions are first-order or second-order, with the latter being of particular interest for this project.

2.1.2 Liquid-gas Phase Transition

In a P-v diagram of a simple liquid, there exist a region on which the two phases coexist, liquid and steam. In that region, the pressure is constant along an isotherm, $P=P_{coex}(T)$. Hence, if we impose a constant pressure $P^*=P_{coex}(T^*)$ for the temperature $T_1=T^*-\delta T$ the system will be on the liquid phase and at $T_2=T^*+\delta T$ it will be on steam phase, regardless of how small δT is. Consequently, by changing the temperature at constant pressure, the specific volume undergoes a jump from $T< T^*$ to $T>T^*$. This same thing happens with the entropy S. At each point of the process we fix T,P then we use the Gibbs free energy G. Writing $T=T^*$ this is represented in Figure 2.1. Since the entropy present a jump, there will be a latent heat involved

$$\Delta S = \frac{\delta Q}{T} \tag{2.1}$$

Note that

$$S = \left(\frac{\partial G}{\partial T}\right)_{P} \tag{2.2}$$

there is a discontinuity on the first derivative of G, hence the transition is of first-order. It is also possible to have a second-order transition where the singularity appears on the heat capacity which is the second derivative. For a system to undergo this type of transition, there must exist an interaction between particles that is attractive for some distances and repulsive for others. The Lennard-Jones potential [5] is a good

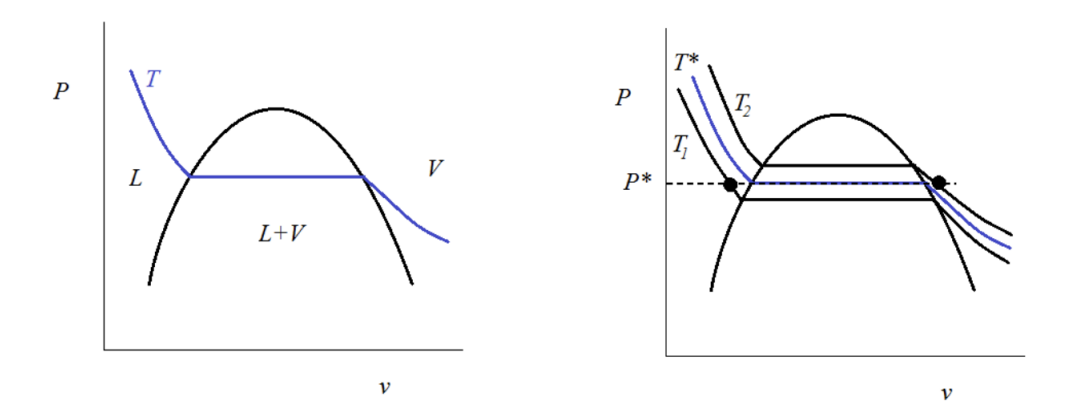


Figure 2.1: P - v diagram of a simple fluid.

approximation for such interaction (2.3):

$$u(r) = 4\epsilon \left[\left(\frac{\sigma}{r} \right)^{12} - \left(\frac{\sigma}{r} \right)^{6} \right]$$
 (2.3)

In order to simplify the computation it is useful to use the following model

$$\begin{cases} u(r) = \infty & r \le \sigma \\ 0 > u(r) > -\epsilon & \sigma < r < r^* \\ u(r) = 0 & r \ge r^* \end{cases}$$
 (2.4)

with this potential we can think that each particle is a hard sphere of diameter σ situated in an attractive potential of range r^* which has a maximum depth ϵ . If we compute the exact partition function $Z_N(V,T)$ (here N is the total number of particles of the system) this will exhibit the following properties: in the thermodynamic limit, that is, when $N,V\to\infty$ and the ratio N/V stays constant, the quantity $\frac{\ln{(Z)}}{N}$ tends to be a function of the specific volume v and the temperature. From the partition function one computes the Helmholtz free energy of the system which allows us to compute the thermodynamic pressure P given by

$$P(v,t) = -\left(\frac{\partial F}{\partial V}\right)_{N,T} = kT\left(\frac{\partial f}{\partial v}\right)_{N,T} \tag{2.5}$$

which is a strictly non-negative quantity. Moreover, the function f(v,T) is everywhere concave, hence the slope $(\partial P/\partial v)$ of the (P,v) curve is never positive. At high temperature the slope is negative for all v but at lower temperatures there may exist regions in which the slope is zero, therefore the systems is infinitely compressible.

The existence of such regions emerge from the coexistence of two or more phases of different density of the system. We are in the presence of a phase transition. It is important to distinguish two different cases, whether one use the *exact* partition function or an approximation. If one use the former, there will be no isotherms with positive slope, otherwise it would appear unphysical regions like it does if one uses the van der Waals model as it will be described below. In order to solve this problem it is common to introduce a flat region where the isotherms slope is positive, then we go from $\frac{\partial P}{\partial v} > 0 \rightarrow \frac{\partial P}{\partial v} = 0$. To do so we use the Maxwell construction of equal areas. This unphysical regions emerge since as one use an approximate partition function, the density is constrained to be constant thus hindering the system from undergoing a transition, where the phases on either side have different densities.

Van der Waals Model

The Van der Waals gas model [6] was one of the first used to describe the gas-liquid phase transition, which can be derived by doing an approximation of rigid sphere. This model obeys the equation of state

$$P = \frac{RT}{v - b} - \frac{a}{v^2} \tag{2.6}$$

where *a* and *b* are constant that measure the attractive force among the molecules and the repulsive force when two particles come too close respectively.

For T above the critical temperature, P decreases monotonically with v. For $T < T_c$ in Figure 2.2 the isotherms shows regions where $\partial P/\partial v > 0$ hence the condition of stable equilibrium is not satisfied. This is corrected with the Maxwell construction, which has a result the flat portion of isotherms as shown in the picture. In that flat interval the substance is in a mixed phase where the transition from liquid to gas state results in a $\Delta v \neq 0$ and $\Delta P = 0$. In the Figure 2.2 the coexistence curve is represented. This curve delimits the zone under which the two phases can coexist, this means that for $v_l < v < v_g$, the system is in a mixed phase and the transition below this curve correspond to a first order phase transition. As the temperature increase, the values of v_g along this curve decreases and the values of v_l increase up to a common value for v_c known as the critical volume which is part of the set known as the critical point.

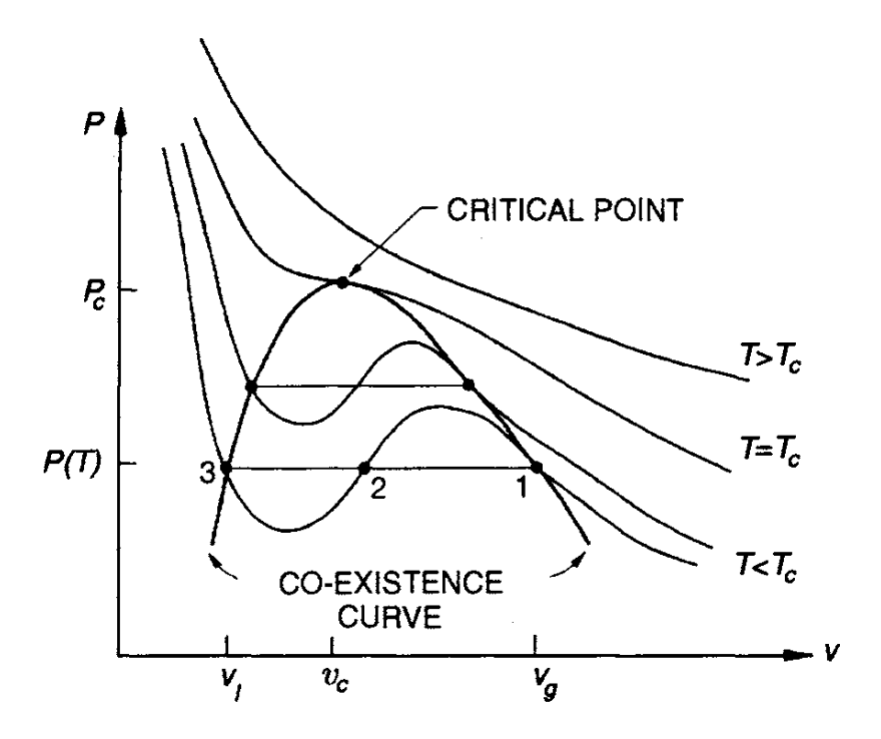


Figure 2.2: Isotherms of a van der Waals system (taken from [7]).

The critical point is the one that verify

$$\left(\frac{\partial P}{\partial v}\right)_T = 0, \qquad \left(\frac{\partial^2 P}{\partial v^2}\right)_T = 0$$

under these conditions in the Van der Walls model we define

$$P_c = \frac{a}{27b^2}, \qquad v_c = 3b, \qquad T_c = \frac{8a}{27bR}.$$

It is possible to define the number K as

$$\mathcal{K} = \frac{RT_c}{P_c v_c} = \frac{8}{3} = 2.666...$$

the values of the temperature, pressure and volume at the critical point differ in one system or another, but the quantity \mathcal{K} is the same for every system that satisfy the van der Waals equation of state, thus value of \mathcal{K} is *universal*. Usually we define reduced

variables¹ as

$$P_r = P/P_c$$
, $T_r = T/T_c$, $v_r = v/v_c$

Thus the equation of state can be written as

$$\left(P_r - \frac{3}{v_r^3}\right) \left(3v_r - 1\right) = 8T_r \tag{2.7}$$

Now let us study what happen with the isothermal compressibility κ_t as we approach to the critical point. By definition at the critical point we have that $P_r = 1$, $v_r = 1$ and $T_r = 1$. Hence, we write close to the criticality

$$P_r = 1 + \pi$$

$$v_r = 1 + \psi$$

$$T_r = 1 + t$$

where in the case of the temperature t is defined as $t = \frac{T - T_c}{T_c}$. We need to compute

$$\kappa_t = -\frac{1}{v} \left(\frac{\partial v}{\partial P} \right)_T$$

Using the reduced variables

$$P = \frac{8}{3} \frac{T}{(v - 1/3)} - \frac{3}{v^2} \tag{2.8}$$

Thus

$$-\left(\frac{\partial v}{\partial P}\right)_T = -\frac{6}{v^3} + \frac{8}{3} \frac{T}{(v - 1/3)^2}$$

Now, let us examine how κ varies as $T \to T_c$ with $T > T_c$ and v = 1 that is the critical volume then

$$\frac{1}{\kappa_t} = -v \left(\frac{\partial P}{\partial v}\right)_T$$
$$= -(6 - \frac{8}{3} \frac{T}{(2/3)^2}) = -6(1 - T) = 6t$$

¹This is because it enables us to abstract away from the specifics of individual systems to uncover and analyze the universal behaviors and properties that many systems share. Besides, it simplifies the mathematical expressions and makes the equations more manageable.

$$\kappa_T = \frac{1}{6t}$$

Therefore we see that as $T \to 1$, (i.e., we approach to the critical point), the isothermal compressibility diverge. This is the typical behavior of a second-order transition where some properties diverge close to the critical point. In order to characterize these kind of divergences we define **critical exponents**. In the case of the compressibility the critical exponent γ is defined such that close to the critical point

$$\kappa_t \propto (T - T_c)^{-\gamma}$$

We found that

$$\kappa_T = \frac{1}{6t} = \frac{1}{6(T_r - 1)} \propto \frac{1}{T - T_c}$$

so the critical exponent $\gamma = 1$.

A problem in the phase transition theory is that as close as we approach to the criticality it is harder and harder to tell on which side of the phase we are, therefore we need a tool in order to infer on which side of the phase we are. To do so, we define a function called **order parameter**, which serves to distinguish each phase. The density ρ is the order parameter in the context of fluids where close to the criticality it behaves as $\rho_l - \rho_g \sim |T - T_c|^{\beta}$. From here we see that we have introduced a new critical exponent, β .

As we approach the phase transition (for instance, by varying the temperature), certain thermodynamic properties exhibit power-law behavior near the critical temperature. In particular, the specific heat C diverges in the neighborhood of T_c as $C \sim |T - T_c|^{-\alpha}$ defining the exponent α .

The study of these critical exponents is a key point, as they characterize a universality class.

2.1.3 Magnetic Phase Transitions

Now we turn to study the magnetic continuous phase transitions, unlike the first order this do not involve an absorption/release of latent heat. It was Pierre Curie [8] that was one of the first to observe a continuous phase transition, he saw how iron transformed from paramagnetic to ferromagnetic up to the temperature $T_c = 1043K$. Element such as iron, cooper or zinc are paramagnetic at $T > T_c$, this means that material is not magnetized in the absence of an applied magnetic field. Though if we apply a weak magnetic field $\bf B$, the material's magnetic moments $\bf m$ is proportional to

the applied field $\mathbf{m} \approx \mu \mathbf{B}$. In contrast, the ferromagnetic state, for $T < T_c$, the material shows a non-zero magnetization even when no external magnetic field \mathbf{B} is applied.

The analogue for the divergence in the isothermal compressibility for the watersteam transition is in the case of iron ferromagnetic-paramagnetic transition at the susceptibility $\chi_T = (\partial m/\partial B) \sim (T - T_c)^{-\gamma}$. In either case, the large values of κ_T and χ_T above T_c give rise to large fluctuations in the density or magnetization. This large fluctuations can be observed experimentally through the phenomenon of critical opalescence.² In the case of the ferromagnetic-paramagnetic transition, we use the magnetization m as order parameter which is defined as:

$$m(T) = \begin{cases} 0 & \text{for } T > T_c, \\ |t|^{\beta} & \text{for } T < T_c \end{cases}$$

Another example of critical exponent we want to introduce is δ which in the context of magnetic materials this critical exponent is defined by how the magnetization \mathcal{M} depends on the external magnetic field B at the critical temperature T_c . Formally, it is written as $\mathcal{M} \sim B^{\frac{1}{\delta}}$ when $T = T_c$.

Finally, a last few words before we proceed to present some models. The amazing thing we want to emphasize is that all these exponents defined above $(\beta, \nu, \delta, \cdots)$ share the same value for magnetism as for the water-steam transition! Surprisingly, two system (which have microscopically nothing in common) behave exactly the same at criticality. This is our first encounter with the concept of universality [9].

The Ising Model

So far we have mentioned the phase transition in an uniaxial magnet but yet did not propose any model. The Ising model [10] is by far the most popular model to model quantitatively the paramagnetic-ferromagnetic transition at least as a first approximation. There are some key features that are essential which must be displayed in the Hamiltonian describing the theory, such as the interaction between spins tending to align them in the case of ferromagnetism. We build this model as electrons placed on a lattice which in general we assume it is a cubic one. This lattice may have dimension one, two or three which will be denoted with the letter *d*. Also we will think that the spin-spin interaction has a short range, therefore we will neglect the interaction between spins enough separated. The simplest quantum Hamiltonian with tendency

²This is a light scattering phenomena where the wavelength of the gas are long enough to scatter visible light. The fluid appears "milky" and the light can not pass through the system.

to align the spins is the quantum Heisenberg model:

$$H = -J \sum_{\langle i,j \rangle} \sigma_i \cdot \sigma_j \tag{2.9}$$

where J is the coupling constant which is positive for the ferromagnetic case, < i, j > means sum over the nearest neighbors and σ_i are the Pauli matrices. Since quantum fluctuations are suppressed by statistical fluctuations, we can replace the Pauli matrices σ by the classical vector S_i of length 1 which defines the classical Heisenberg model. Despite this simplification (from quantum to classical) the model is still too hard to solve, the only analytic solution known up to date is on the d=1 case. The last simplification was proposed by Lenz in 1920 [11], he replaced the classical vector S_i by scalar S_i where $S_i = +1$, -1. Some years later Lenz proposed this model to his student, Ernst Ising, as a model for ferromagnetism. Ising treated the case d=1 which has a analytic solution. In 1942 Onsager [12] solved the case d=2 with no external field applied. Nowadays, we know that the Ising model describe the ferromagnetism qualitatively good but quantitatively it fails to provide accurate predictions.

The main difference between the classical Heisenberg model and the Ising model is that the former takes the spins S_i as three-dimensional vectors, whereas the latter takes the spins as scalar. On account of we say that the Heisenberg model has dimensionality N=3 of the order parameter and the Ising correspond to the N=1. Consequently, the critical exponent computed in each case will differ. As mentioned, the Hamiltonian of the Ising model is given by

$$H = -J \sum_{\langle i,j \rangle} S_i S_j, \quad S_i = \pm 1$$
 (2.10)

For pedagogical reasons, let us compute the partition function from which several thermodynamic quantities can be derived. The partition function Z is

$$Z = \sum_{states} e^{-\beta H} = \sum_{[S_i]} e^{\frac{J}{k_B T} \sum_{\langle i,j \rangle} S_i S_j} \qquad \beta = \frac{1}{k_B T}$$
 (2.11)

where $\sum_{[S_i]}$ runs over all configurations. If we have N sites in the lattice there will be 2^N terms in the partition function.

Let consider the most simple case which is the linear lattice (d = 1). There are many ways to compute the partition function among them the transfer matrix method.

The partition function is

$$Z = (\cosh(K)^{N-1}) \sum_{[S_l]} \prod_{i=1}^{N-1} (1 + S_i S_{i+1} \tanh K)$$

One common method in statistical mechanics is the use of the high-temperature expansion. To apply this one expand the partition function in power of some parameter $\kappa(T)$ such that $\kappa(T) \to 0$ as $T \to \infty$. In this case the $\tanh(K) = \tanh(J/kT) \to 0$ as $T \to \infty$. Therefore we will expand

$$\prod_{i} (1 + S_{i}S_{i+1} \tanh(K)) = 1 + \tanh(K) \sum SS + \tanh(K)^{2} \sum (SSSS) + \cdots$$

For this various terms the only terms that survives is the first of the expansion since for a given configuration with S_k fixed to 1 there is another identical but with $S_k = -1$ and this two cancel each other. When we impose a free boundary condition we arrive at

$$Z = 2^N(\cosh(K)^{N-1})$$

with $K = J/k_BT$. Now that we know the partition function we are allowed to compute any thermodynamic function, in particular the Helmholtz free energy $-k_BT \ln Z$. Recall that a phase transition correspond to a singularity of the thermodynamic function, to see that we have to take the thermodynamic limit $N \to \infty$. The free energy per spin f is in this limit

$$f = \lim_{N \to \infty} \frac{1}{N} F = \lim_{N \to \infty} \left(-\frac{k_B T}{N} \ln Z \right) = k_B T \log(2 \cosh(\frac{J}{k_B T}))$$

Hence f is an analytic function of T and there is no phase transition in one dimension since the temperature of transition is $T_c = 0$. This was also shown by Peierls [13] who predicted a phase transition for d = 2.

Correlation Function

We move forward with the calculation of the correlation function of two spins S_i and S_j . The correlation functions measures the influence exerted, for instance, on the spin S_i due to the spin S_j . At this point we expect the correlation function to decay exponentially as the spins get further and further away. The definition of the correlation

function is

$$G_{ij} = \langle S_i S_j \rangle - \langle S_i \rangle \langle S_j \rangle \tag{2.12}$$

this is actually called *connected correlation function*. If we consider the Ising model with an external magnetic field **B** applied the Hamiltonian becomes

$$H = -J \sum_{\langle i,j \rangle} S_i S_j - \mu \sum_i B_i S_i$$

and the function G_{ij} relates to a second derivative of the partition function $Z[B_i]$

$$\langle S_i \rangle = \frac{1}{Z} \sum_{S_k} S_i e^{-\beta(H_0 - \mu \sum_k B_k S_k)}$$

therefore

$$\langle S_i \rangle = \frac{1}{\beta \mu Z} \frac{\partial Z}{\partial B_i} = \frac{1}{\beta \mu} \frac{\partial \ln Z}{\partial B_i}$$

Then

$$\langle S_i S_j \rangle = \frac{1}{(\beta \mu)^2} \frac{1}{Z} \frac{\partial^2 Z}{\partial B_i \partial B_j}$$

$$G_{ij} = \frac{1}{(\beta \mu)^2} \frac{\partial^2 \ln Z}{\partial B_i \partial B_j}$$

It is worth noting that the correlation function G_{ij} of two spins is computed from the derivatives of log Z, from here we can extend this process and compute the correlation functions of several spins. Due to this fact, the function $Z[B_i]$ is called *generating* function of the correlation functions.

Experimentally it can be shown close to the criticality that for small momentum $q \ll \frac{1}{a}$ the correlation function has the form³

$$\widetilde{G}(\mathbf{q}) = \frac{1}{q^{2-\eta}} f(q\xi) \tag{2.13}$$

where the parameter η is called **anomalous dimension**. In the context of magnetism, we define the critical exponent ν which relates to the **correlation length** ξ . Close to the criticality is found that

$$\xi \sim |T - T_c|^{-\nu} \sim |t|^{-\nu}$$
 (2.14)

 $^{^{3}}a$ is the lattice spacing.

order parameter specific heat susceptibility critical isotherm correlation length
$$\mathcal{M} \sim (T_c - T)^{\beta} \quad (T < T_c)$$
 $\mathcal{C} \sim |T - T_c|^{\alpha} \quad (T \neq T_c)$ $\chi \sim |T - T_c|^{\gamma} \quad (T \neq T_c)$ $\mathcal{B} \sim \mathcal{M}^{\delta} \quad (T = T_c)$ $\tilde{G}(q) \sim q^{\eta - 2} \quad (T = T_c)$

Table 2.1: Characteristic behaviour of ferromagnetic quantities close to criticality.

Its value in the one dimensional Ising model is

$$\xi = \frac{a}{|\ln \tanh J/K_B T|}.$$

As expected, the correlation length decreases as the temperature increase and tends to infinity as the temperature goes to zero (the critical point).

Scaling Relations

The last two equation (2.13) and (2.14) defines the critical exponent η and ν . We can apply a Fourier transformation to G(q) and go back to the coordinate space

$$G(\mathbf{r}) = \frac{g(r/\xi)}{r^{d+\eta-2}} \tag{2.15}$$

where $g(r/\xi)$ behaves as $g(r/\xi) \sim e^{-r/\xi}$ for $r \gg a$. The correlation function $\widetilde{G}(\mathbf{q})$ is finite at q=0, in order to compensate the divergent factor in the denominator the function $f(q\xi)$ should behave as $f(q\xi) \sim (q\xi)^{2-\nu}$. This leads us to

$$\widetilde{G}(0) \sim \xi^{2-\eta} \sim t^{-\nu(2-\eta)}$$
.

The response fluctuation theorem says that

$$\chi \sim N\widetilde{G}(0)$$

and the magnetic susceptibility diverges as $\chi \sim |t|^{-\gamma}$. From here we see that there is a relation between the critical exponent

$$\gamma = -\nu(2 - \eta) \tag{2.16}$$

this is the first scaling law we find. There are six critical exponent $\alpha, \beta, \gamma, \delta, \eta$ and ν

which are not independent of each other, actually there are only two independent (say ν and η) from which one can compute the rest of them. The scaling relation reads as follows

$$\alpha = 2 - \nu d \tag{2.17}$$

$$\beta = \frac{\nu}{2}(d - 2 + \eta) \tag{2.18}$$

$$\gamma = \bar{\nu}(2-\eta) \tag{2.19}$$

$$\delta = \frac{d+2-\eta}{d-2+\eta} \tag{2.20}$$

The liquid-steam transition as well as the ferromagnetic-paramagnetic transition share the same values for the critical exponents, thus we say that both models belong to the same **universality class**.

2.2 Landau's theory of phase transitions

2.2.1 Mean Field Theory

The model proposed by Ising is too hard to solve without a method of approximation. Ising himself solved for d=1, later Onsager did it for d=2 and B=0. Nevertheless, for higher dimension, say d=3 the model has not been solved at B=0 or $B\neq 0$. It is possible to solve the problem in arbitrary dimension within the mean field approximation proposed by Weiss in 1907. This approximation is based on the fact that each spin interact with an average of the spins that surround it, discarding fluctuations. Take for example the spin S_i and assume its energy is E_i which can be computed by replacing all other spins by their average value $\langle S_j \rangle$. If the system is immersed in a B-field then E_i is

$$E_i = -JS_i \sum_{j} \langle S_j \rangle - \mu BS_i.$$

Denote M, the average value of S_j , $M = \langle S_j \rangle$ and q the coordination number (the number of nearest neighbours). The magnetization is

$$M = \langle S_i \rangle = \frac{\sum_{S_i \pm 1} e^{-\beta E_i} S_i}{\sum_{S_i \pm 1} e^{-\beta E_i}} = \tanh\left(\frac{qJM + \mu B}{K_B T}\right)$$
(2.21)

$$\tanh^{-1}(M) = \frac{qJ}{K_B T} M + \frac{\mu B}{K_B T}.$$
 (2.22)

This equation must be solved numerically but it is possible to give a qualitative idea of the solutions by looking at the graph. The solution to this equation is the intersection of the line $(qJ/K_BT) + \mu B/K_BT$ with the curve $\tanh^{-1} M$. When B > 0 there are three solutions, two of them negative which are metastable or unstable. The physically correct solution correspond to the M > 0 (i.e., magnetization in the same direction as B). To have an intersection when $B \to 0^+$ the slope qJ/KT must be greater than 1 for $M \neq 0$. In a zero B-field the mean field predicts a non-zero spontaneous magnetization if $T < T_c = qJ/K$ and zero spontaneous magnetization if $T > T_c$. We define the transition temperature $T_c = qJ/K$.

We can solve (2.22) by doing some approximations. As we approach to T_c and the magnetic field B is small the magnetization is weak $M \ll 1$, this allow as to perform a series expansion of \tanh^{-1}

$$\tanh^{-1}(M) = M + \frac{1}{3}M^3 + \mathcal{O}(M^5).$$

With this approximation the magnetization in zero field is

$$M_0 \simeq \sqrt{-3t}$$

close to T_c the spontaneous magnetization behaves as $(T_c - T)^{1/2}$

$$M_0 \sim (T_c - T)^{1/2}$$
.

Likewise we compute the susceptibility in zero field when $T > T_c$ for $B \to 0$. The total magnetization $\mathcal{M} = N\mu M$ and the magnetic susceptibility in zero field is

$$\chi = \frac{\partial \mathcal{M}}{\partial B} \bigg|_{B=0}$$

$$\chi \approx (T - T_c)^{-1}$$
.

Needless to say the predictions of the mean field approximation are catastrophic when compared with the exact results in d = 1,2 and with the numerical calculations in d = 3. For d = 1 it predicts a phase transition even when it was proven that there was none (recall the Peierls's argument). For d = 2, one arrives to a critical temperature higher than the one computed by Onsager. On one case one arrives at

$$k_B T_c = 4J$$
 $(q = 4)$

whereas Onsager's solution is

$$k_B T_c = 2.27 J.$$

Later we will see that, within this framework, the critical exponent improves as the dimension grows and it becomes exact up from a certain value d_c known as *upper critical dimension*, which in the case of the Ising model is $d_c > 4$.

Critical Exponent	MF	d=2
α	discont.	$\ln T - T_c $
β	0.5	0.125
γ	1	1.75
δ	3	15
ν	1/2	1

Table 2.2: Comparison of the critical exponent predicted by the mean field (MF) theory and the exact result from Onsager.

Comparing the critical exponents derived by Lars Onsager for the two-dimensional Ising model to those predicted by the mean field theory provides insight into the differences in behavior and accuracy between exact solutions and approximations.

2.2.2 The Ginzburg-Landau criterion

The mean field approximation just studied is not accurate for certain dimensions since it neglects the effects of fluctuations. In what follows we will not only see how these effects depend on dimension but also we will find a criterion which will be help us to discern whether the result are reliable or not. The Ginzburg-Landau Hamiltonaian has as its main difference with the Ising model that the former is described by variables φ_i defined on the site i of a lattice with the property of being a continuous variable.

In order to formulate a Hamiltonian to describe the second order transition we have to ask it to fulfill some requirements as we did in the Ising model. First, it must be invariant under $\varphi \to -\varphi$ (i.e., $H[\varphi] = H[-\varphi]$) in the absence of external field. Second, by analogy we need the Hamiltonian to depend on two coefficients and be a polynomial function.

$$H[\varphi] = \frac{1}{2!} r_0 \varphi^2 + \frac{1}{4!} u_0 \varphi^4 \tag{2.23}$$

with r_0 , u_0 functions of the temperature and $u_0 > 0$ in order for the partition function to converge.

The Hamiltonian above do not display any interaction term since it was derived as the one site case. When we have N sites we must include the interactions between the nearest neighbor to make the model reliable. Concretely, if μ is the vector linking the site x_i and the nearest neighbor we describe the interaction between $\varphi(x_i)$ and $\varphi(x_i + \mu)$ through the discretized gradient

$$\partial_{\mu}\varphi(x_i) = \frac{1}{a}(\varphi(x_i + \mu) - \varphi(x_i))$$

$$\sum_{i,\mu} = \frac{1}{a^2} (\varphi(x_i + \mu) - \varphi(x_i)) = \sum_{i} (\nabla \varphi(x_i))^2.$$

In the continuous limit the Ginzburg-Landau Hamiltonian becomes

$$H_{GL} = \int d^d x \left[\frac{1}{2} (\nabla \varphi)^2 + \frac{1}{2} r_0(T) \varphi^2 + \frac{1}{4!} u_0 \varphi^4 \right]. \tag{2.24}$$

The partition function in an external field B(x) is

$$Z[B] = \int \mathcal{D}\varphi(x)e^{-\int d^dx \left[\frac{1}{2}(\nabla\varphi)^2 + \frac{1}{2}r_0(T)\varphi^2 + \frac{1}{4!}u_0\varphi^4 - B\varphi\right]}$$
(2.25)

Landau approximation is based on the assumption that Z[B] is dominated by a single configuration which is the one with the higher probability, that is, the one that minimize the exponent. This conditions satisfy

$$B(x) = \frac{\delta H_{GL}}{\delta \varphi(x)} \Big|_{\varphi = \varphi_0}.$$

As promised we will give a criterion, called Ginzburg criterion, which will help us know if neglecting fluctuations is appropriate or not. To do so, we will compare the average magnetization \mathcal{M} over a volume V against mean-square fluctuation $(\Delta \mathcal{M})^2$

$$\mathcal{M}^2 = \frac{6r_0(T_c - T)V^2}{u_0}$$

The mean-square fluctuation $(\Delta \mathcal{M})^2$ is computed through the integration of the correlation function over the volume V

$$(\Delta \mathcal{M})^2 = \int_{x,y} [\langle \varphi(x)\varphi(y)\rangle - \langle \varphi(x)\rangle \langle \varphi(y)\rangle] = V \int_x G(x)$$

Roughly speaking

$$\int_x G(x) \approx \xi^2 \approx \frac{1}{r_0(T_c - T)}.$$

Then the ratio

$$\frac{(\Delta \mathcal{M})^2}{\mathcal{M}^2} \simeq \frac{u r_0^{\frac{d-4}{2}}}{6} (T_c - T)^{\frac{d-4}{2}}.$$
 (2.26)

This tell us that as we approach to criticality $T \to T_c$ and d > 4, the ratio $\frac{(\Delta \mathcal{M})^2}{\mathcal{M}^2} \ll 1$ and it seems reasonable to apply the Landau approximation for describing the critical behaviour. Since for dimensions above 4 this approximation remains applicable we call it *upper critical dimension* (i.e., dimension from which the mean field is valid). However, when d < 4 the ratio diverges and this approximation is no longer suitable.

2.3 Renormalization Group and Universality

2.3.1 Renormalization Group

In this section, we will discuss one of the most successful tools to study phase transitions. Normally when a system composed by a large number of molecules interacting weakly one another its study can be performed by applying perturbative methods. The weakly interaction can be characterized by some "interaction length" which will be bigger than the correlation length of the system itself. An example of this last is a diluted gas described, in a first approximation, by the ideal gas equation when performing the virial expansion, for instance. The hard things come when the number of degrees of freedom interacting diverges. This is the case of a critical phenomena. In this case, near the critical point the number of degree of freedom interacting is $\sim \xi^d$, and since second order transitions are characterized for being long range interaction, the correlation length diverges $\xi \to \infty$. In this scenario, perturbative methods fails to give an accurate result, since they are build to solve problems where a few degrees of freedoms interact. To save the day, first Kadanoff [14] and later and more importantly Kenneth Wilson [15] developed the ideas of what it is nowadays known as the renormalization group (RG). The main idea behind this framework is the sensitivity of the system to a length transformation, or change of scale, is significantly reduced. Accordingly, not too far from the critical point the transformed system resemble to the original one after the change of scale, say from the $a \rightarrow a' = sa$ where a is the lattice spacing and s > 1 a constant.

Wilson's renormalization group method relies on reduce systematically the num-

ber of degrees of freedom interacting by integrating over short wavelength fluctuation. To put an idea into concrete terms, think about a spin system on a lattice whose spacing is a. The first step is to integrate over fluctuation of wavelength $a < \lambda < sa$, here the fluctuations of wavelength greater than sa remains untouched and therefore the transformed system and the original behaves in the same way at long distances. This kind of transformation is called *renormalization group transformation* (RGT). In this new transformed system, the natural unit of length will be sa but the lattice spacing is not the only parameter of the system that underwent a change; the correlation length of the new system is ξ/s , hence the number of degree of freedom effectively interacting reduced from $\xi^d \to (\xi/s)^d$. By iterating over the renormalization group transformation we can make the correlation length to be of the order of the "interacting length" and hopefully solve the problem with perturbative method.

Blocks of spins

One way of integrating over short-wavelength fluctuation is to form blocks of spins. Let work with the Ising model in dimension d=2 on a square lattice whose spacing is a. The idea is to form block of spins and work with the interaction among them rather than look at each spin individually. For correctness, let make a block of spin four individual spin. Originally each spin has value $S_i = +1$, -1 then the value block S'_{α} will depend on its constituents spins.

$$S'_{\alpha} = f(S_i).$$

Of course this value should represent the configuration of the block, the intuitive choice is to take the average of the spins. This new configuration has the double size compared to the first one, we need to revert to the initial lattice in order to compare both systems on the same lattice.

The probability of observing a given configuration [S'] of blocks is related to the former Hamiltonian via

$$e^{-H'[S'_{\alpha}]} = \sum_{[S_i]} \prod_{\alpha} \delta(S'_{\alpha} - f(S_i)) e^{-H[S_i]}$$
(2.27)

this delta function yield to

$$Z = \sum_{[S_i]} e^{-H[S_i]} = \sum_{[S'_{\alpha}]} e^{H'[S'_{\alpha}]} = Z'$$
(2.28)

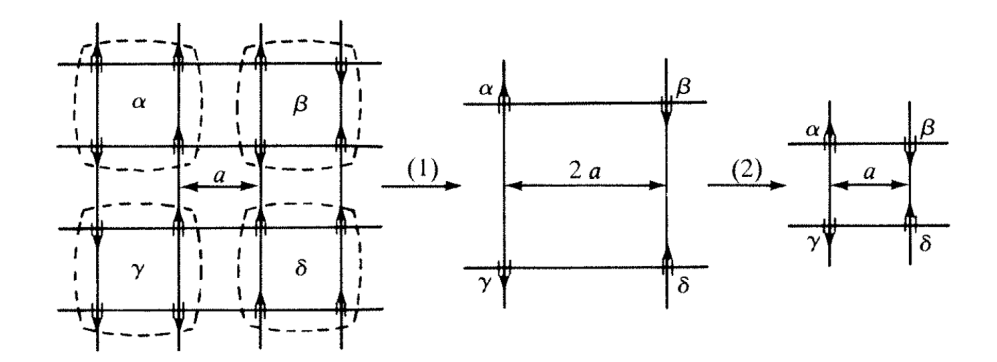


Figure 2.3: Formation of blocks of spins and rescaling [9].

The partition function are exactly the same and so the Helmholtz free energy i.e., the same physics is described. At this point we must note that the new Hamiltonian $H'[S'_{\alpha}]$ should have the Ising form but it may come with new terms

$$-H' = K_1 \sum_{\langle i,j \rangle} S_i S_j + K_2 \sum_{\langle i,j \rangle} S_i S_j + K_3 \sum_{\langle ijkl \rangle} S_i S_j S_k S_l$$
 (2.29)

where the second terms refers to the next-nearest neighbours and the third to "plaquettes". The coefficient K_i are called coupling constant and together they define a parameter space μ .

A RGT is a non-linear map on the coupling constant space

$$\mu' = R(\mu). \tag{2.30}$$

The RG method consist in apply RGT many times, under this consideration the parameter space have the form

$$\mu^{(n)} = R^{(n)}\mu = R \circ R \circ R \cdots \circ R\mu. \tag{2.31}$$

Before we continue, we have to introduce some assumptions

- The coupling constant K_i are analytic function of the temperature and the K'_i are smooth functions of the K_i .
- The RGT do not introduce any long-range interaction
- After many iteration, eventually, $\mu^{(n)} = \mu^{(n-1)}$. This mean there exist a *fixed point*.

It is possible to divide the function $f(S_i)$ into two categories, the linear transformation and the non-linear transformation. Now let see an example of linear transformation defined as:

 $S_{\alpha}' = \frac{\lambda(s)}{s^d} \sum_{i \in \alpha} S_i$

 $\lambda(s)$ is a function of the dilatation factor that will be explained later. Note that in this case the spin block no longer have the value +1, -1. The RGT now requires to work with continuous variable $\varphi \in \mathbb{R}$, we can take the Ginzburg-Landau Hamiltonian.

$$H = \int d^d x \left\{ \frac{c_0}{2} (\nabla \varphi)^2 + \frac{r_0}{2} \varphi^2 + \frac{u_0}{4!} \varphi^4 + \frac{v_6}{6!} \varphi^6 + \frac{v}{2} \varphi^2 (\nabla \varphi)^2 + \cdots \right\}$$

With this Hamiltonian the parameter space is defined by $\mu = \{c, r_0, u_o, u_6, v, \cdots\}$

$$\left\langle S'_{\alpha}S'_{\beta} \right\rangle = \sum_{S'_{\beta}} \frac{e^{-H'[S']}S'_{\alpha}S'_{\beta}}{Z'}$$

$$= \frac{1}{Z'} \sum S'_{\gamma} \sum_{S_{i}} e^{-H[S]} \prod_{\gamma} \delta(S'_{\gamma} - \frac{\lambda(s)}{s^{d}} \sum_{i \in \alpha}) S'_{\alpha}S'_{\beta}$$

$$= \frac{1}{Z} \sum_{S_{i}} e^{-H[S]} \frac{\lambda^{2}(s)}{(s^{d})^{2}} \sum_{i \in \alpha} S_{i} \sum_{j \in \beta} S_{j} = \frac{\lambda^{2}(s)}{(s^{d})^{2}} \sum_{i \in \alpha} \sum_{j \in \beta} \left\langle S_{i}S_{j} \right\rangle$$

$$\approx \lambda^{2}(s) \left\langle S_{i}S_{j} \right\rangle$$

in the last step we assume the distance between two block $r_{\alpha\beta}\gg sa$. In general we can deduce

$$\langle S'_{\alpha_1} \cdots S'_{\alpha_n} \rangle = \lambda^n(s) \langle S_{i_1} \cdots S_{i_n} \rangle.$$

For distances $r \gg a$ we can relate the two correlation functions

$$G\left(\frac{r}{s}, \mu'\right) \simeq \lambda^2(s)G(r, \mu)$$
 (2.32)

Then under a RGT the correlation functions scales as (2.32). Moreover, this last equation yields to a form for $\lambda(s)$. For instance, the transformation of blocks $(s_1s_2)^d$ has same result as the product of two RGT, that is, the formation of blocks of s_1^d and s_2^d . This mean that $\lambda(s)$ satisfies

$$\lambda(s_1, s_2) = \lambda(s_1)\lambda(s_2)$$

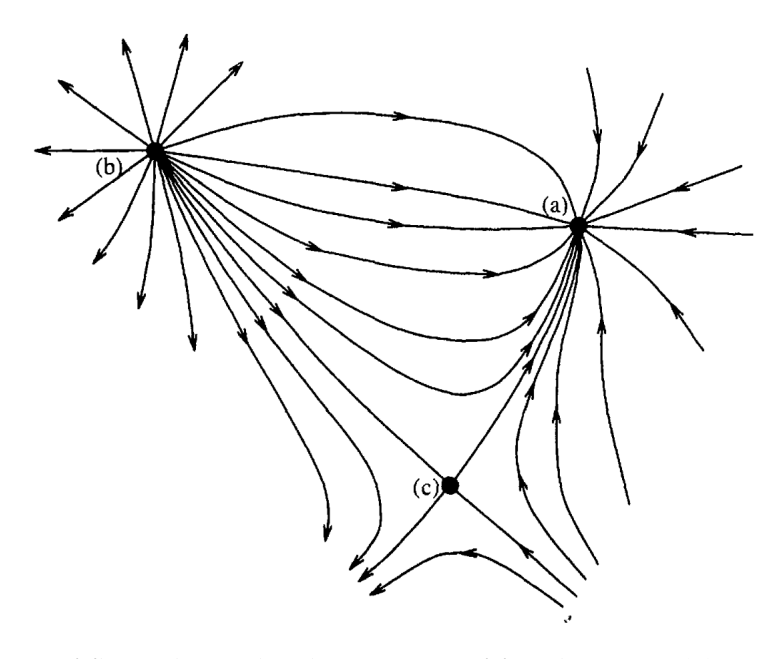


Figure 2.4: Lines of flow about the three types of fixed points: (a) attractive, (b) repulsive and (c) mixed [16].

From here we see that the dilatation factor has the form

$$\lambda(s) = s^{d_{\varphi}} \tag{2.33}$$

where d_{φ} is the anomalous dimension of the field. The dimension of the field will play a crucial role when doing a dimensional analysis of the β -functions. The computation of these functions will be one of the key points of this projects since they describes the running of the coupling. We will see more of these functions in detail in Chapter 3.

2.3.2 Critical Surface and Fixed Points

We just learnt that the RG requires to integrate over the microscopic fluctuations which is taken into account by changing the system parameter. That is, we iterate over and over using the operator \mathcal{R} of the RG. This process generates a system of trajectories called the renormalization flow. This trajectories could be cycles, fixed points or strange attractor but for us the crucial ingredient is the existence of a fixed point where close to it we restrict our attention to a finite number of parameters. Likewise, fixed points can be classified in three different categories, attractive, repulsive or mixed. An attractive fixed point is the one that all points in every direction (in the neighbourhood) converges to it.

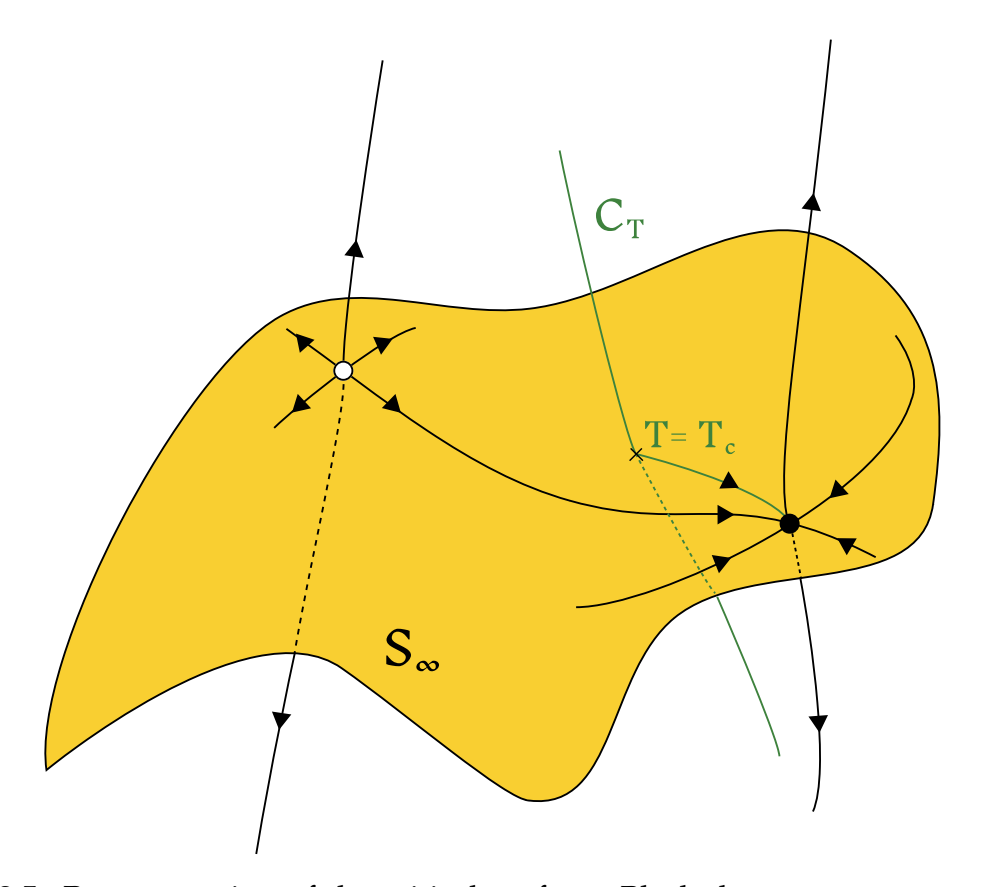


Figure 2.5: Representation of the critical surface. Black dot represent an attractive (stable) fixed point while the white represent an unstable fixed point.

In this phase space there is a special manifold of interest called the critical surface or critical manifold. The critical surface S_{∞} is the geometric place where the coupling constant are evaluated at the critical temperature T_c . Recall that at criticality $\xi \to \infty$, whence by applying a RGT to the parameter space $K_c \to \mathbf{K'}$ where ξ' also diverges. This means that the transformed parameter remains in criticality, i.e., $\mathbf{K'} \in S_{\infty}$.

Unlike the points in the critical surface, those outside it will go further and further away the critical surface. This is because the initial point has correlation length finite and as one goes from $Q \to Q'$ the transformed point will have correlation length $\xi' = \xi/s$.

Recall the RGT \mathcal{R} acts as

$$\mathcal{R}(K^n) = K^{n+1} \tag{2.34}$$

then when it acts on a fixed point K^*

$$\mathcal{R}(K^*) = K^*. \tag{2.35}$$

By studying the vicinity of the fixed point we can compute the desired critical exponent by linearizing the RG equations near that point.

Let K_{α} be a point in the parameter space near the fixed point described by K_{α}^* . Linearizing close to the fixed point yield to

$$K_{\alpha} = K_{\alpha}^* + \delta K_{\alpha}. \tag{2.36}$$

As usual, the transformed point under an RGT is $K'_{\alpha} = \mathcal{R}K_{\alpha}$.

There is a relation between $\delta K'_{\alpha}$ and K_{α} which is approximately linear

$$\delta K_{\alpha}' = \sum_{\beta} T_{\alpha\beta}(s) \delta K_{\beta} \tag{2.37}$$

where

$$T_{\alpha\beta}(s) = \frac{\partial \mathcal{R}_{\alpha}}{\partial K_{\beta}} \bigg|_{\mathbf{K}^*} \tag{2.38}$$

is the stability matrix which depend on the parameter s. This matrix is not diagonal but we will suppose it is diagonalizable and its eigenvector are denoted as $e^{(i)}$ and its eigenvalues are $\lambda_i = s^{y_i}$ therefore it will satisfy

$$\sum_{\beta} T_{\alpha\beta}(s) e_{\beta}^{(i)} = s^{y_i} e_{\alpha}^{(i)}$$
(2.39)

We can express any point of the parameter space using the basis $\{e^i\}$.

$$\delta K_{\beta} = \sum_{i} t_{i} e_{\beta}^{i} \tag{2.40}$$

the t_i are called the *scaling parameter*. In the same way we can write

$$\delta K'_{\beta} = \sum_{i} t_{i} s^{y_{i}} e_{\beta}^{(i)}$$

From here it is seen that the RGT multiplies the scaling field by s^{y_i} . After n—iterations the $t_i^{(n)}$ scaling field will be $t_i s^{y_i n}$.

- $y_i > 0$: the scaling field increase on each iteration of the RGT $\Rightarrow t_i$ is called a *relevant parameter*
- $y_i < 0$: the scaling field decrease on each iteration of the RGT $\Rightarrow t_i$ is called a *irrelevant parameter*
- $y_i = 0$: the scaling field remains on each iteration of the RGT $\Rightarrow t_i$ is called a *marginal*

If we have *M* relevant direction, then, we will have to fine-tune *M* parameters to be on the critical surface. For a second order phase transition the critical surface is reached by varying one parameter, for example the temperature, whence there is only one relevant direction⁴.

We can use the language of magnetic system for the study of the correlation function and compute the critical exponent, even though the discussion is general.

Consider a fixed point with scaling field $t_1, t_2, t_3, \dots, t_i, \dots$ where $y_1 > 0 > y_2 > y_3 > \dots > y_i > \dots$. When applying the RGT the representative point approaches to the fixed point, and after a long time will eventually diverge along e_1 (the relevant axis). The aim of all this is to compute the critical exponent which will be related to the eigenvalues of the stability matrix, also the correlation function is a function of the scaling fields and for the sake of simplicity we assume the field t_1 must vanish linearly on the critical surface.

$$t_1 \sim t = \frac{T - T_c}{T_c} \tag{2.41}$$

We already know the transformation law for the correlation function is

$$G(r/s, \mu') \simeq \lambda^2(s)G(r, \mu) \Rightarrow G(r; t_1, t_2, \dots) = s^{-2d_{\varphi}}G(r/s; t'_1, t'_2, \dots)$$
 (2.42)

Starting on the critical surface $t_1 = 0$ and choosing s = r. This last choice correspond to integrate out all fluctuations between a and r

$$G(r; t_2, \cdots) = r^{-2d_{\varphi}}G(1; 0, r^{y_2}t_2, \cdots)$$
 (2.43)

⁴There is one more parameter which is relevant, this is the magnetic field but in what follow we will work in the case B = 0

If $r^{y_2}t_2 \ll 1$, the equation shows that at the critical point the correlation functions behaves as power law and the critical exponent η is linked to d_{φ} by matching with equation (2.15).

$$d_{\varphi} = \frac{D-2+\eta}{2} \tag{2.44}$$

Now, let analyze the case where we do not departure from the critical surface $(t_1 \neq 0)$. Iterating enough times the scaling field will be

$$s^{y_1}t_1 \sim \pm 1$$

Denote ξ the quantity $|t_1|^{-1/y_1} \sim |t|^{-1/y_1}$

$$G(r) = s^{-2d_{\varphi}}G(r/s; \pm (\frac{s}{\xi})^{y_1}, s^{y_2}t_2, \cdots)$$
 (2.45)

Because of its definition $s\sim \xi$, and writing $s=\xi$ correspond to integrate over fluctuations between a and ξ .

$$G(r) = \xi^{-2d_{\varphi}} G(\frac{r}{\xi}, \pm 1, \xi^{y_2} t_2)$$
 (2.46)

with $\xi^{y_2}t_2 \ll 1$ we arrive to

$$G(r) = r^{-2d_{\varphi}} f_{\pm}(r/\xi)$$
 (2.47)

in the view of the equation (2.14), we identify the critical exponent ν with the inverse of the largest eigenvalue of the RG flow equation.

Exploring how the correlation function change under the RG transformation allow us to compute critical exponent and derive scaling laws presented in (2.17). For instance, the next step could be to study the correlation function with external magnetic field and reach a formula for the critical exponent δ and β . Last but not least, there is another critical exponent that we want to compute and it is independent of the ones defined above: this is ω and it is the second largest eigenvalue of the stability matrix.

2.3.3 Universality

There is no doubt, that one of the greatest achievement of the RG, is to give an accurate proof of universality [17, 18]. The concept of universality refers to the observation of system which differ completely microscopical, share the same macroscopic behavior whence approach to the criticality. As it was shown, the scaling behavior described by power laws of the form $\propto t^{\alpha}$ provides a set of exponents which together defines an

universality class. This means that physical systems belonging to an universality class approaching to the critical point share the same set of critical exponents while as they are far from this regime they behave radically different. The typical example of two system belonging to a same universality class are fluid (the water-steam transition) and magnets (the ferromagnetic-paramagnetic transition). These two systems are part of the Ising universality⁵ class which is the particular class of the O(N)-model when N=1.

Now let us see an explanation for the existence of universality through the RG. As we mentioned the basic ingredients of the RG is a coarse-graining followed by a rescale (just as we did with the block spins). This procedures yield to a new renormalized Hamiltonian. As we continue with the iterations, this procedure leads to a flow on the space of Hamiltonians where we look for fixed points. Since the fixed points is a property of the transformation itself all details of the system have been eliminated. Therefore, those systems that flow to the same fixed point belong to the same universality class and they will show the same macroscopic scaling behavior.

2.4 Universality Classes with O(N) Symmetry

When we refer to the O(N) symmetry we first need to understand what kind of theory are we facing. The O refers to the orthogonal group, that is, the group of real orthogonal matrices such that

$$\mathbf{O}^{\mathbf{T}}\mathbf{O} = 1$$

from here we see that $\det \mathbf{O} = \pm 1$ since

$$\det \mathbf{O}^T\mathbf{O} = \det \mathbf{O}^T \det \mathbf{O} = (\det \mathbf{O})^2 = 1$$

The group SO(N) is the subgroup of the O(N) consisting of the matrices O with $\det O = 1$. The special orthogonal group is also known as the rotation group and together with the orthogonal group are Lie group separately. The set of orthogonal matrices with determinant -1 do not form a group since the product of two its elements has determinant 1.

$$\det \mathbf{O_1} = \det \mathbf{O_2} = -1$$
$$\det(\mathbf{O_1O_2}) = 1$$

⁵Here we need to set the dimension d = 3

The symmetry that arise from the set of matrices with $\det \mathbf{O} = -1$ is reflection. In dimension two it is possible to write every rotation as the product of two reflections. The N refers to the order parameter or to the number of component field, that is why the O(N)-model is also known as the N-vector model.

In the following we give a brief description of each class of universality of interest, that is the XY universality N=2, the Heisenberg universality class N=3 and two special cases regarding random walks, that is the self-avoiding random walk N=0 and the loop-erased random walk N=-2.

2.4.1 N = 2 XY

Despite the N=1 Ising model where the spin only take two possible directions, up or down, the N=2 case is much more interesting since it display a different phase transition where spins have greater flexibility of orientation. In this model, each spin is capable of pointing in any direction within some given plane, meaning that the spin \mathbf{s} is a two component vector. The unit-length vector $\mathbf{s}_j=(\cos\theta_j,\sin\theta_j)$ and the Hamiltonian which is invariant under rotations in this plane (it has O(2) symmetry) is given by

$$H = -J \sum_{\langle i,j \rangle} \mathbf{S_i} \cdot \mathbf{S_j} = -J \sum_{\langle i,j \rangle} cos(\theta_i - \theta_j).$$
 (2.48)

When d = 1 and a free boundary condition is impose (in external zero field), the model is solvable and its exact solution of the partition function is

$$Z = (2\pi)^m (I_0(\beta J))^{m-1}$$
(2.49)

where m is the number of total spins and I_0 is the modified Bessel function of the first kind. From here one is able to compute any thermodynamic quantity. As in the Ising model, there is no divergence in the specific heat in this dimension and no other physical quantity diverges, therefore there is no phase transition when d = 1.

The curious case is the d=2 since it delimit the frontier between having or not a phase transition. Bellow d=2 there is no phase transition and at d=2 we define the the Kosterlitz-Thouless (KT) universality class [19]. This case is very special due to the existence of vortex and antivortex has a great influence in how the system undergoes the phase transition.

Another interesting case of study is the three-dimensional XY universality class

which describe the superfluid transition in ${}^4He^6$, unlike the liquid-vapor where the transition occur in a point (the critical point), in this case the transition takes place along the λ -line of its phase diagram [20].

2.4.2 N=3 Heisenberg

The three-dimension Heisenberg universality class is characterized by a three component order parameter. This is useful to describe the behavior of isotropic magnets such as Ni and EuO. It is important to bear in mind that the isotropic Heisenberg Hamiltonian is a simplified model for magnets since it may neglect other kind of interaction present in a real material [21, 22], for instance, interaction with cubic anisotropy.

Theoretically, estimates of the critical exponent are obtained by different approaches such as Monte Carlo simulation and High Temperature expansion⁷.

2.4.3 N = 0 SAW

The $N \to 0$ limit is an interesting case of application of the O(N) model to real life phenomena in nature. The long polymer chain can be described as critical phenomena. This was discovered by de Gennes who in 1972 [23], inspired by the recent breakthrough of Kenneth Wilson on his renormalization group method, was able to make a link between the O(N) model and the polymer physics. This accomplishment allowed to gain knowledge about the universal properties of long polymer chains through the connection with the O(N) model. Once this was known, other authors explained the SAW problem without appeal to the n-vector model, for example, by treating the generating function for SAW as a grand partition function[24]. This kind of approach lead to a single scaling field which has as a result that all critical exponent are related to a single one. This result was also shown by Flory (1969) where there is an extra equation for the scaling law which relates ν and η .

On his paper, De Gennes defines the partition function needed to determine the average end to end separation R of a self-avoiding polymer. It is the mean square length the quantity that behaves as a scaling law in the criticality.

$$\left\langle R_N^2 \right\rangle \approx N^{2\nu}$$

⁶Do not confuse with ³He which has a superfluid transition but different treatment since they are fermions.

⁷We show the results of these methods in the following section.

where *N* is the number of steps the SAW performed. It is possible to compute this relation by making a random walk in a lattice where the self-intersection are not allowed, this is the excluded volume problem.

2.4.4 N = -2 LERW

The LERW (loop-erased random walk) [25, 26] are those obtained from a random walk erasing the self-intersect. The SAW as well as the LERW have various application in mathematics and statistical physics. In contrast to the SAW described by the limit $N \to 0$ of the O(N) symmetry, the LEWR has no solid field theoretical description. One candidate is the O(N)-model at N=-2, whose links to this model was in d=2 because of conformal field theory. Similar to the SAW the end to end distance R scales with the intrinsic length ℓ as $R \sim \ell^{1/d_f}$ where d_f is the fractal dimension. On both cases, their fractal dimension differs despite both being random walks.

2.4.5 Large-N

The large-*N* limit represents a powerful analytical approach in the study of quantum field theories and statistical physics, particularly due to its exact resolution. This allows us to test whether our scheme for solving this model aligns with the exact result. The large *N*-limit actually relates to the spherical model [27] which was introduces by Berlin and Kac in 1952. Their model has a variant respect to the Ising model, the spins are subject to the condition

$$\sum_{j=1}^{N} \sigma_j^2 = N.$$

It was found by Stanley the equivalence between the spherical model and a spin model with O(N) symmetry in the limit $N \to \infty$. Concretely, Stanley proved that the model with Hamiltonian

$$H = -J \sum_{\langle ij \rangle} \vec{\sigma}_i \cdot \vec{\sigma}_j$$

where each spin is an *N*-dimensional vector which satisfy $|\vec{\sigma_i}|^2 = N$ is equivalent to the spherical model.

2.4.6 State of the Art data for Critical Exponents

In this section, we collect the most updated values for critical exponent computed through different numerical method. The most accurate result have been obtained from the high temperature expansion (HT) [28], Monte Carlo simulation (MC) [29], and perturbative field theory such as the ϵ -expansion or the loop expansion at certain order. In recent years, the implementation of the Conformal Bootstrap (CB) [30, 31, 32, 33, 34, 35, 36], has been known to give the most precise values and in this project we will compare and see if our results are in agreement with the one predicted by this method.

Method	ν	ω	η
LPA, improved	0.5925	0.66	0
$\mathcal{O}(\partial^2)$,raw	0.5878	1.0489	0.0388
$\mathcal{O}(\partial^2)$,improved	0.5879(13)	1.00(19)	0.0326(47)
$\mathcal{O}(\partial^4)$,raw	0.5875	0.901	0.0292
$\mathcal{O}(\partial^4)$,improved	0.5876(2)	0.901(24)	0.0312(9)
MC [37, 29]	0.58759700(40)	0.899(14)	0.0310434(30)
six-loop PT	0.5882(11)	0.812(16)	0.0284(25)
ε^6 , ε -exp	0.5874(3)	0.841(13)	0.0310(7)
CB [38]	0.5876(12)		0.0282(4)

Table 2.3: Critical exponent for the O(0) symmetric scalar model in d=3. DE at LPA, $\mathcal{O}(\partial^2)$ and $\mathcal{O}(\partial^4)$ [39], Monte-Carlo simulation, six-loop perturbation theory at fixed d=3 [40], $d=4-\epsilon$ at ϵ^6 [41], the conformal bootstrap and the large-N expansion [42, 43, 44]

Method	ν	ω	η
LPA, improved	0.64956	0.654	0
$\mathcal{O}(\partial^2)$,raw	0.62752(245)	0.8707(410)	0.04551(921)
$\mathcal{O}(\partial^2)$, improved	0.6308(27)	0.870(55)	0.0387(55)
$\mathcal{O}(\partial^4)$, raw	0.63057(60)	0.8321(24)	0.03357(272)
$\mathcal{O}(\partial^4)$, improved	0.62989(25)	0.832(14)	0.0362(12)
MC	0.62998(5)	0.832(6)	0.036284(40)
six-loop PT	0.6304(13)	0.799(11)	0.0335(25)
ε^6 , ε -exp	0.6292(5)	0.820(7)	0.0362(6)
СВ	0.629971(4)	0.82951(61)	0.0362978(20)

Table 2.4: Critical exponent for the O(1) symmetric scalar model in d=3. DE at LPA, $\mathcal{O}(\partial^2)$, $\mathcal{O}(\partial^4)$ improved and raw with exponential cut-off from [45], Monte-Carlo simulation [46, 47], six-loop perturbation theory at fixed d=3 [40], $d=4-\epsilon$ expansion at ϵ^6 [41], the conformal bootstrap [33, 48].

Method	ν	ω	η
LPA, improved	0.7090	0.672	0
$\mathcal{O}(\partial^2)$,raw	0.6663	0.7972	0.0480
$\mathcal{O}(\partial^2)$,improved	0.6725(52)	0.789(34)	0.0410(59)
$\mathcal{O}(\partial^4)$,raw	0.6732	0.793	0.0350
$\mathcal{O}(\partial^4)$,improved	0.6716(6)	0.791(8)	0.0380(13)
MC [49]	0.67169(7)	0.789(4)	0.03810(8)
six-loop PT	0.6703(15)	0.789(11)	0.0354(25)
ε^6 , ε -exp	0.6690(10)	0.804(3)	0.0380(6)
CB [50]	0.671754(99)	0.794(8)	0.03818(4)

Table 2.5: Critical exponent for the O(2) symmetric scalar model in d=3. DE at LPA, $\mathcal{O}(\partial^2)$ and $\mathcal{O}(\partial^4)$ (raw computed with exponential regulator) [39], Monte-Carlo simulation, six-loop perturbation theory at fixed d=3[40], $d=4-\epsilon$ at ϵ^6 [41], the conformal bootstrap.

Method	ν	ω	η
LPA, improved	0.7620	0.702	0
$\mathcal{O}(\partial^2)$,raw	0.7039	0.7516	0.0476
$\mathcal{O}(\partial^2)$,improved	0.7125(71)	0.754(34)	0.0408
$\mathcal{O}(\partial^4)$,raw	0.7136	0.773	0.0347
$\mathcal{O}(\partial^4)$,improved	0.7114(9)	0.769(11)	0.0376(13)
MC [51, 52]	0.7116(10)	0.773	0.0378(3)
MC (2020)[53]	0.71164(10)	0.759(2)	0.03784(5)
six-loop PT	0.7073(35)	0.782(13)	0.0355(25)
ε^6 , ε -exp	0.7059(20)	0.795(7)	0.0378(5)
CB (2016) [33, 34]	0.7120(23)	0.791(22)	0.0385(13)
CB (2021) [54]	0.71168(41)	0.7668(100)	

Table 2.6: Critical exponent for the O(3) symmetric scalar model in d=3. DE at LPA, $\mathcal{O}(\partial^2)$ and $\mathcal{O}(\partial^4)$ (raw computed with exponential regulator) [39], Monte-Carlo simulation, six-loop perturbation theory at fixed d=3 [40], $d=4-\epsilon$ at ϵ^6 [41], the conformal bootstrap.

Method	ν	ω	η
LPA, improved	0.805	0.737	0
$\mathcal{O}(\partial^2)$,raw	0.7396	0.7274	0.0455
$\mathcal{O}(\partial^2)$,improved	0.749(8)	0.731(34)	0.0389(56)
$\mathcal{O}(\partial^4)$,raw	0.7500	0.765	0.0332
$\mathcal{O}(\partial^4)$,improved	0.7478(9)	0.761(12)	0.0360(12)
MC [52, 55]	0.7477(8)	0.765	0.0360(4)
six-loop PT	0.741(6)	0.774(20)	0.0350(45)
ε^6 , ε -exp	0.7397(35)	0.794(9)	0.0366(4)
CB [34, 32]	0.7472(87)	0.817(30)	0.0378(32)

Table 2.7: Critical exponent for the O(4) symmetric scalar model in d=3. DE at LPA, $\mathcal{O}(\partial^2)$ and $\mathcal{O}(\partial^4)$ (raw computed with exponential regulator) [39], Monte-Carlo simulation, six-loop perturbation theory at fixed d=3 [40], $d=4-\epsilon$ at ϵ^6 [41], the conformal bootstrap and the large-N expansion [42, 43, 44].

Method	ν	ω	η
LPA, improved	0.839	0.770	0
$\mathcal{O}(\partial^2)$,raw	0.7722	0.7199	0.0425
$\mathcal{O}(\partial^2)$	0.782(8)	0.724(34)	0.0364(52)
$\mathcal{O}(\partial^4)$	0.7797(9)	0.760(18)	0.0338(11)
six-loop PT	0.766		0.034
large-N	0.71(7)	0.51(6)	0.031(15)

Table 2.8: Critical exponent ν , ω and η of the O(5) symmetric scalar model in d=3. DE results are final estimate from [45], six-loop [56] and the large-N expansion [42, 43, 44].

Method	ν	ω	η
LPA, improved	0.919	0.874	0
∂^2 ,raw	0.8772	0.7853	0.0279
$\mathcal{O}(\partial^2)$	0.877(11)	0.788(26)	0.0240(34)
$\mathcal{O}(\partial^4)$	0.8776(10)	0.807(7)	0.0231(6)
six-loop PT	0.859		0.024
large-N	0.87(2)	0.77(1)	0.023(2)

Table 2.9: Critical exponent ν , ω and η of the O(10) symmetric scalar model in d=3. DE results are final estimate from [45] (raw computed with exponential regulator), six-loop [56] and the large-N expansion [42, 43, 44].

Method	ν	ω	η
LPA, improved	0.9610	0.938	0
∂^2 ,raw	0.9414	0.8867	0.0151
$\mathcal{O}(\partial^2)$	0.9414(49)	0.887(14)	0.0130(19)
$\mathcal{O}(\partial^4)$	0.9409(6)	0.887(2)	0.0129(3)
six-loop PT	0.930		0.014
large-N	0.941(5)	0.888(3)	0.0128(2)
СВ	0.9416(87)		0.0128(16)

Table 2.10: Critical exponent ν , ω and η of the O(20) symmetric scalar model in d=3. DE results are final estimate from [45], conformal bootstrap [32], six-loop [56] and the large-N expansion [42, 43, 44].

Method	ν	ω	η
LPA, improved	0.9925	0.9882	0
$\mathcal{O}(\partial^2)$,raw	0.98908	0.9781	0.00310
$\mathcal{O}(\partial^2)$	0.9892(11)	0.9782(26)	0.00257(37)
$\mathcal{O}(\partial^4)$	0.9888(2)	0.9770(8)	0.00268(4)
large-N	0.9890(2)	0.9782(2)	0.002681(1)

Table 2.11: Critical exponent ν , ω and η of the O(100) symmetric scalar model in d=3. DE results are final estimate from [45] and the large-N expansion [42, 43, 44].

Method	ν	ω	η
LPA, improved	1/2	0.700	0
$\mathcal{O}(\partial^2)$	0.5000(12)	0.84(19)	0.0000(47)
$\mathcal{O}(\partial^4)$	0.5001(1)	0.838(24)	0.0004(9)
six-loop PT		0.83(1)	
exact	1/2		0

Table 2.12: Critical exponent ν , ω and η of the O(-2) symmetric scalar model in d=3. DE results are final estimate from [45] and perturbative results can be found in [25, 26].

Chapter 3

Functional Renormalization Groups

This chapter aims to introduce three main topics. First, to complete the introduction of the theoretical concepts necessary to fully address the theory; in this regard, we introduce and explain what the effective action is - i.e. the functional that describe the overall statistical and quantum physics of the system. Second, we provide an introduction to the frameworks of perturbative and non-perturbative renormalization group, which will serve as a comparison to our results. Finally, we present our novel scheme *Functional Dimensional Regularization*, its derivation and physical foundations. We conclude with a pedagogical introduction, for all approaches we will give the beta functionals for the potential V and wave function Z; deriving and comparing them in the simplest case: the Ising model, showing how to find the fixed point and how to compute the critical exponents.

3.1 Effective Action

Recall from section 2.2.2 the Ginzburg-Landau formulation of statistical mechanics where the partition function is written in terms of a functional integral in the continuum limit (2.25). We saw that Landau's theory taught us that the theory of phase transition is an Euclidean statistical field theory, now to adapt the notation to the field theory context we will make a slight change of notation. We can extend and generalize this formalism by taking the Ginzburg-Landau partition function (2.25), change the external field for a general source $B \rightarrow J$ and instead of using the Ginzburg-Landau Hamiltionian H_{GL} write a general action S:

$$Z[J] = \int \mathcal{D}\phi \, e^{-S[\phi] + \int d^d x \, \phi J}$$
 (3.1)

The functional Z[J] is the generating functional of the correlation function and W (Helmholtz free energy) relates to the partition function as:

$$W[J] = \log Z[J] \tag{3.2}$$

W is also known as the generating functional of the connected correlation functions [9, 16]. The expectation value of the field is computed as

$$\varphi(x) = \langle \phi(x) \rangle = \frac{\int \mathcal{D}\phi \, \phi(x) e^{-S[\phi]}}{\int \mathcal{D}\phi \, e^{-S[\phi]}} = \frac{\delta W}{\delta J(x)} \Big|_{J=0}$$
(3.3)

and the connected two-point function or propagator is derived as

$$G_c(x,y) = \langle \phi(x)\phi(y) \rangle - \langle \phi(x) \rangle \langle \phi(y) \rangle = \frac{\delta^2 W}{\delta J(x)\delta J(y)} \bigg|_{I=0}$$
 (3.4)

Note that both W and Z are functional of J(x) and that the n-functional derivatives of W with respect to the sources give as a result the connected n-point function $G_c(x_1, \dots, x_n)$

$$G_c(x_1, \dots, x_n) = \frac{\delta^n W}{\delta J(x_1) \cdots \delta J(x_n)} \bigg|_{I=0}$$
(3.5)

When the source is non zero the expectation value of φ has a dependence on J

$$\varphi_{J}(x) = \langle \phi(x) \rangle_{J} = \frac{\delta W}{\delta J(x)}$$
 (3.6)

We want to work with an action of φ and not of J since the field φ has a physical meaning, it is the mean field of φ and is the right variable to use. To eliminate the dependence on J we use a mathematical trick, the Legendre transform. The Legendre transform of W is the effective action (EA) Γ

$$\Gamma[\varphi] = -W[J] + \int d^d x \phi(x) J(x)$$
 (3.7)

Note that the variation of the effective action with respect to the field is the source

$$\frac{\delta\Gamma}{\delta\varphi(x)} = -\int \frac{\delta W}{\delta I} \frac{\delta J}{\delta\varphi} + \frac{\delta J}{\delta\varphi} \varphi + J(x) = J(x)$$
 (3.8)

Using the background field method we can write the effective action by expanding the classical field around a background field $\chi = \phi - \varphi$ together with equation (3.7) and (3.8)

$$e^{-\Gamma[\varphi]} = \int \mathcal{D}\chi e^{-S[\varphi + \chi] + \int d^d x \frac{\delta \Gamma}{\delta \varphi} \chi}$$
(3.9)

This is an exact integro differential formula for the effective action which will be our starting point for further analysis; in particular the ability to compute Γ opens the way to understanding the entire problem of phase transitions and universality.

In this chapter we will consider an Euclidean action for a first part a single component scalar field in *d* dimension and work with a general potential. Thus the action is of the form

$$S = \int d^d x \left\{ \frac{1}{2} (\partial \phi)^2 + V(\phi) \right\}$$
 (3.10)

From equation (3.9) we can proceed in two ways; either we take the path of perturbation theory or we apply technics of the non-perturbative renormalization group. In the following sections we explore both directions to give an overview of these two traditional approaches.

3.2 Functional Perturbative RG (FPRG)

In this section, we first introduce the loop expansion, whose goal is to illustrate how corrections to the effective action arise. We then briefly explain the processes of regularization and perturbative renormalization, as well as the method for transitioning from a series of functions to a functional. Finally, we conclude with an example taken from the literature, which helps compare the results of this method with those obtained in the present project.

3.2.1 Loop Expansion

We aim to find a perturbative formula for the effective action in a loop expansion by the saddle point method [3, 57]. We take as starting point the formula (3.9) and we introduce a parameter \hbar and perform a shift $\chi \to \sqrt{\hbar} \chi$. We will expand the action in

 $^{^{1}\}text{Note}$ that the fluctuation field has vanishing expectation value $\left\langle \chi\right\rangle =0.$

power of the fluctuation²

$$\frac{1}{\hbar}S[\varphi + \sqrt{\hbar}\chi] = \frac{1}{\hbar}S[\varphi] + \frac{1}{\hbar}S^{(1)}[\varphi]\chi + \frac{1}{2}S^{(2)}[\varphi]\chi\chi + \frac{\sqrt{\hbar}}{3!}S^{(3)}[\varphi]\chi\chi\chi + \frac{\hbar}{4!}S^{(4)}[\varphi]\chi\chi\chi\chi + \cdots$$
(3.11)

We also expand the effective action as

$$\Gamma[\varphi] = S[\varphi] + \hbar \Gamma_1[\varphi] + \hbar^2 \Gamma_2[\varphi] + \cdots$$
 (3.12)

Plugging (3.11) and (3.12) into (3.9) we find

$$\begin{split} e^{-\hbar\Gamma_{1}[\varphi]-\hbar^{2}\Gamma_{2}[\varphi]+\cdots} &= \int \mathcal{D}\chi e^{-\frac{1}{2}S^{(2)}[\varphi]\chi\chi-\sqrt{\hbar}(\frac{1}{3!}S^{(3)}[\varphi]\chi\chi\chi-\Gamma_{1}^{(1)}[\varphi]\chi)-\frac{\hbar}{4!}S^{(4)}[\varphi]\chi\chi\chi\chi+\cdots} \\ &= \int \mathcal{D}\chi e^{-\frac{1}{2}S^{(2)}[\varphi]\chi\chi} \left[1-\sqrt{\hbar}\left(\frac{1}{3!}S_{123}^{(3)}[\varphi]\chi_{1}\chi_{2}\chi_{3}-\Gamma_{1,1}^{(1)}[\varphi]\chi_{1}\right) \right. \\ &\left. +\frac{\hbar}{2}\left(\frac{1}{3!}S_{123}^{(3)}[\varphi]\chi_{1}\chi_{2}\chi_{3}-\Gamma_{1,1}^{(1)}[\varphi]\chi_{1}\right)^{2} \\ &\left. -\frac{\hbar}{4!}S_{1234}^{(4)}[\varphi]\chi_{1}\chi_{2}\chi_{3}\chi_{4}+\mathcal{O}(\hbar^{3/2})\right] \end{split}$$

We have written our integral in a Gaussian shape keeping in mind that $\langle \chi \rangle = 0$, thus the only integral surviving are those even in χ . Therefore, the term proportional to $\sqrt{\hbar}$ will be zero since it is the multiplication of a Gaussian function times an odd function. The one loop effective action will be

$$e^{-\Gamma_1[\varphi]} = \int \mathcal{D}\chi e^{-\frac{1}{2}S^{(2)}[\varphi]\chi\chi} = \left(\det S^{(2)}[\varphi]\right)^{1/2} \tag{3.13}$$

therefore

$$\Gamma_1[\varphi] = \frac{1}{2} \operatorname{Tr} \log S^{(2)}[\varphi] \tag{3.14}$$

Similarly we compute the two-loop contribution as

$$\Gamma_{2}[\varphi] = -\frac{1}{2} \left(\frac{1}{3!}\right)^{2} S_{123}^{(3)}[\varphi] S_{456}^{(3)}[\varphi] \langle \chi_{1} \chi_{2} \chi_{3} \chi_{4} \chi_{5} \chi_{6} \rangle
+ \frac{1}{3!} S_{123}^{(3)}[\varphi] \Gamma_{1,4}^{(1)}[\varphi] \langle \chi_{1} \chi_{2} \chi_{3} \chi_{4} \rangle - \frac{1}{2} \Gamma_{1,1}^{(1)}[\varphi] \Gamma_{1,2}^{(1)}[\varphi] \langle \chi_{1} \chi_{2} \rangle
+ \frac{1}{4!} S_{1234}^{(4)}[\varphi] \langle \chi_{1} \chi_{2} \chi_{3} \chi_{4} \rangle$$

²We use a condensed notation avoiding to write the integrals explicitly.

To compute all this factors we need to introduce the propagator G_{ij} defined as the inverse of the second derivative of the action $G_{ij} = (S_{ij}^{(2)})^{-1}$. Together with Wick's theorem [9, 57] which allows us to easily compute the n-point correlation functions we find

To construct the diagrams above think as, for instance, the $S^{(3)}$ is a vertex from which three line goes out. Then with the aid of Wick's theorem we connect this lines in all possible ways as for the first strucutre there are two possible diagrams with the corresponding symmetry factor.

For the case of the $\Gamma^{(1)}$ we use equation (3.14) from where we get

$$\Gamma_{1,1}^{(1)}[\varphi] = \frac{1}{2} S_{123}^{(3)}[\varphi] G_{23}[\varphi]$$

A key different between the first and the second diagram in the first line is that the former is non-reducible and the latter is reducible, to see this just "cut" the internal line in the second diagram joining the two bubbles from where you get two diagrams that can not be further reduces. That it is what we mean when a diagram is not reducible, they are the so-called "1-PI" diagrams [9, 57, 58]. The two loops effective action is the sum of two 1PI diagrams

$$\Gamma_2[\varphi] = -rac{1}{12} \left(
ight) \ +rac{1}{8} \left(
ight)$$

The loop expansion for the effective action up to two loops is the sum of each contribution

$$\Gamma[\varphi] = S + \frac{1}{2} \operatorname{Tr} \log S^{(2)} + \frac{1}{8} S_{xyzw}^{(4)} G_{xy} G_{zw} - \frac{1}{12} S_{xyz}^{(3)} S_{abc}^{(3)} G_{xa} G_{yb} G_{zc} + \cdots$$
(3.15)

The first term of (3.15) is called the tree-level which is the contribution one gets discarding fluctuations – i.e its contains the mean field physics; in the context of particle physics of ϕ^4 – theory, the tree level process refer to those processes where no self interaction are taken into account. The second term is the dominant contribution of statistical and quantum fluctuations: the one-loop correction to the effective action; finally the last two terms correspond to the next-leading-order two-loop contributions. Clearly, the computation presented in this section can be further continued to arbitrary loop order.

3.2.2 Perturbative Regularization and Renormalization

As it is well known the effective action (3.15) comes with divergent contributions which we must first regularize and then renormalize with the addition of counter terms [9, 57]. Within the renormalization group we find several ways to regularize a theory or divergent integrals. One option is to introduce a cut-off in the momentum integral in order to avoid ultraviolet divergences, another method is the Pauli-Villar regularization or more importantly for this project the dimensional regularization (DR). The DR is one of the most convenient ways to regularize integral since it preserve gauge invariance. The DR scheme is performed as follows: Instead of working in $d_c = 4$ as it is generally done in QFT we write integral in momentum in an arbitrary d and perform the integral which has as result different factors times a Gamma function which depends on the dimension d_c and presents poles in various dimension, especially $d_c = 4$. After that we expand the resulting integral with a Laurent series around $\varepsilon = 0$ for this we put $d_c = 4 - \varepsilon$ and the divergent part comes in form of $\frac{1}{\varepsilon}$ while other terms remains finite. The divergent part which come from the $\frac{1}{\varepsilon}$ pole are canceled by adding counterterms to the Lagrangian, this counterterms are introduced in order to absorb the divergences and have a finite physical result. Apart from a regularization scheme, we need a subtraction scheme or subtraction rule. Since we add counterterms to our Lagrangian to absorb the divergences, the subtraction rule is essential because it specifies how those divergences should be subtracted. In this work we use the modified minimal subtraction MS rule, which unlike the minimal subtraction scheme it absorbs all divergences plus any universal quantity that may arise.

A key feature of DR is that the $\frac{1}{\varepsilon}$ -poles are directly related to the RG beta functions [59, 60]. Concretely, the beta functionals β_V and β_Z – describing the RG flow of the potential V and of the wave function renormalization functional Z – at a given loop

order L – is given by:

$$\Gamma_{div}^{(L)} = -\frac{1/L}{\varepsilon} \int d^{d_c} x \left\{ \beta_V^{(L)}(\phi) + \beta_Z^{(L)}(\phi) \frac{1}{2} (\partial \phi)^2 + \cdots \right\} + O\left(\frac{1}{\varepsilon^2}\right)$$
(3.16)

where $\Gamma_{div}^{(L)}$ is the simple pole contribution (including possible counterterms). The beta functionals in FPRG are computed as the sum of each beta function at a certain loop order, namely³

$$\beta_V^{\text{FPRG}} = \sum_L \beta_V^{(L)} \qquad \qquad \beta_Z^{\text{FPRG}} = \sum_L \beta_Z^{(L)} \qquad (3.17)$$

Perturbativly – and for a single field theory – each universality class is related one to one with a particular upper critical dimension d_c ; for example, the Ising universality class is the one with $d_c = 4$ while the Lee Yang is the one with $d_c = 6$. To calculate the beta functionals β_V^{FPRG} and β_Z^{FPRG} for a given universality class related to d_c one uses (3.16) and (3.17) around the respective d_c . An interesting feature that emerges from the use of the functional perturbative renormalization group is that the leading order (LO) and next-to-leading order (NLO) coefficients are universal quantities of the given universality class. It is also worth mentioning that some universality classes are "hidden" in the loop expansions; that is, their first non-zero contribution occurs at a loop order beyond one. For instance, the tricritical universality class has a critical dimension $d_c = 3$ and an L_{LO} of 2 while the tricritical Lee-Yang first appears at $d_c = 10/3$ and an L_{LO} of 3.

In the following section, we will examine the functionals for the potential *V* and wave function renormalization for some universality classes of great interest.

3.2.3 Local Potential Approximation (LPA') in FRPG

We will present the beta functions for the potential and the wave function renormalization, based on the results available in the literature. It is important to note that, in this subsection, the LPA' approximation indicates that the β_V and β_Z flows are generated only by the potential.

In the case $d = 4 - \epsilon$, that is, the *Ising* universality class one finds at two loop order

³We now use the superscript FPRG to clearly denote the framework used but later we will change to the superscript DR since it is the chosen scheme.

the following results computed in [61]:

$$\beta_V^{\text{FPRG}} = \frac{1}{(4\pi)^2} \frac{1}{2} (V^{(2)})^2 - \frac{1}{(4\pi)^4} \frac{1}{2} V^{(2)} (V^{(3)})^2 + \cdots$$
 (3.18)

$$\beta_Z^{\text{FPRG}} = -\frac{1}{(4\pi)^4} \frac{1}{6} (V^{(4)})^2 + \cdots$$
 (3.19)

The *Lee-Yang* universality class has upper critical dimension $d_c = 6$ and is also a single component scalar theory. In the case $d = 6 - \epsilon$ one finds at two loop order the following results [61]:

$$\beta_{V}^{\text{FPRG}} = -\frac{1}{(4\pi)^{3}} \frac{1}{6} (V^{(2)})^{3} - \frac{1}{(4\pi)^{6}} \frac{23}{144} (V^{(2)})^{3} (V^{(3)})^{2} + \cdots$$

$$\beta_{Z}^{\text{FPRG}} = -\frac{1}{(4\pi)^{3}} \frac{1}{6} (V^{(3)})^{2} - \frac{1}{(4\pi)^{6}} \frac{13}{216} (V^{(3)})^{4} + \cdots$$

The last example we want to bring from literature is the *Sine-Gordon* universality class which has upper critical dimension $d_c = 2$. Then in $d = 2 - \epsilon$ we find [61]:

$$eta_V^{ ext{FPRG}} = -rac{1}{(4\pi)}(V^{(2)})$$

Unlike any other universality class, there are no higher loop contributions for the β_V in d=2.

3.3 Functional Non-Perturbative RG (NPRG)

In this section we aim to introduce the basic notions of the non-perturbative renormalization group where the main goal is to derive the flow equation i.e., an equation that describes the scale dependence of the effective average action Γ_k . The effective average action (EAA) is closely related to the effective action defined in (3.9). When defining the EAA we do an average of field taken within a volume of size k^{-d} . The idea resemble the Wilsonian idea of block-spin approach on a lattice but in this case we work in continuous Euclidean space which preserve all space-time symmetries. When Wilson and Kadanoff [15] introduced the concept of a block spin, that is, an average of the field over a block of lattice site, they defined an effective action for block spins with blocks of size k^{-d} . As we will see below, the effective action Γ_k involves an integration over all modes but the contribution of modes low momenta are sup-

pressed by a mass term⁴. There are different ways to implement the non perturbative renormalization group nevertheless all of them has as root Kadanoff-Wilson's ideas of block spins, the coarse-graning and effective long distance theories. Nonetheless, this various ways to implement the NPRG differ completely in one case or another. Among the different framework two of them stand out, the Wilson-Polchinski approach [62] and the effective average action [63, 64, 65, 66]. In what follow we will focus on the effective average action method.

3.3.1 EAA and the Wetterich-Morris Equation

Concretely, we want to construct a one parameter family of modes indexed by a scale k. We require that (1) when $k = \Lambda$, $\Gamma_{k=\Lambda}[\varphi] = S[\varphi]$ and (2) when k = 0, $\Gamma_{k=0}[\varphi] = \Gamma[\varphi]$. The former is the case where no fluctuation where integrated out (the Gibbs free energy is the microscopic Hamiltonian) and the latter is the case where all fluctuation are integrated out and $\Gamma_{k=0}$ is just the Gibbs free energy of the original model. This method, therefore, provides an interpolation between microscopic and macroscopic physics. The integral equation (3.9) now becomes

$$e^{-\Gamma_k[\varphi]} = \int \mathcal{D}\chi e^{-S[\varphi + \chi] - \Delta S_k[\chi] + \int \frac{\delta \Gamma_k}{\delta \varphi} \chi}$$
 (3.20)

In order to construct a one parameter family of Γ_k we want to decouple the slow modes of the model in the partition function. Therefore, this method is based on consider an extra term proportional to the momentum dependent mass term

$$\Delta S_k[\varphi] = \frac{1}{2} \int_{x,y} \varphi(x) R_k(x - y) \varphi(y) = \frac{1}{2} \int_{p} \varphi(p) R_k(p) \varphi(-p)$$
 (3.21)

The function $R_k(p)$ is called cut-off or regulator. This function must satisfy certain conditions;

- For k = 0, $R_{k=0}(p) = 0$ for all p. This ensures that $Z_{k=0}[J] = Z[J]$ or in other words the EEA at k = 0 is as we just described the Gibbs free energy or effective action Γ .
- For $k = \Lambda$, $R_{k=\Lambda}(p) = \infty$ for all p. For this condition all modes should be frozen, typically rather than choose the function $R_k = \Lambda$ equal to infinite we choose as the order of k^2 .

⁴By mass term we mean a term quadratic in the field.

• For $0 < k < \Lambda$ the regulator goes to zero sufficiently fast. This will ensure the fast momentum modes are integrated out unsuppressed.

$$R_k(|p| > k) \simeq 0$$

There are many ways to choose the function R_k that meet the conditions above. In the literature the most common are the following

$$R_k(q^2) = k^2 e^{-\frac{q^2}{k^2}} (3.22)$$

$$R_k(q^2) = k^2 \frac{q^2/k^2}{e^{q^2/k^2} - 1}$$
 (3.23)

$$R_k(q^2) = (k^2 - q^2)\Theta(k^2 - q^2)$$
 (3.24)

In terms of dimensionless variable we can express the cut-off as

$$R_k(q^2) = k^2 r(y), \qquad y = \frac{q^2}{k^2}$$

where r is a dimensionless function of y which is also dimensionless. Thus the cut-offs presented above adapt the form

$$R_k(q^2) = k^2 e^{-y} (3.25)$$

$$R_k(q^2) = k^2 \frac{y}{e^y - 1} (3.26)$$

$$R_k(q^2) = k^2(1-y)\Theta(1-y)$$
 (3.27)

The cut-offs (3.25), (3.26), (3.27) are commonly known as the exponential cut-off, Wetterich cut-off and Litim or optimized cut-off respectively.

We know that up to a factor of $-K_BT$ the Helmholtz free energy W is

$$W_k[J] = \log\left[Z_k\right] \tag{3.28}$$

which depends on the scale k and the regulator. We want to work with Legendre transformation of W_k but in a general way

$$\Gamma_k[\varphi] + \frac{1}{2} \int_{x,y} \varphi(x) R_k(|x-y|) \varphi(y) = -W_k + \int_x J(x) \varphi(x)$$
 (3.29)

where

$$\varphi(x) = \frac{\delta W_k}{\delta J(x)} = \langle \phi(x) \rangle$$

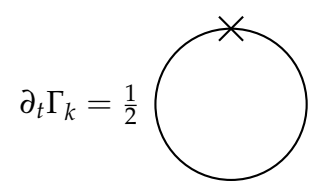


Figure 3.1: Diagrammatic representation of the RG equation. The line represent the propagator and the cross is $\partial_t R_k$, the closed loop means integration over q.

Taking (3.29) as starting point we can derive a flow equation for the effective action,

$$\partial_t \Gamma_k[\varphi] = \frac{1}{2} \int_{x,y} \partial_t R_k(|x-y|) \frac{\delta^2 W_k}{\delta J(x) \delta J(y)}$$
(3.30)

where we used the variable $t \equiv \log(k/\Lambda)$ known as the RG time and the full propagator $G_k(x,y)$ is

$$G_k(x,y) \equiv \frac{\delta^2 W_k}{\delta J(x)\delta J(y)} = \left(\frac{\delta^2 \Gamma_k}{\delta \phi(x)\delta \phi(y)} + R_k(|x-y|)\right)^{-1}$$

Therefore we find Wetterich-Morris equation [63, 66, 67]

$$\partial_t \Gamma_k[\varphi] = \frac{1}{2} \int_{x,y} \partial_t R_k(|x-y|) \left(\Gamma_k^{(2)} + R_k\right)_{x,y}^{-1}$$
(3.31)

A detailed derivation of equation (3.31) can be found in appendix A. Before study the approximation procedures let see some properties.

- 1. This equation is exact since no approximation where made, although is too hard to solve that is why we require an approximation procedure.
- 2. As it is seen the equation for the evolution of Γ_k involves $\Gamma_k^{(2)}$ then it does not have a closed form. In general the flow equation for $\Gamma^{(n)}$ involves $\Gamma^{(n+1)}$ and $\Gamma^{(n+2)}$.
- 3. If we substitute $\Gamma_k^{(2)} \to S^{(2)}$ we see that. $\partial_t \Gamma_k = \frac{1}{2} \widetilde{\partial}_t \text{Tr} \Big[\log(S^{(2)} + R_k) \Big]$ which resemble the 1-loop contribution⁵ of equation (3.15).

⁵Here $\tilde{\partial}_t$ acts only on the regulator R_k

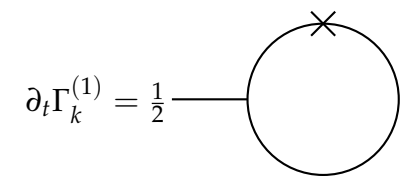


Figure 3.2: Diagrammatic representation of $\partial_t \Gamma_k^{(1)}$.

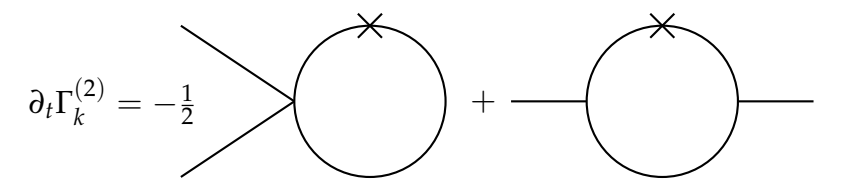


Figure 3.3: Diagrammatic representation of $\partial_t \Gamma_k^{(2)}$.

3.3.2 Approximation Schemes

The first approximation scheme we present here is the Green function approach or the vertex expansion. Imagine we want to close the equation by looking for $\Gamma^{(2)}$. Then

$$\frac{\delta}{\delta\phi(x_1)}\partial_t\Gamma_k = \partial_t \frac{\delta\Gamma_k}{\delta\phi(x_1)} = \partial_t\Gamma_k^{(1)} = \frac{1}{2} \int_{x,y} \partial_t R_k(|x-y|) \frac{\delta^3 W_k}{\delta J(x)\delta J(y)\delta\phi(x_1)}
= -\frac{1}{2} \int_{x,y,z,u} \partial_t R_k(|x-y|) G_k(y,z) \Gamma_k^{(3)}(z,x_1,u) G_k(u,x)$$

In momentum space we have

$$\partial_t \Gamma_k^{(1)}(p) = \int_{q's} \dot{R}_k(q_1) G_k(q_1, -q_2) \Gamma_k^{(3)}(q_2, p, -q_3) G_k(q_3, -q_1)$$

and by the same reasoning

$$\partial_{t}\Gamma_{k}^{(2)}(p,p') = -\frac{1}{2}\int \dot{R}_{k}(q_{1})G_{k}(q_{1},-q_{2})\Gamma_{k}^{(4)}(q_{2},p,p',-q_{3})G_{k}(q_{3},-q_{1}) + \int \dot{R}_{k}(q_{1})G_{k}(q_{1},-q_{2})\Gamma_{k}^{(3)}(q_{2},p,-q_{3})G_{k}(q_{3},-q_{4})\Gamma_{k}^{(3)}(q_{4},p',-q_{5})G_{k}(q_{5},-q_{1}).$$
(3.32)

Here we clearly see what was mentioned before, the $\Gamma_k^{(2)}$ depends on $\Gamma_k^{(3)}$ and $\Gamma_k^{(4)}$, hence, in order to solve this infinite tower of equation we must apply a truncation. Usually we work in a uniform field configuration where the momentum is conserved at each vertex and propagator. One possible truncation consist in keeping only $\Gamma_k^{(4)}$ and neglect higher order or to give ansatz of $\Gamma_k^{(6)}$ in terms or $\Gamma_k^{(2)}$ and $\Gamma_k^{(4)}$. In any case, the system is now closed and could be solved.

On the other hand, a widely used method is the derivative expansion (DE). This technique involves expanding the effective action in powers of derivatives of the fields, typically starting with local potential terms and then including terms with an increasing number of derivatives. This method is particularly useful for dealing with strongly interacting systems, as we are in the regime of low momenta ($q \rightarrow 0$), where it seems plausible to expand the action in powers of derivatives of the fields. The lowest order of the DE is the Local Potential Approximation (LPA) which is based on writing the effective action in terms of the effective potential V_k plus a kinetic term

$$\Gamma_k^{LPA}[\varphi] = \int_r \left(\frac{1}{2}(\partial \varphi)^2 + V_k(\varphi)\right)$$
 (3.33)

Despite the simplicity of the LPA it is poor in determine the critical exponent η since it predicts a value $\eta = 0$, to solve that it is possible to make a tiny variation and perform the LPA' where a field renormalization factor Z_k is included

$$\Gamma_k^{LPA'}[\varphi] = \int_r \left(\frac{1}{2} Z_k(\partial \varphi)^2 + V_k(\varphi)\right) \tag{3.34}$$

More reliable estimate for the critical exponent are computed when considering the second order of the DE

$$\Gamma_k^{DE2}[\varphi] = \int_r \left(\frac{1}{2} Z_k(\varphi) (\partial \varphi)^2 + V_k(\varphi)\right)$$
 (3.35)

where unlike the LPA' the wave-function renormalization function has now a dependence on the field [68].

3.3.3 Local Potential Approximation (LPA') in NPRG

Let us take a look, just for completeness, of how the beta function are in the NPRG. The explicit expressions for the potential V and the function Z are

$$(4\pi)^{\frac{d}{2}} \beta_V^{\text{NPRG}} = \frac{1}{2} Q_{\frac{d}{2}} [G_k]$$
 (3.36)

and

$$(4\pi)^{\frac{d}{2}} \beta_Z^{\text{NPRG}} = (V_k''')^2 \left\{ Q_{\frac{d}{2}}[G_k^2 G_k'] + Q_{\frac{d}{2}+1}[G_k^2 G_k''] \right\}$$
(3.37)

All functions have argument $z=q^2$. We used the Mellin transform Q-functional notation

$$Q_n[f] = \frac{1}{\Gamma(n)} \int_0^\infty dz \, z^{n-1} f(z) \, \partial_t R_k(z)$$
 (3.38)

The Q-functional contains the integration over the modulus of the momentum. Finally, we recall that the regularized inverse propagator is

$$G_k(z,\phi) = \frac{1}{Z_k(\phi)z + V_k''(\phi) + R_k(z)}.$$
(3.39)

These relations are valid for an arbitrary cutoff function and in any dimension.

To show an example let us see how the beta function (3.36) is computed from the Q-functional notation with the choice of the Litim cutoff (3.27). The way to proceed is straightforward, we just need to compute the integral defined in (3.38) identifying before the each term of the integrand. The result of the time derivative of the regulator is⁶

$$\partial_t R_k = 2k^3 Z_k (k^2 - z) \delta(k^2 - z) + 2k^2 Z_k \Theta(k^2 - z)$$

By plugging the propagator (3.39) in (3.38) we arrive at the following form

$$(4\pi)^{d/2} \beta_V^{\text{NPRG}} = \frac{1}{2\Gamma(d/2)} \int_0^\infty dz \, z^{d/2-1} \frac{2k^2 Z_k}{V_k'' + Z_k k^2} \Theta(k^2 - z)$$

$$= \frac{2k^2 Z_k}{2\Gamma(d/2)(V_k'' + Z_k k^2)} \int_0^\infty dz \, z^{d/2-1} \Theta(k^2 - z)$$

$$= \frac{2}{\Gamma(d/2)d} \frac{k^d}{1 + \frac{V''}{Z_k k^2}}$$
(3.40)

which is the beta function found in the literature [69] for the potential V with the LPA' approximation. Similarly we can compute the β_Z^{NPRG}

$$(4\pi)^{d/2}\beta_{Z}^{\text{NPRG}} = (V_{k}''')^{2} \left\{ \int_{0}^{\infty} \frac{\mathrm{d}z \, z^{d/2-1}}{\Gamma(\frac{d}{2})} G_{k}^{2} G_{k}'(2k^{2} Z_{k} \Theta(k^{2}-z)) + \int_{0}^{\infty} \frac{\mathrm{d}z \, z^{\frac{d}{2}}}{\Gamma(\frac{d}{2}+1)} G_{k}^{2} G_{k}''(2k^{2} Z_{k} \Theta(k^{2}-z)) \right\}$$

We identify that

$$G' = -G^2(Z_k + R'_k)$$
 $G'' = -2G^3(Z_k + R'_k) - G^2R''$

⁶Here we insert a factor Z_k in front of the regulator.

then

$$G^{2}G' = \frac{-Z_{k}(1 + \Theta(k^{z} - z))}{(V_{k}'' + k^{2}Z_{k})^{4}}$$

$$G^{2}G'' = \frac{-2Z_{k}(1 - \Theta(k^{2} - z))}{(V_{k}'' + k^{2}Z_{k})^{5}} - \frac{Z_{k}\delta(k^{2} - z)}{(V_{k}'' + k^{2}Z_{k})^{4}}$$

we plug it in the integral and perform the integration in z, therefore we arrive at

$$(4\pi)^{d/2} \beta_Z^{\text{NPRG}} = \frac{(V_k''')^2 Z_k^2}{d\Gamma\left(\frac{d}{2}\right)} \left\{ -\frac{4k^{d+2}}{\left(k^2 Z_k + V_k''\right)^4} \right\}$$
(3.41)

This last equation, which can be found in [69], can be used to determine the anomalous dimension η within the LPA' approximation. In a future paper [70] we study the connection between the beta functions derived with the NPRG and those derived from the FDR.

3.4 Functional Dimensional Regularization (FDR)

We now introduce our novel approach *Functional Dimensional Regularization*. The key insight is that traditional dimensional regularization (DR) in MS or $\overline{\text{MS}}$ scheme can be generalized and transformed into a functional RG by the simple act of subtracting *all* $1/\epsilon$ poles that arise in perturbation theory – and not only the specific one of interest at a given d_c – as is usually done in perturbation theory and ϵ -expansion. This will result in a *sum of all possible critical dimensions* which will result in a fully fledged functional RG with good convergence properties and all the analytical advantages of DR.

3.4.1 Beta Functionals

As we explained in section 3.2, the bare action, which contains the bare parameters, is plagued by the problem of divergences when computing physical observables. To solve this problem, the renormalization strategy is to write the bare parameters in terms of the regularized parameters. From here one can note that the bare action relates with the renormalized action as follow

$$S = S_R + \Delta S_1 + \cdots \tag{3.42}$$

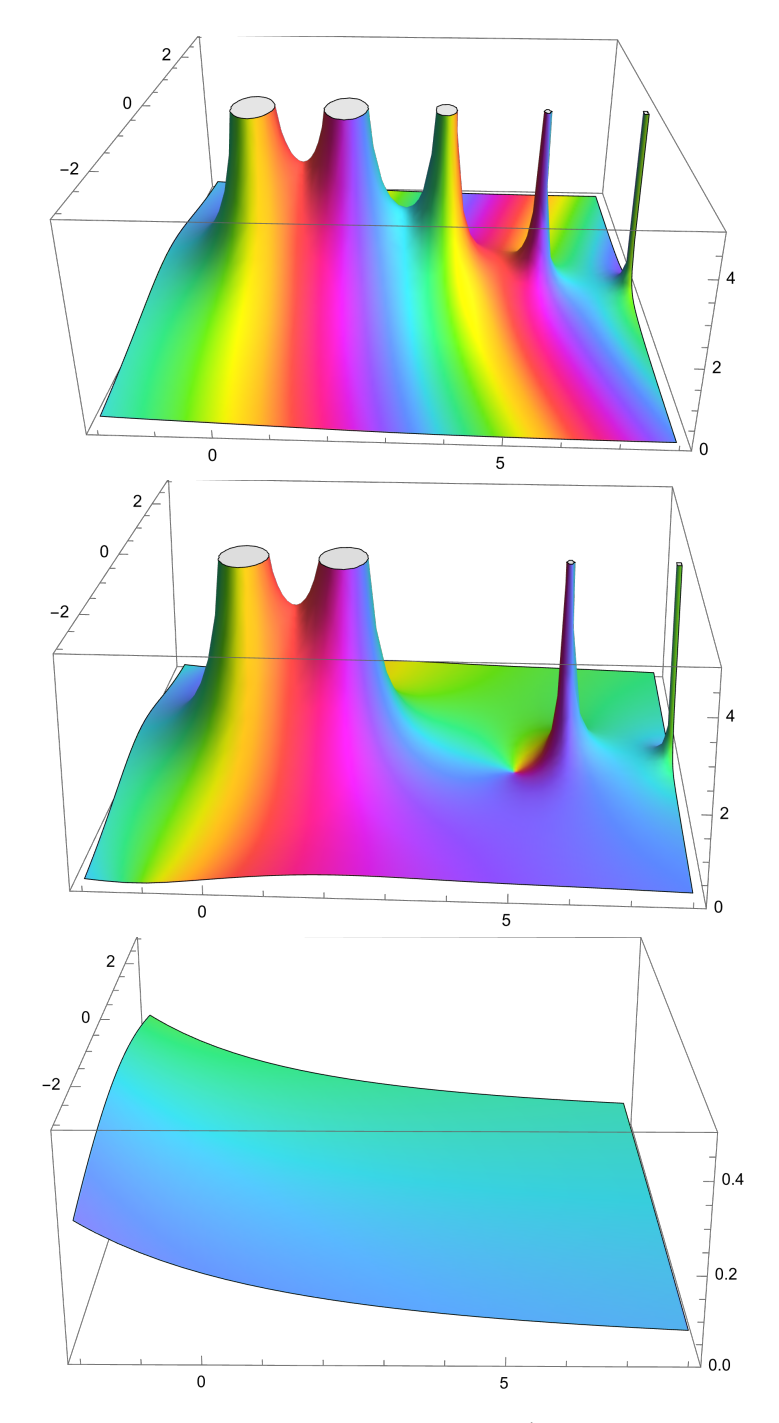


Figure 3.4: Top: Poles of the Gamma function $\Gamma(-\frac{d}{2})$ in the complex plane. Middle: Poles of the Gamma function with d=4 pole regularized. Bottom: Gamma function in the complex plane with all poles regularized.

where S is the bare action which do not depend on the renormalization scale μ , S_R is the renormalized action and ΔS_1 is the counterterm at one loop. We will now express the action as a sum of terms where each term is a coupling constant multiplied by a corresponding operator or functional of the fields

$$S = \sum_{i} g_{i} \mathcal{O}^{i} \qquad S_{R} = \sum_{i} g_{i}^{R} \mathcal{O}^{i}$$

where we use the notation \mathcal{O}^i to stand for integrated operators (for example $\int \frac{1}{i!} \phi^i$). A key difference between the coupling g and g^R is that the former does not depend on the renormalization scale μ . At the same time the counterterm is fixed as $\Delta S_1 = -\Gamma|_{div}$, where the divergent part of the effective action has the form (3.16) but now we are considering all simple poles (at all d_c 's)

$$\Gamma|_{div} = \sum_{i} \sum_{d_c} \frac{\mu^{d-d_c}}{d-d_c} \beta_i^{DR}(d_c) \mathcal{O}^i$$
(3.43)

where the residues are the beta functions in DR. Then (3.42) becomes

$$S = S_R - \sum_i \sum_{d_c} \frac{\mu^{d-d_c}}{d-d_c} \beta_i^{DR}(d_c) \mathcal{O}^i + \cdots$$
(3.44)

By taking the μ -derivative on both sides of this equation and using $\partial_{\mu}S=0$ we find the following relation

$$\mu \partial_{\mu} S = \mu \partial_{\mu} S_{R} - \mu \partial_{\mu} \left(\sum_{d_{c}} \frac{\mu^{d-d_{c}}}{d-d_{c}} \sum_{i} \beta_{i}^{DR}(d_{c}) \mathcal{O}^{i} \right)$$

$$0 = \sum_{i} \left(\beta_{i}^{FDR}(d) - \sum_{d_{c}} \mu^{d-d_{c}} \beta_{i}^{DR}(d_{c}) \right) \mathcal{O}^{i}$$
(3.45)

where we defined $\beta_i^{\text{FDR}}(d) \equiv \mu \partial_\mu g_i^R$. Note that beyond LO one will have to act also on the term $\beta^{\text{DR}}(d_c)$ on the rhs, but since its results gives a higher order contribution we will discard it here. Our final result is that the FDR beta functions for the g_i couplings are obtained as a sum over all critical dimensions (those that appear at one loop) of the respective beta functions of traditional DR. This is our master formula and the main result of our approach

$$\beta_i^{\text{FDR}}(d) \equiv \sum_{d_c} \mu^{d-d_c} \beta_i^{\text{DR}}(d_c)$$
 (3.46)

In the following we will show that such RG scheme has very interesting properties. The master formula can obviously be extended to beta functionals for the potential *V* and the wave function renormalization Z:

$$\beta_V^{\text{FDR}}(d) \equiv \sum_d \mu^{d-d_c} \beta_V^{\text{DR}}(d_c)$$
 (3.47)

$$\beta_V^{\text{FDR}}(d) \equiv \sum_{d_c} \mu^{d-d_c} \beta_V^{\text{DR}}(d_c)$$

$$\beta_Z^{\text{FDR}}(d) \equiv \sum_{d_c} \mu^{d-d_c} \beta_Z^{\text{DR}}(d_c)$$
(3.47)
$$(3.48)$$

Similar expressions clearly apply to all higher-order functionals that enter the derivative expansion of the effective action and can also be extended beyond leading order.

3.4.2 **Dimensional Analysis**

Dimensional analysis is a simple yet very powerful tool. By inspecting the possibles one-loop diagrams, we can extract the fundamental building blocks for the one-loop eta_V^{DR} and eta_Z^{DR} functions. In order to construct these building blocks we need first to determine the vertex set, that is, the structure of all possibles diagrams written as products of the derivatives of the potential at a given loop order. Therefore, the contribution to functional β_V^{DR} and β_Z^{DR} will be a polynomial built out of the possible vertices in the vertex multiplied by the appropriate powers of $V^{(2)}$, i.e the mass insertion, determined with the aid of dimensional analysis. In the following section, we will show how to calculate the one-loop beta function and subsequently determine the coefficients for this theory.

$$\beta_V^{\mathrm{DR}}$$
 at $L=1$

In order to compute the $\beta_V^{\rm DR}$ function we need to study the 1–loop function. Recall that the divergent part of the effective action has the following form.

$$\Gamma|_{div} = -\frac{1}{\epsilon} \int d^d x \left\{ \beta_V^{DR} + \beta_Z^{DR} \frac{1}{2} (\partial \phi)^2 + \cdots \right\} + O\left(\frac{1}{\epsilon^2}\right). \tag{3.49}$$

Since the effective action must be dimensionless we see that the $\beta_V^{\rm DR}$ must have dimension d. By counting the dimension we find that $[V^{(n)}] = d - n(\frac{d}{2} - 1)$ and the mass insertion is proportional to $(V'')^k$ where k is the number of insertions in the loop. The most complete form of the β_V^{DR} at 1-loop is trivial given that the building

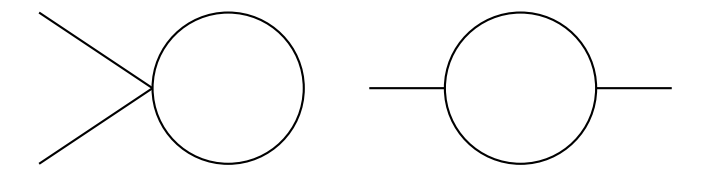


Figure 3.5: Feynman diagram for the $\beta_Z^{\rm DR}$ at 1 loop

block is just $(V'')^k$. Thus, by dimensional analysis

$$\left(d-2\left(\frac{d}{2}-1\right)\right)k=d \quad \Rightarrow \quad 2k=d \quad \Rightarrow \quad k=\frac{d}{2} \tag{3.50}$$

This gives the following structures:

d_c	$eta_V^{ m DR}$
2	a_2V''
4	$a_4(V'')^2$
6	$a_6(V'')^3$
:	
2 <i>n</i>	$a_{2n}(V'')^n$

This Table defines the coefficients a_n to be determined in a later section.

$$\beta_Z^{\mathrm{DR}}$$
 at $L=1$

When its come to the β_Z^{DR} at 1 loop, there are two possible diagrams as shown in the Figure 3.5.

The building block of the diagram on the left has the form $V^{(4)}(V'')^k$. It can be shown that this diagram does not contribute to the $\beta_Z^{\rm DR}$ but in order to be complete we will add it and then justify why it does not appear. On the other hand, the diagram on the right has the form $(V^{(3)})^2(V'')^k$. The diagram which is proportional to $(V^{(3)})^2$ is known as the polarization diagram and the one proportional to $V^{(4)}$ is known as the tadpole. When performing the dimensional analysis this time we have to keep in mind that the $\beta_Z^{\rm DR}$ must be dimensionless, so equations provided from dimensional analysis will be set equal zero. For the first diagram we have

$$d - 4\left(\frac{d}{2} - 1\right) + 2k = 0 \quad \Rightarrow \quad k = \frac{d}{2} - 2$$

Applying the same analysis to the second diagram we find

$$2\left(d-3\left(\frac{d}{2}-1\right)\right)+2k=0 \quad \Rightarrow \quad k=\frac{d}{2}-3$$

Note that for d = 2 and d = 4 the value of k is negative. This kind of solution, as well as fractional, will be discarded since it is the power of the potential and has no physical interpretation. The results is:

d_c	$eta_Z^{ m DR}$
2	0
4	$c_4'V^{(4)}$
6	$c_6(V^{(3)})^2 + c_6'V^{(4)}V''$
8	$c_8(V^{(3)})^2V'' + c_8'V^{(4)}(V'')^2$
:	:
n	$c_n(V^{(3)})^2(V'')^{\frac{n}{2}-3} + c'_n V^{(4)}(V'')^{\frac{n}{2}-2}$

and defines the coefficients c_n and c'_n where the c'_n are zero in DR. We still need to compute the coefficients a_n and c_n , we will do it in the next section. After that we will compare the results which comes from the non-perturbative renormalization group to compare its results with those that arise from our calculation.

3.4.3 Calculation of the a_n and c_n coefficients

In this subsection it is shown how to compute the coefficients a_n and c_n which belong to the β_V and β_Z functions respectively. This is the first concrete example where we show how the FDR is carried out. Regarding the a_n coefficient we will present a simple computation that uses the Heat Kernel starting from the one-loop effective action (3.14)

$$\Gamma_1[\phi] = \frac{1}{2} \text{Tr} \log S^{(2)}[\phi]$$
 (3.51)

Since we are working at the LPA level the action reads

$$S[\phi] = \int d^d x \left\{ \frac{1}{2} \partial_\mu \phi \partial^\mu \phi + V(\phi) \right\}$$
 (3.52)

From here we can compute the Hessian $S^{(2)}$ as

$$S^{(2)}[\phi] = \left\{-\Box + V''(\phi)
ight\}\delta_{xy}$$

which we can insert into (3.51) and then perform some basic Heat Kernel manipulations (we are assuming ϕ constant and we are inserting an IR mass regulator μ in the final step)

$$\Gamma_{1} = \frac{1}{2} \operatorname{Tr} \log(-\Box + V'')$$

$$= -\frac{1}{2} \int_{0}^{\infty} \frac{\mathrm{d}s}{s} \operatorname{Tr} e^{-s(-\Box + V'')}$$

$$= -\frac{1}{2} \int_{0}^{\infty} \frac{\mathrm{d}s}{s} \frac{1}{(4\pi s)^{\frac{d}{2}}} e^{-sV''}$$

$$= -\frac{1}{2} \frac{1}{(4\pi)^{\frac{d}{2}}} \int_{0}^{\infty} \mathrm{d}s \, s^{-(\frac{d}{2}+1)} e^{-sV''} e^{-s\mu^{2}}.$$

Now we expand the exponential in the potential and use the fact that $d_c=2n$ and $d=d_c-\varepsilon=2n-\varepsilon$

$$\begin{split} \Gamma_1 &= -\frac{1}{2} \frac{1}{(4\pi)^{d/2}} \int_0^\infty ds \sum_{n=0}^\infty s^{n-(1+d/2)} \frac{(-V'')^n}{n!} e^{-s\mu^2} \\ &= -\frac{1}{2} \frac{1}{(4\pi)^{d/2}} \sum_{n=0}^\infty \Gamma\left(n - \frac{d}{2}\right) \mu^{d/2 - n} \frac{(-V'')^n}{n!}. \end{split}$$

Our definition of β_V requires to look only the divergent part of Γ_1 , then

$$\Gamma_{1|div} = -\frac{1}{2} \frac{1}{(4\pi)^{d_{c}/2}} \Gamma\left(\frac{\varepsilon}{2}\right) \frac{(-V'')^{d_{c}/2}}{(d_{c}/2)!}$$

$$= -\frac{1}{\varepsilon} \frac{1}{(4\pi)^{d_{c}/2}} \frac{(-V'')^{d_{c}/2}}{(d_{c}/2)!}.$$

where in the last step we used that $\Gamma(\frac{\varepsilon}{2}) = \frac{2}{\varepsilon} + \cdots$. Finally the coefficients a_{d_c} with $d_c = 2n$ turn out to be

$$a_{2n} = \frac{(-1)^n}{(4\pi)^n n!} \tag{3.53}$$

For the c_n coefficients we have to consider the polarization diagram for the one loop two point function shown in the Figure 3.5 and expand in powers of $\omega \equiv V''$

$$\begin{aligned} \text{polarization} &= -\frac{(V^{(3)})^2}{2} \int_q \frac{1}{(q^2 + \omega)((q+p)^2 + \omega)} \\ &= -\frac{(V^{(3)})^2}{2} \int_q \left(\sum_{n_1=0}^{\infty} \frac{(-\omega)^{n_1}}{q^{2(n_1+1)}} \right) \left(\sum_{n_2=0}^{\infty} \frac{(-\omega)^{n_2}}{(q+p)^{2(n_2+1)}} \right) \\ &= -\frac{(V^{(3)})^2}{2} \sum_{n_1=0}^{\infty} \sum_{n_2=0}^{\infty} (-\omega)^{n_1+n_2} \int_q \frac{1}{q^{2(n_1+1)}(q+p)^{2(n_2+1)}} \end{aligned}$$

We have reduced the diagram to the one loop master integral

$$\int_{q} \frac{1}{q^{2\alpha}(q+p)^{2\beta}} = \frac{1}{(4\pi)^{\frac{d}{2}}} \frac{\Gamma(\frac{d}{2}-\alpha)\Gamma(\frac{d}{2}-\beta)\Gamma(\alpha+\beta-\frac{d}{2})}{\Gamma(\alpha)\Gamma(\beta)\Gamma(d-\alpha-\beta)} \left(p^{2}\right)^{\frac{d}{2}-\alpha-\beta}$$
(3.54)

with $\alpha = n_1 + 1$ and $\beta = n_2 + 1$. We are looking for the p^2 terms so $\frac{d}{2} - 2 - n_1 - n_2 = 1$ which implies $n \equiv n_1 + n_2 = \frac{d}{2} - 3$. Under this condition the polarization diagram becomes

$$\text{polarization}|_{p^2} = -\frac{(V^{(3)})^2}{2(4\pi)^{\frac{d}{2}}} p^2 \sum_{n_1+n_2=n} (-\omega)^n \frac{\Gamma(\frac{d}{2}-1-n_1)\Gamma(\frac{d}{2}-1-n_2)}{\Gamma(n_1+1)\Gamma(n_2+1)} \frac{\Gamma(n+2-\frac{d}{2})}{\Gamma(d-2-n)}.$$

This formula gives us divergences for $d_c = 6, 8, 10, ...$ We find the pattern

Thus the coefficients c_{d_c} turn out to be

$$c_{2n+4} = \frac{(-1)^n}{6(4\pi)^{n+2}(n-1)!}$$
(3.55)

with $d_c = 2n + 4$. In the following section we use the coefficients found to finally compute our first beta functions by summing over all possible upper critical dimension at one loop.

3.4.4 Local Potential Approximation (LPA') in FDR

We can now compute the first non-trivial beta functional in the FDR using the results for the coefficients a_{d_c} given in (3.53) and the coefficients c_{d_c} given in (3.55). The β_V^{DR} together with the coefficient a_n has the form

$$\beta_V^{\text{DR}}(d_c = 2n) = \frac{(-1)^n}{(4\pi)^n n!} (V'')^n$$
(3.56)

Inserting into (3.47) gives an easy summation

$$\beta_V^{\text{FDR}}(d) = \sum_{n=0}^{\infty} \mu^{d-2n} \frac{(-1)^n}{(4\pi)^n n!} (V'')^n = \mu^d \sum_{n=0}^{\infty} \frac{1}{n!} \left(\frac{-V''}{4\pi \mu^2} \right)^n = \mu^d e^{-\frac{V''}{4\pi \mu^2}}$$

The FDR-LPA beta functional is thus very simple

$$\beta_V^{\text{FDR}}(d) = \mu^d \, e^{-\frac{V''}{4\pi\mu^2}} \tag{3.57}$$

Now is the turn to compute the $\beta_Z^{\text{FDR}}(d)$ at L=1. Proceeding in an analogous way we insert the coefficient (3.55) into the equation (3.48)

$$\begin{split} \beta_{Z}^{\text{FDR}}(d) &= \sum_{d_{c}} \mu^{d-d_{c}} \beta_{Z}^{\text{DR}}(d_{c}) = \sum_{d_{c}} \mu^{d-d_{c}} c_{d_{c}} (V''')^{2} (V''')^{\frac{d_{c}}{2} - 3} \\ &\stackrel{d_{c}=2n+4}{=} \sum_{n=1}^{\infty} \mu^{d-(2n+4)} \frac{(-1)^{n}}{(4\pi)^{n+2}(n-1)!} (V''')^{2} (V''')^{n-1} \\ &= \frac{\mu^{d-6} (V''')^{2}}{6(4\pi)^{3}} \sum_{n=1}^{\infty} \mu^{-2(n-1)} \frac{(-1)^{n} (V'')^{n-1}}{(4\pi)^{n-1}(n-1)!} \\ &= -\frac{\mu^{d-6} (V''')^{2}}{6(4\pi)^{3}} \sum_{n=1}^{\infty} \frac{1}{(n-1)!} \left(\frac{-V''}{4\pi\mu^{2}}\right)^{n-1} \end{split}$$

The beta function of the wave function renormalization turns out to be

$$\beta_Z^{\text{FDR}}(d) = -\mu^{d-6} \frac{1}{6} \frac{(V^{(3)})^2}{(4\pi)^3} e^{-\frac{V''}{4\pi\mu^2}}$$
(3.58)

As for the potential, this beta functions also turns to be remarkably simple. In the following section we will see how to compute the dimensionless flow equations and test for the first time the beta functions just found.

3.5 Fixed Point Analysis (FPRG vs NPRG vs FDR)

3.5.1 Dimensionless Flow Equation for β_V & β_Z

Up to this point, we have introduced a new method for computing the β -function using a novel RG scheme and applied it to the N=1 case of the O(N) model. This case presents fewer difficulties compared to the general N case. Moreover, we focused on the lowest order of the derivative expansion, not only because it is simpler but also because it is more pedagogical. Now, it is time to test these functions and determine the critical exponents using this approach. Before deriving the beta functions from the beta functionals, we need to rewrite them in terms of dimensionless variables defined as:

$$\tilde{\varphi} = \varphi \mu^{d_{\varphi}} = \varphi \mu^{\frac{1}{2}(d-2+\eta)}, \quad \tilde{V}(\tilde{\varphi}) = \mu^{-d}V, \quad \tilde{Z} = \mu^{\eta}Z$$
(3.59)

where μ is the renormalization scale, $\tilde{\varphi}$ the dimensionless field and η is the anomalous dimension. We express the dimensionless potential and wave function renormalization function as

$$v(\varphi) \equiv \tilde{V}(\tilde{\varphi})$$
 $z(\varphi) \equiv \mu^{\eta} Z(\varphi \mu^{\frac{1}{2}(d-2+\eta)})$ (3.60)

The dimensionless beta functionals $\beta_v \equiv \mu \partial_{\mu} v$ and $\beta_z \equiv \mu \partial_{\mu} z$ are easily obtained by deriving (3.60):

$$\partial_t(\mu^d v) = \partial_t V = \beta_V$$
$$\mu^d dv + \mu^d \partial_t v - \mu^d d_{\varphi} v' = \beta_V$$
$$\mu^d \beta_v = -d\mu^d v + \mu^d d_{\varphi} \varphi v' + \beta_V$$

Performing a similar computation we find the expression for β_z , then the two dimensionless flow equation are

$$\beta_v = -dv + \frac{1}{2}(d - 2 + \eta)\varphi v' + \mu^{-d}\beta_V$$
 (3.61)

$$\beta_z = \eta z + \frac{1}{2} (d - 2 + \eta) \varphi z' + \mu^{\eta} \beta_Z$$
 (3.62)

The anomalous dimension η is determined self consistently, imposing the normalization condition z(0) = 1 on equation (3.62) when $\beta_z = 0$

$$\eta = -\mu^{\eta} \beta_Z \Big|_{\varphi \to 0} \tag{3.63}$$

If we expand the dimensionless potential in Taylor series (\mathbb{Z}_2 even and odd operators), then the coefficients are the dimensionless running coupling constants λ_n

$$v(\varphi) = \sum_{n=1}^{\infty} \frac{\lambda_n}{n!} \varphi^n \tag{3.64}$$

and their dimensionless beta functions $\beta_n \equiv \mu \, \partial_\mu \lambda_n$ can be straightforwardly extracted inserting (3.61) in

$$\beta_n = \frac{\partial^n}{\partial \varphi^n} \beta_v(\varphi) \Big|_{\varphi \to 0} \tag{3.65}$$

The final step to determine the existence of a universality class in a given d_c is to solve for the fixed points

$$\beta_i = 0 \tag{3.66}$$

Let's see how it is applied for the Ising universality class in d = 3.

3.5.2 Fixed Points and Critical Exponents in $d = 4 - \varepsilon$

Before analysing the fixed points and subsequently calculating the critical exponents in d=3 using FDR, let us first examine the structure of the beta functions as derived through the ε -expansion. This involves expanding around the upper critical dimension, which means setting $d=d_c-\varepsilon$ [4]. We want to show which is the functional form of the beta functions within this theoretical framework. To proceed, we substitute equation (3.18) into equation (3.61), noting that at this stage, we set $d=4-\varepsilon$. Then using (3.65) we find the following system of beta functions (we re-scaled factors of 4π for clarity)

$$\beta_{1}^{\text{FPRG}} = -(3 - \frac{\epsilon}{2})\lambda_{1} + \lambda_{2}\lambda_{3} - \frac{1}{2}\lambda_{3}^{2} - \lambda_{2}\lambda_{3}\lambda_{4} + \frac{1}{12}\lambda_{1}\lambda_{4}^{2}$$

$$\beta_{2}^{\text{FPRG}} = -2\lambda_{2} + \lambda_{4}\lambda_{2} + \lambda_{3}^{3} - \frac{5}{2}\lambda_{3}^{2}\lambda_{4} - \frac{5}{6}\lambda_{2}\lambda_{4}^{2}$$

$$\beta_{3}^{\text{FPRG}} = -(1 + \frac{\epsilon}{2})\lambda_{3} + 3\lambda_{4}\lambda_{3} - \frac{23}{4}\lambda_{3}\lambda_{4}^{2}$$

$$\beta_{4}^{\text{FPRG}} = -\epsilon + 3\lambda_{4}^{2} - \frac{17}{3}\lambda_{4}^{3}$$

For this set of equations, the fixed points are determined to subsequently calculate the critical exponents. We will present the results derived from this method at the end of the chapter. The fixed point for this set of equation is found by setting $\beta_i = 0$ which for this case we find

$$\lambda_1^* = 0$$
 $\lambda_2^* = 0$ $\lambda_3^* = 0$ $\lambda_4^* = \frac{\epsilon}{3} - \frac{17}{81}\epsilon^2 + \mathcal{O}(\epsilon^3)$

In the ϵ -expansion for the O(N) theory the critical exponent have the following form at two-loop order [71]:

$$\nu = \frac{1}{2} + \frac{N+2}{4(N+8)}\epsilon + \frac{N^3 + 25N^2 + 106N + 120}{8(N+8)^3}\epsilon^2 + \mathcal{O}(\epsilon^3)$$

$$\omega = \epsilon - \frac{3(3N+14)}{(N+8)^2}\epsilon^2 + \mathcal{O}(\epsilon^3)$$

$$\eta = \frac{N+2}{2(N+8)^2}\epsilon^2 + \mathcal{O}(\epsilon^3)$$
(3.67)

In our case of interest we set N=1 and $\epsilon=1$ since we want to see the result for d=3, this yields

$$\nu = 0.626543$$
 $\omega = 0.37037$
 $\eta = 0.0185185$

We will assess the quality of these estimates in the following.

3.5.3 Fixed Points and Critical Exponents in d = 3 at FDR-LPA

Now that we have presented all the necessary elements to calculate the critical exponents, we will proceed to develop an example in the most pedagogical way possible. Specifically, we aim to compare the three theoretical frameworks previously discussed and demonstrate the procedure required for a concrete example. To this end, we will solve the flow equation at the lowest order of the derivative expansion in the case of three dimensions.

The first step is to find the beta functions in their dimensionless form, as explained throughout this chapter, which in the case of the FDR takes the form

$$\beta_v^{\text{FDR}}(\varphi) = -3v(\varphi) + \frac{1}{2}\varphi v'(\varphi) + e^{-\frac{v''(\varphi)}{4\pi}}$$
(3.68)

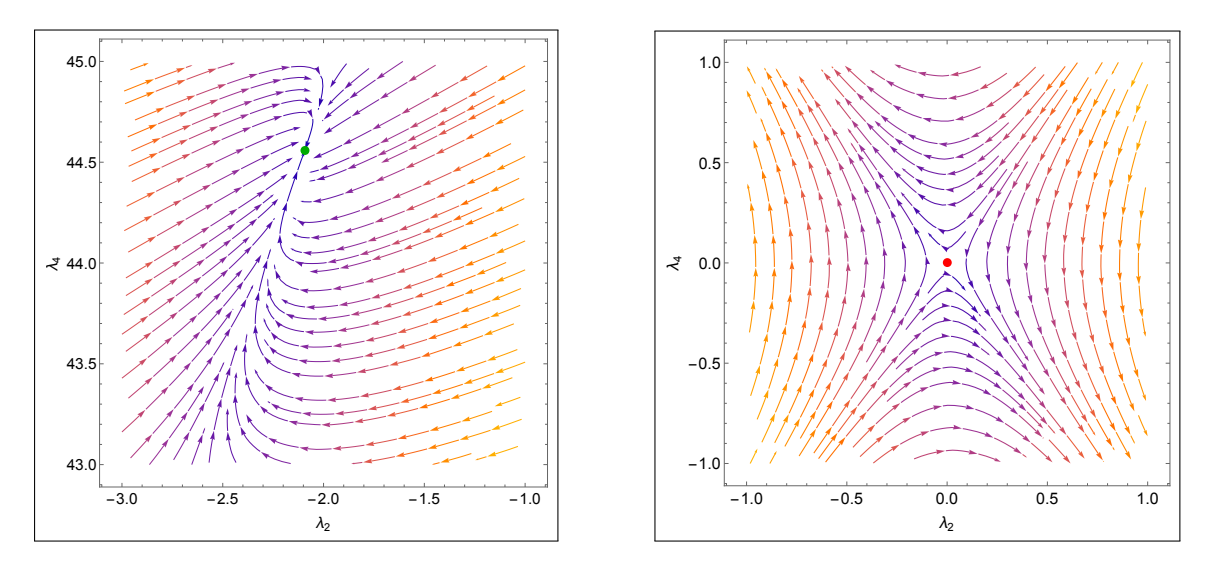


Figure 3.6: Flow in the (λ_2, λ_4) plane in d = 3. The Gaussian (red) and Wilson-Fisher (green) fixed point.

Instead of solving the partial differential equation (3.68) we employ a polynomial truncation on the potential where we expect \mathbb{Z}_2 symmetry at the fixed point, thus we keep only even couplings in (3.64), note that this expansion is valid for the three framework (FPRG, NPRG and FDR). With these considerations, the local potential takes the following form

$$v(\varphi) = \sum_{n=1}^{N_{tr}} \frac{\lambda_{2n}}{(2n)!} \varphi^{2n} = \frac{\lambda_2}{2} \varphi^2 + \frac{\lambda_4}{4!} \varphi^4 + \frac{\lambda_6}{6!} \varphi^6 + \cdots$$
 (3.69)

where N_{tr} is the truncation order. By plugging (3.69) in (3.68) we find that for $N_{tr} = 2$ the β_v takes the form⁷

$$\beta_v(\varphi) = -\lambda_2 \varphi^2 - \frac{1}{24} \lambda_4 \varphi^4 + e^{-\frac{\lambda_4 \varphi^2 + 2\lambda_2}{8\pi}}$$
 (3.70)

then the beta functions as defined in (3.65) are

$$\beta_2 = -2\lambda_2 - \frac{\lambda_4}{4\pi} e^{-\frac{\lambda_2}{4\pi}} \qquad \beta_4 = -\lambda_4 + \frac{3\lambda_4^2}{(4\pi)^2} e^{-\frac{\lambda_2}{4\pi}}$$
(3.71)

The fixed point equations are transcendental but can still be solved exactly in the lowest cases. The Ising-Wilson-Fisher fixed point is

⁷To alleviate the notation, from this point onward we will no longer use the FDR superscript, and all the beta functions presented will correspond to this scheme.

$$\beta_2 = \beta_4 = 0 \qquad \Rightarrow \qquad \lambda_2^* = -\frac{2\pi}{3} \qquad \lambda_4^* = \frac{16\pi^2}{3\sqrt[6]{e}}$$
 (3.72)

The stability matrix, used to determine the critical exponent, is defined as $M_{ij} = \frac{\partial \beta_{2i}}{\partial \lambda_{2j}}$. Evaluated at the Wilson-Fisher (WF) fixed point, the stability matrix is:

$$\mathbb{M} = \begin{pmatrix} -\frac{5}{3} & -\frac{4\pi}{3\sqrt[6]{e}} \\ -\frac{6\sqrt{e}}{4\pi} & 1 \end{pmatrix}$$
 (3.73)

and has eigenvalues

$$\{\Lambda_1, \Lambda_2\} = \left\{\frac{-\sqrt[6]{e} - \sqrt{19}\sqrt[6]{e}}{3\sqrt[6]{e}}, \frac{\sqrt{19}\sqrt[6]{e} - \sqrt[6]{e}}{3\sqrt[6]{e}}\right\} = \{-1.7863..., 1.11963...\}$$

The exponents are thus $\nu(N_{tr}=2)=-1/\Lambda_1=0.559816...$ and $\omega(N_{tr}=2)=\Lambda_2=1.11963...$ When the $N_{tr}=3$ the dimensionless beta functionals is

$$\beta_v(\varphi) = -\lambda_2 \varphi^2 - \frac{1}{24} \lambda_4 \varphi^4 + e^{-\frac{\lambda_6 \varphi^4 + 12\lambda_4 \varphi^2 + 24\lambda_2}{96\pi}}$$
(3.74)

from this using (3.65) the beta functions are

$$\beta_{2} = -2\lambda_{2} - \frac{3e^{-\frac{\lambda_{2}}{4\pi}}\lambda_{4}}{4\pi}$$

$$\beta_{4} = -\lambda_{4} + \frac{9e^{-\frac{\lambda_{2}}{4\pi}}\lambda_{4}^{2}}{(4\pi)^{2}} - \frac{5e^{-\frac{\lambda_{2}}{4\pi}}\lambda_{6}}{4\pi}$$

$$\beta_{6} = \frac{45e^{-\frac{\lambda_{2}}{4\pi}}\lambda_{4}\lambda_{6}}{(4\pi)^{2}} - \frac{27e^{-\frac{\lambda_{2}}{4\pi}}\lambda_{4}^{3}}{(4\pi)^{3}}$$
(3.75)

Now the stability matrix takes the form

$$\mathbf{M} = \begin{pmatrix}
-\frac{3}{2} & -\frac{2\pi}{3\frac{4}{\sqrt{e}}} & 0 \\
-\frac{3\frac{4}{\sqrt{e}}}{4\pi} & 2 & -\frac{6\pi}{\frac{4}{\sqrt{e}}} \\
0 & -\frac{5\frac{4}{\sqrt{e}}}{4\pi} & \frac{15}{2}
\end{pmatrix}$$
(3.76)

whose eigenvalues are

$$\{\Lambda_1, \Lambda_2, \Lambda_3\} = \{-1.67498, 1.03671, 8.63827\}$$

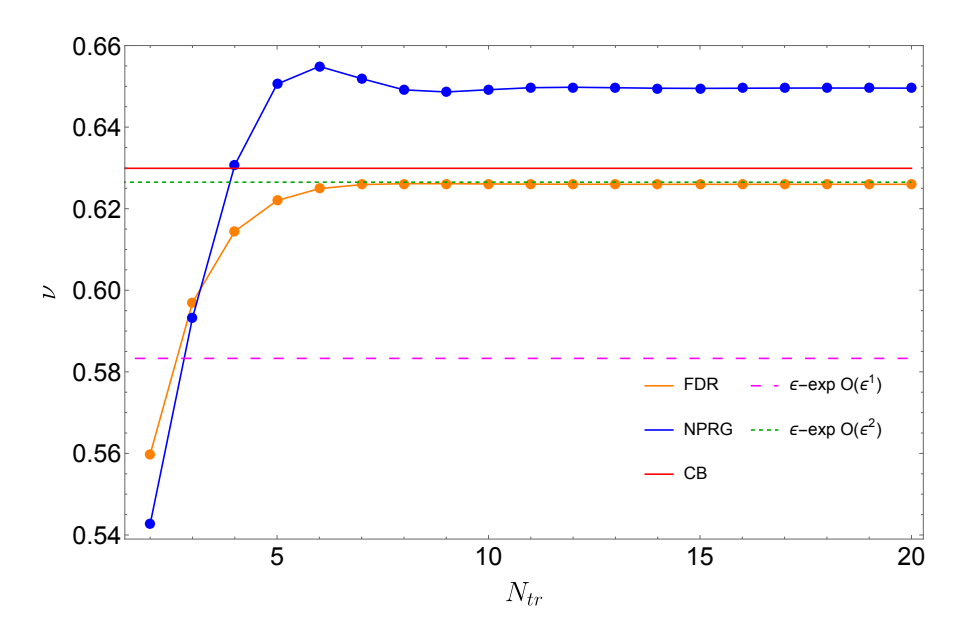


Figure 3.7: Comparison of the convergence of the critical exponent ν in d=3 among the FDR-LPA, NPRG-LPA + Litim cutoff and FPRG.

then $\nu(N_{tr}=3)=-1/\Lambda_1=0.597051...$ and $\omega(N_{tr}=3)=\Lambda_2=1.03671...$ The result of the full analysis is shown in Figures 3.7 and 3.8: convergence to the Bootstrap values (in red) is quite remarkable considering the simplicity of the approximation involved! It is also evident the better convergence with respect to traditional NPRG-LPA with optimized Litim cut-off. For the green line in Figure 3.7 we use the value which come from (3.67). As shown the two loop ϵ -expansion is comparable with our value for the FDR which only has information coming from a one-loop computation whereas the case of ω in the perturbative scenario is quite far from our and the conformal bootstrap result.

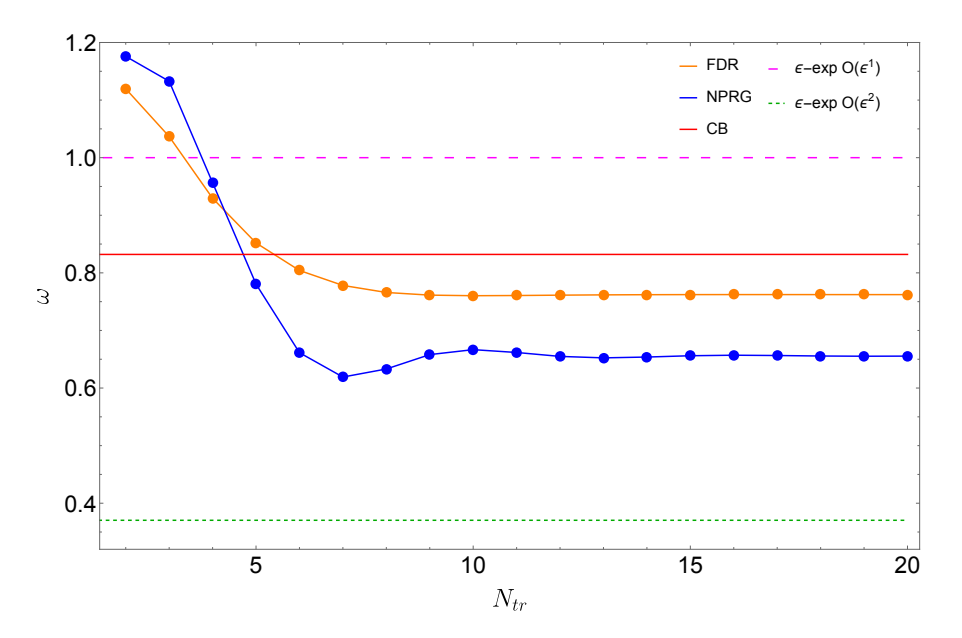


Figure 3.8: Convergence of the critical exponent ω in the FDR-LPA approximation in d=3. Comparison is shown against the state-of-the-art Bootstrap value, the NPRG-LPA + Litim cutoff and FPRG.

The follwing table summarize the final results for the critical exponent withing the varoius methods. It must been said that the fact that the two-loop ϵ -expansion approaches to the CB results is just a coincidence. This can be seen by inspecting the ω critical exponent where this "accuracy" is lost.

Method	ν	
FDR	0.6259	
NPRG	0.6495	
ε -exp $\mathcal{O}(\varepsilon)$	0.5833	
ε -exp $\mathcal{O}(\varepsilon^2)$	0.6265	
СВ	0.6299	

Method	ω	
FDR	0.7622	
NPRG	0.6554	
ε -exp $\mathcal{O}(\varepsilon)$	1	
ε -exp $\mathcal{O}(\varepsilon^2)$	0.37037	
СВ	0.82951	

Table 3.1: Comparison of the ν and ω critical exponents against the differents methods

Chapter 4

Functional Dimensional Regularization for the O(N) Model

In this section, we will study the scalar field O(N) model in three dimensions using our new technique, Functional Dimensional Regularization. We begin by deriving the lowest order in the derivative expansion, specifically the Local Potential Approximation (LPA) for arbitrary N. The critical exponents ν , ω , and η obtained will be compared against those from NPRG-LPA and the derivative expansion (DE) at orders $\mathcal{O}(\partial^2)$ and $\mathcal{O}(\partial^4)$, when appropriate.

As will be shown, we compute the flow equation via two methods: expanding the potential around zero and around a non-vanishing minimum (the spontaneously broken regime). In a subsequent section, we will compute the β -functions using the derivative expansion at order $\mathcal{O}(\partial^2)$, providing a pedagogical explanation of how these equations are derived. Finally, we compare all these results with the state of the art.

4.1 O(N) Local Potential Approximation

4.1.1 FDR-LPA

In this subsection, we focus exclusively on deriving the β_U equation, which describes the RG flow of the potential U for general N. Note that from now on, we will use U for the potential instead of V as we did previously for the N=1 case since the potential U now depends on the variable $\rho=\frac{1}{2}\varphi_i\varphi_i$, unlike the potential V, which depended on φ .

To calculate the β_U function at one loop, recall that the term contributing to the $\frac{1}{\epsilon}$ -pole comes from $\Gamma_1 = \frac{1}{2} \text{Tr} \log \mathbb{S}^{(2)}$, as we saw in the previous chapter. This time, we need to calculate the Hessian $\mathbb{S}^{(2)}$ for N components starting from the action

$$S = \int d^d x \left\{ \frac{1}{2} \partial_\mu \varphi_a \partial^\mu \varphi_a + U(\rho) \right\}. \tag{4.1}$$

Additionally, it will be very useful to define the projectors onto the longitudinal and transverse subspaces; the longitudinal projector is defined by

$$P_{ij} \equiv \frac{\varphi_i \varphi_j}{\varphi^2}$$

while the transverse projector is defined as $\delta_{ij} - P_{ij}$.

Let us motivate the generalization of the equation (3.57) for β_V^{DR} to N components. It will be useful to write down a table of the beta functions (in DR) of the potential in the multi-component case in order to reach a general expression:

	N=1	General N
d_c	eta_V^{DR}	eta_V^{DR}
2	a_2V''	a_2V_{ii}
4	$a_4(V'')^2$	$a_4V_{ij}V_{ji}$
6	$a_6(V'')^3$	$a_6 V_{ij} V_{jk} V_{ki}$
:	:	
2 <i>n</i>	$a_{2n}(V'')^n$	$a_{2n}V_{i_1i_2}V_{i_2i_3}V_{i_ni_1}$

Where the coefficients a_{2n} are defined in (3.53)

$$a_{2n}V_{i_1i_2}V_{i_2i_3}..V_{i_ni_1} = a_{2n}\text{Tr}\mathbb{V}^n$$

From which we obtain the FDR β_V by usual resummation

$$\beta_{V} = \sum_{n=0}^{\infty} \mu^{d-2n} a_{2n} \operatorname{Tr} \mathbb{V}^{n}$$

$$= \sum_{n=0}^{\infty} \mu^{d-2n} \frac{(-1)^{n}}{n!} \frac{1}{(4\pi)^{n}} \operatorname{Tr} \mathbb{V}^{n}$$

$$= \mu^{d} \sum_{n=0}^{\infty} \frac{1}{n!} \operatorname{Tr} \left(\frac{-\mathbb{V}}{4\pi\mu^{2}}\right)^{n}$$

CHAPTER 4. FUNCTIONAL DIMENSIONAL REGULARIZATION FOR THE O(N) MODEL 70

Finally the FDR–LPA beta functional for general *N* is

$$\beta_V(d) = \mu^d \operatorname{tr} e^{-\frac{\mathbb{V}}{4\pi\mu^2}}$$
(4.2)

where $(V)_{ij} \equiv V_{ij}$ is the multi-field Hessian.

The Hessian U_{ij} of the effective potential is

$$U_i \equiv rac{\partial U}{\partial arphi_i} = U' \partial_i
ho = U' arphi_i \qquad \qquad U_{ij} \equiv rac{\partial^2 U}{\partial arphi_i \partial arphi_j} = U' \delta_{ij} + U'' arphi_i arphi_j$$

and can be conveniently decomposed using the projectors as

$$U_{ij} = U'(1-P)_{ij} + (U'+2\rho U'')P_{ij}$$

Thus the multi-component Hessian is

$$V = U'(1 - P) + (U' + 2\rho U'')P$$
(4.3)

Inserting it into the multi-component beta functional, which has the form of (4.2) gives

$$\operatorname{Tr}\left\{e^{-\frac{V}{4\pi\mu^{2}}}\right\} = \operatorname{Tr}\left\{\mathbb{1}e^{-\frac{V}{4\pi\mu^{2}}}\right\} = \operatorname{Tr}\left\{\left[(\mathbb{1} - \mathbb{P}) + \mathbb{P}\right]e^{-\frac{V}{4\pi\mu^{2}}}\right\} \\
= \operatorname{Tr}\left\{(\mathbb{1} - \mathbb{P})e^{-\frac{U'}{4\pi\mu^{2}}(\mathbb{1} - \mathbb{P}) - \frac{U' + 2\rho U''}{4\pi\mu^{2}}}\mathbb{P}\right\} + \operatorname{Tr}\left\{\mathbb{P}e^{-\frac{U'}{4\pi\mu^{2}}(\mathbb{1} - \mathbb{P}) - \frac{U' + 2\rho U''}{4\pi\mu^{2}}}\mathbb{P}\right\} \tag{4.4}$$

If now we expand the exponential in series and use the orthogonality properties we find for the first term of (4.4)

$$(\mathbb{1} - \mathbb{P}) \quad \sum_{n=0}^{\infty} \frac{1}{n!} \left(\frac{-1}{4\pi\mu^2} \right)^n \left[U'(\mathbb{1} - \mathbb{P}) + (U' + 2\rho U'') \mathbb{P} \right]^n$$

$$= (\mathbb{1} - \mathbb{P}) \quad \sum_{n=0}^{\infty} \frac{1}{n!} \left(\frac{-1}{4\pi\mu^2} \right)^n (U')^n$$

$$= (\mathbb{1} - \mathbb{P}) \quad e^{-\frac{U'}{4\pi\mu^2}}$$
(4.5)

where we used

$$\left[U'(\mathbb{1} - \mathbb{P}) + (U' + 2\rho U'') \mathbb{P} \right]^n = (U')^n (\mathbb{1} - \mathbb{P}) + (U' + 2\rho U'')^n \mathbb{P}$$

Taking the trace of (4.5) and noting that tr(1 - P) = N - 1 we find

$$Tr\{(\mathbb{1} - \mathbb{P})e^{-\frac{U'}{4\pi\mu^2}}\} = (N-1)e^{-\frac{U'}{4\pi\mu^2}}$$
(4.6)

By doing the same analysis to the second term of (4.4) using that tr $\mathbb{P} = 1$ we arrive at

$$Tr\{\mathbb{P}e^{-\frac{U''+2\rho U''}{4\pi\mu^2}}\} = e^{-\frac{U''+2\rho U''}{4\pi\mu^2}}$$
(4.7)

Finally we add (4.6) and (4.7) in order to find the O(N) beta functional for the potential $U(\rho)$ (which has a longitudinal and a tangential part):

$$\beta_{U}(d) = \mu^{d} (N-1) e^{-\frac{U'}{4\pi\mu^{2}}} + \mu^{d} e^{-\frac{U'+2\rho U''}{4\pi\mu^{2}}}$$
(4.8)

It is clear that in the $N \to 1$ limit only the longitudinal part survives, thus recovering the Ising beta functional of the previous chapter.

The final step is to write the dimensionless form of the beta functional:

$$\beta_u = -du + (d-2)\rho u' + (N-1)e^{-\frac{u'}{4\pi}} + e^{-\frac{u'+2\rho u''}{4\pi}}$$
(4.9)

There are at least two things to remark about this equation. First, despite it is valid for any dimension d, we will fix d=3. Because of the rapid convergence provided by the exponential it is possible to study the solutions of $\beta_u=0$ using a polynomial expansion. Second, this is the same β_u found using the Proper time RG [72, 73, 74, 75, 76] which yields to very good results on the exponent ν [77]. The noteworthy aspect is that many questioned the validity of this approach since it was not originally derived from first principles. However, it has now been established on a more solid foundation.

4.1.2 NPRG-LPA

In a previous chapter, we discussed how the Wetterich equation (3.31) describes the flow of the average effective action. We observed that, to solve this equation, it is necessary not only to provide an Ansatz but also to specify the regulator. To study the flow equation for the O(N) model in d dimension we pick the following action

(which is the action corresponding to (4.1))

$$\Gamma_k = \int d^d x \left(\frac{1}{2} \partial_\mu \phi_a \partial^\mu \phi_a + U_k(\rho) \right) \tag{4.10}$$

which is the leading order in the derivative expansion, the local potential approximation (LPA). By plugging this Ansatz in the Wetterich equation and using the Litim cut-off (3.27) we arrive at the flow equation in its dimensionful form [78]

$$\beta_U = \mu^{d+2}(N-1)\frac{c_d}{\mu^2 + U'} + \mu^{d+2}\frac{c_d}{\mu^2 + U' + 2\rho U''}$$
(4.11)

where $c_d = \frac{2}{d(4\pi)^{d/2}\Gamma(d/2)}$. Passing to dimensionless variables we find the flow equation has the following form

$$\beta_u = -du + (d-2)\rho u' + (N-1)\frac{c_d}{1+u'} + \frac{c_d}{1+u'+2\rho u''}$$
(4.12)

This equation (4.12) display two scaling solution for $3 \le d < 4$, which refer to the Gaussian and Wilson-Fisher fixed point. The former has the trivial solution $u^* = cte$ and the latter has a non trivial fixed point which is the case of interest. The study of this equation with this and other choice for the cutoff can be found in [69, 78, 79, 80, 81, 82].

4.1.3 Fixed Points and Critical Exponents

Almost all ingredients have been presented to compute the flow equation and, with it, the universal critical exponents. The last but not least important decision to make is regarding the potential. Here, we employ a polynomial truncation, of the scaling potential, which means expanding the potential to order $\phi^{2N_{tr}}$ up to a truncation number N_{tr} .

There are two ways to perform this polynomial expansion. The first is around zero, where $u(\rho = 0) = 0$, and the second is around the minimum of the potential, $\rho = \rho_0$, where $u'(\rho = \rho_0) = 0$. Thus, with the first expansion, the potential is

$$u(\rho) = \sum_{n=1}^{N_{tr}} \frac{\lambda_n}{n!} \rho^n \tag{4.13}$$

where λ_n are the running couplings. The second expansion, which approximate

around the minimum has the form

$$u(\rho) = \sum_{n=2}^{N_{tr}} \frac{1}{n!} \lambda_n (\rho - \lambda_1)^n$$
(4.14)

Here λ_1 is the position of the minimum. Moreover, note that the potential is normalised as $u(\lambda_1) = 0$. Now, we have N_{tr} coupled ordinary differential equations $\partial_t \lambda_i \equiv \beta_i(\lambda_n)$ for the entire set of couplings. In this section we compare the NPRG-LPA-Litim [78, 83] with the novel FDR-LPA. We perform both an expansion around zero and around the minima.

Expansion around zero For the expansion around zero we computed the different critical exponents for N=0,1,2,3,4,5,10,20,100 at $N_{tr}=20$. Results are reported in Table 4.1 for the critical exponents ν, ω, ω_3 and ω_4 (following the conventions of [78]) while the convergences of the truncation is shown in Figures 4.1 and 4.2.

N	ν (2-digits)	ν	ω	ω_3	ω_4
0	0.58	0.5827	0.7818	3.8989	7.48507
1	0.63	0.6259	0.7622	3.6853	7.03162
2	0.67	0.6689	0.7457	3.4930	6.62476
3	0.71	0.7103	0.7345	3.3258	6.27486
4	0.75	0.7485	0.7296	3.1850	5.98801
5	0.78	0.7825	0.7313	3.07	5.75845
10	0.89	0.8867	0.7916	2.8267	4.92327
20	0.9 5	0.9483	0.8823	2.8310	5.02247
100	0.99	0.9907	0.976	2.9592	4.94072

Table 4.1: FDR-LPA with expansion around zero (4 significant digits). The first column shows in bold face those two significant digits for the exponent ν which match state-of-the-art estimates.

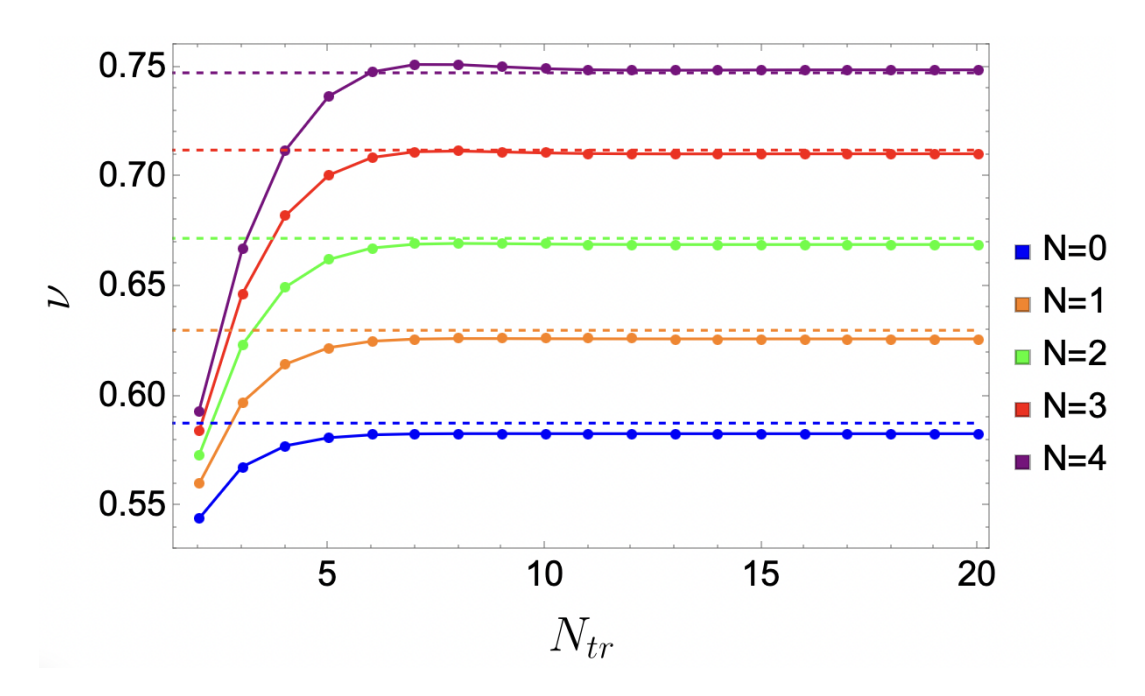


Figure 4.1: Convergence of the critical exponent ν in the FDR-LPA applied to O(N) models. Comparison is made with state-of-the-art estimates (CB).

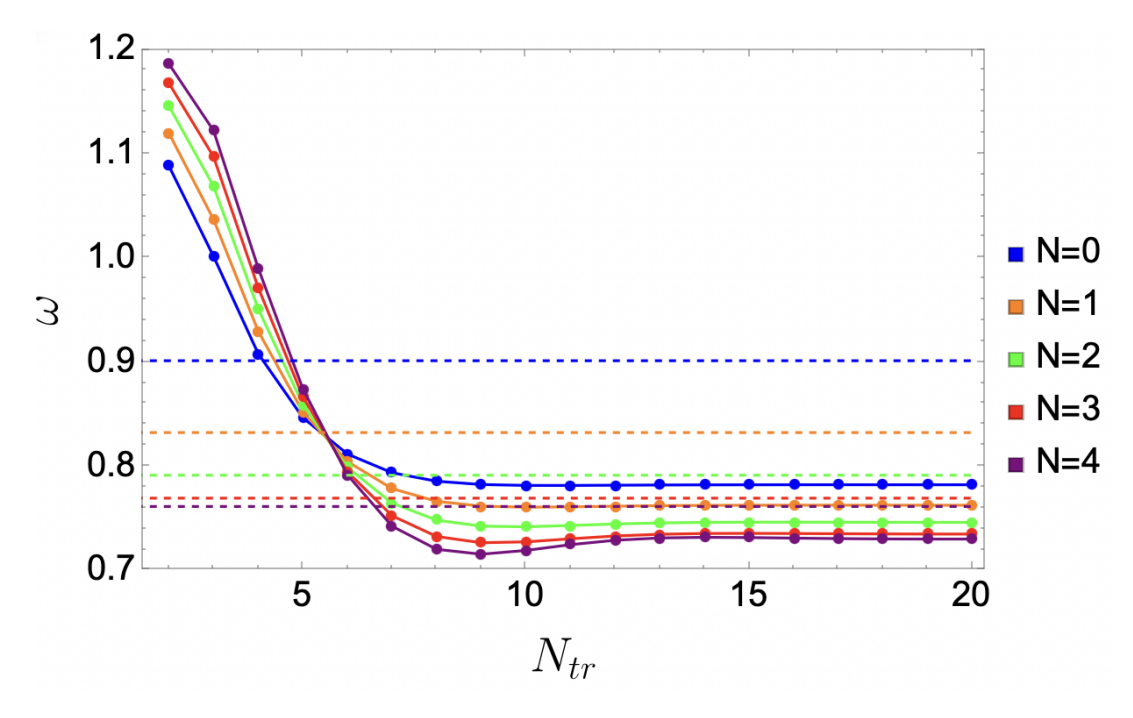


Figure 4.2: Convergence of the critical exponent ω in the FDR-LPA applied to O(N) models. Comparison is made with state-of-the-art estimates DE at $\mathcal{O}(\partial^4)$ [39].

Expansion around minima For the expansion around the minima, we find almost the exact same values as in the expansion around zero. The advantage of this ap-

N	ν	ω	ω_3	ω_4
0	0.5827	0.7818	3.8986	7.49054
1	0.6259	0.7622	3.6845	7.03796
2	0.6689	0.7457	3.4914	6.62782
3	0.7103	0.7345	3.3235	6.26572
4	0.7485	0.7298	3.1829	5.94951
5	0.7825	0.7316	3.0708	5.70194
10	0.8868	0.7906	2.8306	5.02365
20	0.9483	0.8831	2.8342	4.81965
100	0.9907	0.9768	2.9592	4.9384

Table 4.2: FDR-LPA with expansion around the minima (4 significant digits).

proach is the fast convergence. The computation of the beta functions for the minima λ_1 and for the couplings λ_n are a little bit different from the expansion around zero. We follow the approach from [82] where we learnt that the running of the minimum is obtained by taking a total t-derivative of the condition $u'(\lambda_1) = 0$

$$\frac{\mathrm{d}}{\mathrm{d}t}u'(\lambda_1) = u''\frac{\partial\lambda_1}{\partial t} + \frac{\partial u'}{\partial t} = 0$$

This means that

$$\frac{d\lambda_1}{dt} = \beta_{\lambda_1} = -[u''(\lambda_1)]^{-1} \frac{\partial u'}{\partial t} \Big|_{\rho = \lambda_1}$$
(4.15)

In this regime the evolution equation for the couplings λ_n are computed as

$$\frac{d\lambda_n}{dt} = \beta_{\lambda_n} = \frac{\partial u^{(n)}}{\partial t} \Big|_{\rho = \lambda_1} + \lambda_{n+1} \frac{d\lambda_1}{dt}$$
(4.16)

Results are reported in Table 4.2 for the critical exponents ν , ω , ω_3 and ω_4 (following the conventions of [78]) while the results of the convergences is reported in Figures 4.3 and 4.4.

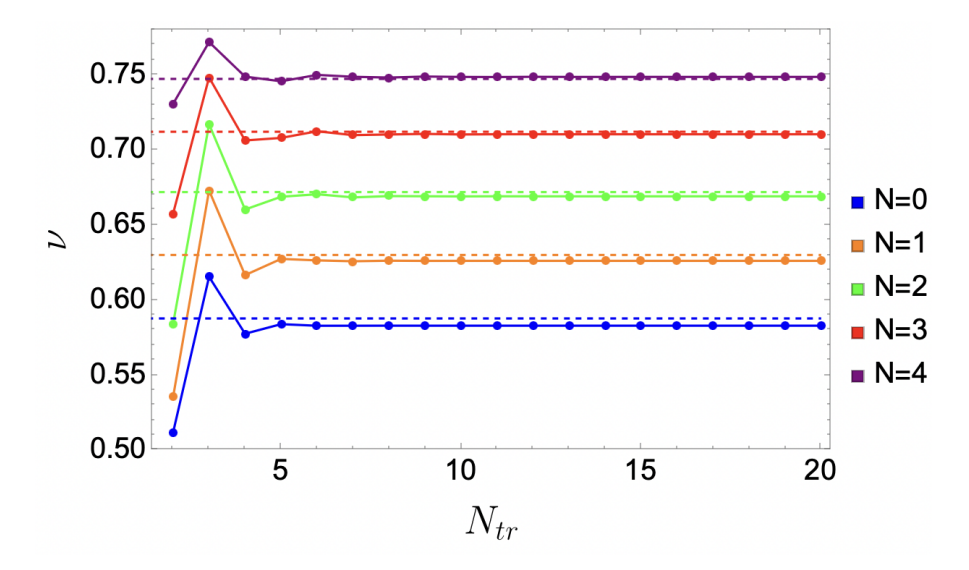


Figure 4.3: Convergence of the critical exponent ν in the FDR-LPA around the minima applied to O(N) models. Comparison is made with state-of-the-art estimates (CB) dashed lines.

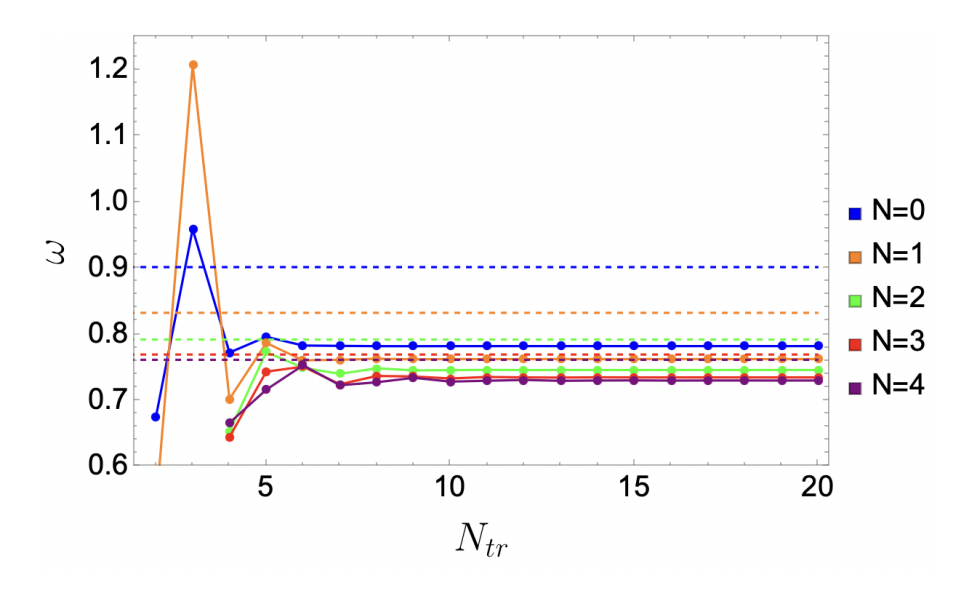


Figure 4.4: Convergence of the critical exponent ω in the FDR-LPA around the minima applied to O(N) models. Comparison is made with state-of-the-art estimates DE at $\mathcal{O}(\partial^4)$ [39].

4.1.4 Comparison with NPRG-Litim

We conclude this section by showing the comparison for the third and fourth subleading critical exponents. Although their computation is not common, we include it for completeness. The critical exponent computed by the author in [78] are shown in Table 4.3 and 4.4 to be compared with our results.

CHAPTER 4. FUNCTIONAL DIMENSIONAL REGULARIZATION FOR THE O(N) MODEL 77

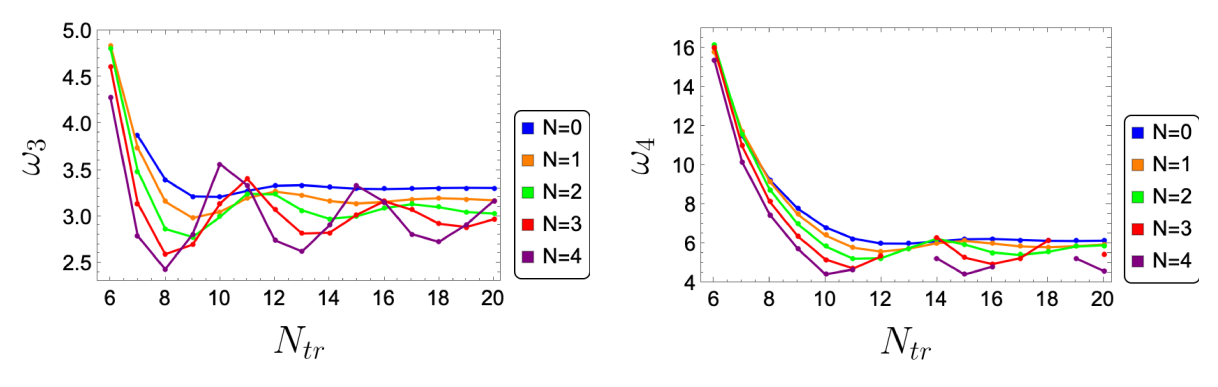
Figure 4.5 shows that the convergence of the critical exponents ω_3 and ω_4 in the case of NPRG is not as good as that obtained with the FDR. The latter exhibits rapid convergence using only $N_{tr}=20$ as the number of truncation, whereas in the NPRG formalism, convergence is only achieved at N=0. Additionally, it is evident that as the number N increases, the tendency to converge is lost.

N	$v^{ m NPRG}$	$\nu^{ ext{FDR}}$	ω^{NPRG}	$\omega^{ ext{FDR}}$
0	0.592083	0.582784	0.65788	0.781865
1	0.649562	0.625979	0.655746	0.762214
2	0.708211	0.668978	0.671221	0.745742
3	0.761123	0.710327	0.699837	0.734503
4	0.804348	0.748549	0.733753	0.729699
5	0.837741	0.782514	0.766735	0.731383
10	0.918605	0.886757	0.871311	0.791678

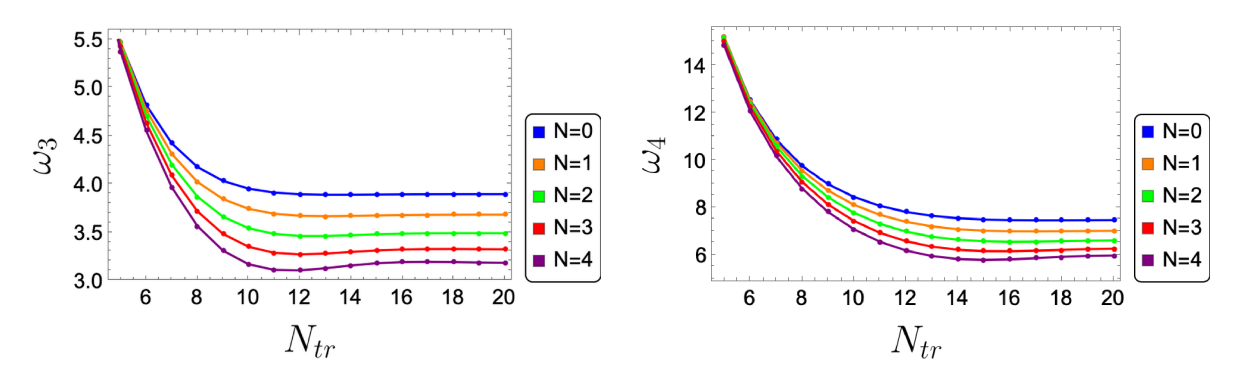
Table 4.3: Comparision between the critical exponent ν and ω for the NPRG and FDR at LPA level.

N	ω_3^{NPRG}	$\omega_3^{ ext{FDR}}$	ω_3^{NPRG}	$\omega_4^{ ext{FDR}}$
0	3.308	3.89896	6.16	7.48507
1	3.180	3.68532	5.912	7.03162
2	3.0714	3.49307	5.679	6.62476
3	2.9914	3.3258	5.482	6.27486
4	2.9399	3.1850	5.330	5.98801
5	2.9180	3.07	5.2195	5.75845
10	2.89846	2.82675	5.00420	4.92327

Table 4.4: Comparision of the sub-leading critical exponent within the NPRG and FDR $\,$



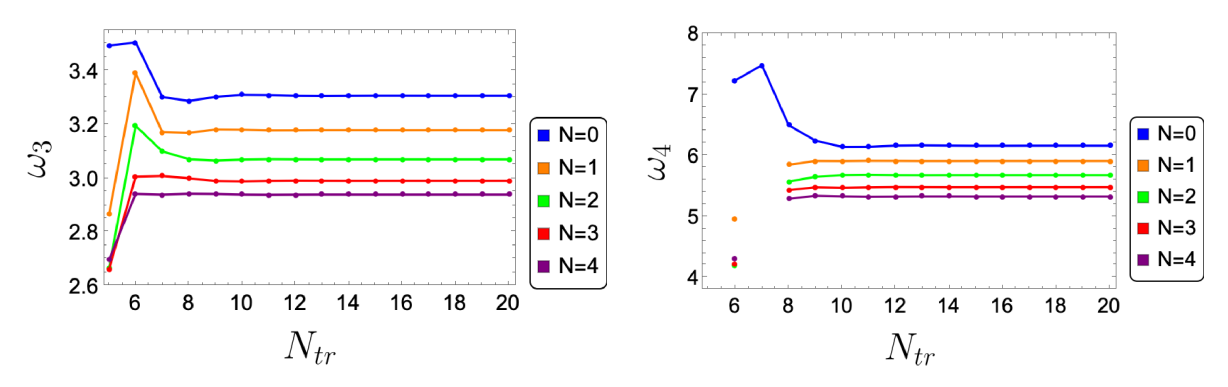
- (a) ω_3 critical exponent for the NPRG-LPA Litim case around zero
- (b) ω_4 critical exponent for the NPRG-LPA Litim case around zero.



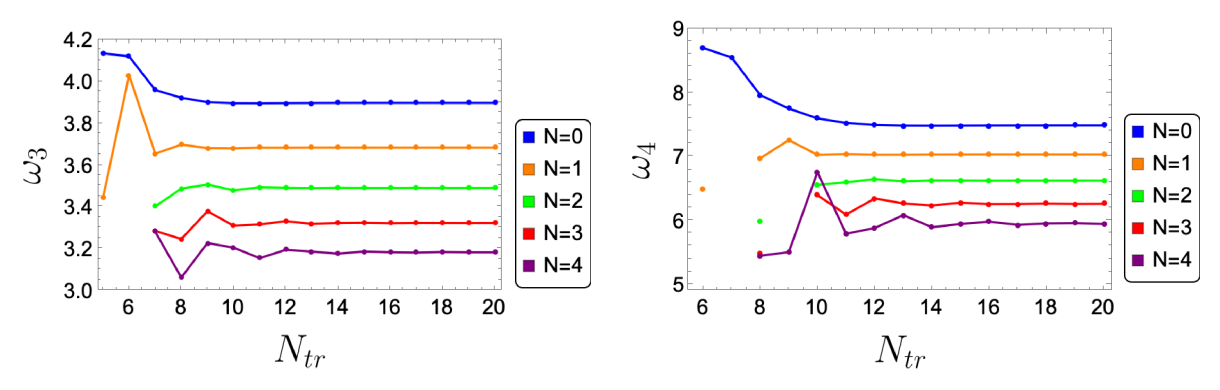
(c) ω_3 critical exponent for the FDR-LPA (d) ω_4 critical exponent for the FDR-LPA around zero.

Figure 4.5: Comparison of the critical exponent ω_3 and ω_4 computed from the Litim equations and the FDR at the LPA around zero.

In contrast, Figure 4.6 demonstrates that the convergence of ω_3 and ω_4 for NPRG around the minima is much better than that computed around zero. As mentioned in [84, 85], the study performed using field truncation indicates that the expansion around the minima has better convergence compared to the expansion around zero. Our results for the FDR are consistent with this observation. Moreover, unlike NPRG with the expansion around zero, the convergence for the critical exponents is present for all N in the FDR. As the reader might noted some of the curves for the NPRG approach are not continous, this is because the results for that critical exponent at this truncantion number has a small imaginary part as stated in [78] and therefore not plotted.



- around the minima.
- (a) ω_3 critical exponent for the NPRG-LPA case (b) ω_4 critical exponent for the NPRG-LPA case around the minima.



(c) ω_3 critical exponent for the FDR-LPA (d) ω_4 critical exponent for the FDR-LPA around the minima. around the minima.

Figure 4.6: Comparison of the critical exponent ω_3 and ω_4 computed from the Litim equations and the FDR at the LPA around the minima.

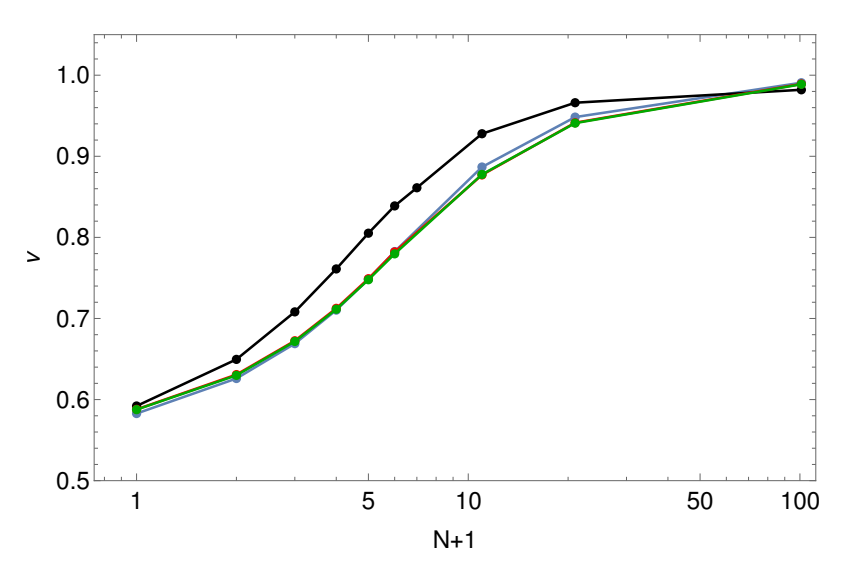


Figure 4.7: Estimate of the critical exponent ν as a function of N at d=3 at order LPA (black), order $\mathcal{O}(\partial^2)$ (red), order $\mathcal{O}(\partial^4)$ (green), FDR(blue).

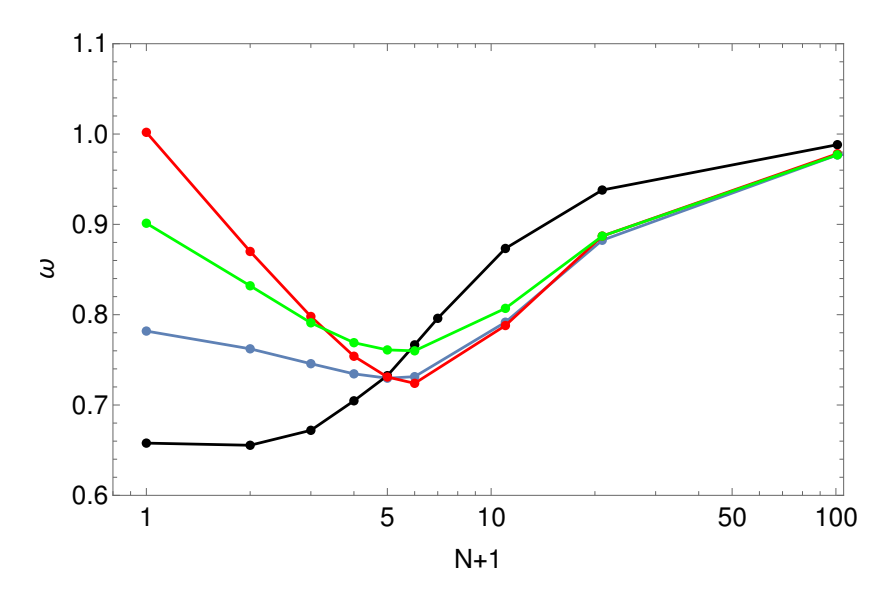


Figure 4.8: Estimate of the critical exponent ω as a function of N at d=3 at order LPA (black), order $\mathcal{O}(\partial^2)$ (red), order $\mathcal{O}(\partial^4)$ (green), FDR at LPA (blue).

We conclude this section by showing the critical exponents ν and ω as functions of N in three dimensions. The Figures 4.7 and 4.8 presents the final estimates for these critical exponents within the framework of NPRG for orders $\mathcal{O}(\partial^0)$, $\mathcal{O}(\partial^2)$, and $\mathcal{O}(\partial^4)$ compared with results of the FDR. For the critical exponent ω , it is noteworthy that, unlike LPA-NPRG, the LPA-FDR yields the same shape as for $\mathcal{O}(\partial^2)$, and $\mathcal{O}(\partial^4)$.

4.2 O(N) **Derivative Expansion**

In this section we present the result for the O(N) with the Functional Dimensional Regularization using the derivative expansion [86]. We will show how to derive the beta function for the potential, the wave function renormalization and the Y function. At the end we will compare the outcoming results with the NPRG and the state-of-the-art predictions.

4.2.1 Action

For the study of the O(N) model by means of the derivative expansion at second order $\mathcal{O}(\partial^2)$ the action is constructed by the addition of two functions $Z(\rho)$ and $Y(\rho)$ [65]

$$S = \int d^{d}x \left\{ \frac{1}{2} (\partial_{\mu} \varphi_{i} \partial^{\mu} \varphi^{i}) + U(\rho) + \frac{1}{2} Z(\rho) (\partial_{\mu} \varphi_{i} \partial^{\mu} \varphi^{i}) + \frac{1}{4} Y(\rho) \partial_{\mu} \rho \partial^{\mu} \rho \right\}$$
(4.17)

Note that unlike traditionally done, we separate the functional *Z* from the kinetic term, which makes it convenient to work with the equivalent parametrization

$$S = \int d^d x \left\{ \frac{1}{2} (\partial_\mu \varphi_i \partial^\mu \varphi^i) + U(\rho) + \left[Z_T(\rho) (\delta_{ij} - P_{ij}) + Z_L(\rho) P_{ij} \right] \frac{1}{2} (\partial_\mu \varphi^i \partial^\mu \varphi^j) \right\}$$
(4.18)

where we use the defined longitudinal $P_{ij}=\frac{\phi_i\phi_j}{\phi^2}$ and transverse $\delta_{ij}-P_{ij}$ projectors. To transition from one parametrization to another, simply map $Z=Z_T$ and $Y=\frac{Z_L-Z_T}{\rho}$. The benefit of using (4.18) becomes apparent in the limit as $N\to 1$, where $P_{ij}\to 1$ and $(\delta_{ij}-P_{ij})\to 0$. Consequently, in this limit, $Z_{N=1}(\phi)=Z_L(\rho)$.

4.2.2 β_U in presence of Z and Y

Since in the second order of the derivative expansion $(\mathcal{O}(\partial^2))$ we have the presence of the functions Z and Y, the functional form of the β_U changes from the LPA. To proceed with the calculation of β_U , we follow the method similar to the one used previously. First, we need to calculate the Hessian of the action (4.17) at a constant field, insert it in one loop contribution and extract the $\frac{1}{\epsilon}$ -poles. The Hessian $S^{(2)}$ of the action (4.18) at constant field reads

$$(S^{(2)}(q))_{ij} = (U' + q^2(1+Z))\delta_{ij} + \rho(2U'' + q^2Y)P_{ij}$$

= $(U' + q^2(1+Z))(\mathbb{1} - \mathbb{P}) + (2U''\rho + U' + q^2(1+Z+\rho Y))\mathbb{P}.$

Recall the one loop effective action where we plug the Hessian

$$\Gamma_{1} = -\frac{1}{2} \int_{0}^{\infty} \frac{ds}{s} \int_{q} \operatorname{tr} e^{-s[S^{(2)}(q)]_{ij}}
= -\frac{1}{2} \int_{0}^{\infty} \frac{ds}{s} \int_{q} \operatorname{tr} \left\{ (\mathbb{1} - \mathbb{P}) e^{-s(q^{2}(1+Z)+U')} + \mathbb{P} e^{-s(q^{2}(1+Z+\rho Y)+U'+2\rho U'')} \right\}
= -\frac{1}{2} \int_{0}^{\infty} \frac{ds}{s} \int_{q} \left\{ (N-1) e^{-s(q^{2}(1+Z)+U')} + e^{-s(q^{2}(1+Z+\rho Y)+U'+2\rho U'')} \right\}$$

If we plan to work on the (U, T, L) basis it is possible to identify

$$Z_T \rightarrow Z \qquad Z_L \rightarrow Z + \rho Y$$

 $\omega_T \rightarrow U' \qquad \omega_L \rightarrow U' + 2\rho U''$

Then Γ_1 is

$$\Gamma_1 = -\frac{1}{2} \int_0^\infty \frac{ds}{s} \int_q \left\{ (N-1)e^{-s(q^2(1+Z_T)+\omega_T)} + e^{-s(q^2(1+Z_L)+\omega_L)} \right\}$$

As usual the integral in the momentum q splits in two, one part which contains the angular factor $S_d = \frac{2\pi^{d/2}}{\Gamma(d/2)}$ and another which is the integral in the momentum; after we perform both we find

$$\Gamma_1 = -\frac{1}{2(4\pi)^{d/2}} \int_0^\infty ds \, s^{-(\frac{d}{2}+1)} \left\{ (N-1) \frac{e^{-s\omega_T}}{(1+Z_T)^{\frac{d}{2}}} + \frac{e^{-s\omega_L}}{(1+Z_L)^{\frac{d}{2}}} \right\}$$
(4.19)

Now we do the proper-time integral which gives Gamma functions

$$\Gamma_{1} = -\frac{\Gamma\left(-\frac{d}{2}\right)}{2(4\pi)^{d/2}} \left\{ (N-1) \left(\frac{\omega_{T}}{1+Z_{T}}\right)^{\frac{d}{2}} + \left(\frac{\omega_{L}}{1+Z_{L}}\right)^{\frac{d}{2}} \right\}$$
(4.20)

This Gamma function present divergences when $d=2n\equiv d_c$ with integer n. As our definition of beta functions requires to look for the $\frac{1}{\epsilon}$ -poles in the complex d-plane we just need to use the relation $\Gamma\left(-\frac{d}{2}\right)=\frac{1}{\epsilon}(-1)^{d_c/2}\frac{2}{(d_c/2)!}+...$ The beta functionals at d_c are minus the respective residue

$$\beta_{U}^{\text{DR}}(d_{c}) = \frac{(-1)^{\frac{d_{c}}{2}}}{(4\pi)^{\frac{d_{c}}{2}} \left(\frac{d_{c}}{2}\right)!} \left\{ (N-1) \left(\frac{\omega_{T}}{1+Z_{T}}\right)^{\frac{d_{c}}{2}} + \left(\frac{\omega_{L}}{1+Z_{L}}\right)^{\frac{d_{c}}{2}} \right\}$$
(4.21)

Finally we apply the master formula (3.47) and sum over all critical dimensions $d_c = 0, 2, 4, 6, 8, ...$

$$\beta_{U}(d) = \sum_{d_{c}=0}^{\infty} \mu^{d-d_{c}} \frac{1}{\left(\frac{d_{c}}{2}\right)!} \left\{ (N-1) \left(\frac{-\omega_{T}}{4\pi(1+Z_{T})} \right)^{\frac{d_{c}}{2}} + \left(\frac{-\omega_{L}}{4\pi(1+Z_{L})} \right)^{\frac{d_{c}}{2}} \right\}$$
(4.22)

which is the series for exponential functions and returns the FDR–DE2 beta functional for the potential

$$\beta_U = \mu^d (N - 1) e^{-\frac{U'}{4\pi\mu^2(1 + Z_T)}} + \mu^d e^{-\frac{U' + 2\rho U''}{4\pi\mu^2(1 + Z_L)}}.$$
 (4.23)

From here it is clear that in the case N = 1 we get the Ising flow at order FDR-DE2

$$\beta_V(\varphi) = \mu^d e^{-\frac{V''}{4\pi\mu^2(1+Z)}}. (4.24)$$

This is exactly what we get when we consider the case of N=1 and the action only contains a potential V and $Z(\phi)\frac{1}{2}(\partial\phi)^2$. By direct computation we see that $V''(\phi)=U'(\rho)+2\rho U''(\rho)$ where V is the potential for the one field component case which we write as a function of the field ϕ .

4.2.3 Feynman Rules

When working at second order in the derivative expansion, there are two diagrams that contribute: the tadpole diagram and the polarization diagram. We will discuss these diagrams in more detail in the next subsection. The key aspect of these diagrams is that they involve functional derivatives of the effective action. Specifically, the tadpole diagram involves a fourth derivative, while the polarization diagram involves a third derivative. Therefore, in this subsection, we explicitly derive the Feynman rules of the theory.

Let us call S_1 to the term in action (4.17) regarding the kinetic term, S_2 to the effective potential, S_3 and S_4 to the Z and Y term respectively. To illustrate how the calculations are performed, we focus on the contribution from S_3 . The contributions from S_2 and S_4 are analogous, and their derivation can be found in Appendix B. On the other hand, S_1 contributes only to the propagator, as its result is null starting from the third derivative. As mentioned

$$S_3 = \int_{\mathcal{X}} \frac{1}{2} Z(\rho) (\partial_{\mu} \varphi_i \partial^{\mu} \varphi^i).$$

The third variation has several terms, most of them proportional to $\partial \varphi$ which are zero once we take the field constant and the term that survives has the form:

$$\delta^{3}S_{3} = 3 \int Z'(\varphi \cdot \delta \varphi)(\partial \delta \varphi)^{2} = 3Z' \int \delta_{ij} \varphi_{k} \delta \varphi_{k} \partial \delta \varphi_{i} \partial \delta \varphi_{j}$$
 (4.25)

Continuing with the calculation we can rewrite the variations of the field, being care-

ful with the indices, in the following way $\delta \varphi_i \rightarrow \delta_{xx_2} \delta_{ib}$

$$\frac{\delta^{3}S}{\delta\varphi_{1a}\delta\varphi_{2b}\delta\varphi_{3c}} = Z' \int_{x} \left\{ \varphi_{k}\delta_{xx_{1}}\delta_{ak}\partial_{x}\delta_{xx_{2}}\delta_{ib} \cdot \partial_{x}\delta_{xx_{3}}\delta_{ic} + \text{combinations} \right\}$$

$$= Z' \int_{x} \varphi_{a}\delta_{xx_{1}}\partial_{x}\delta_{xx_{2}}\partial_{x}\delta_{xx_{3}}\delta_{bc} \rightarrow \varphi_{a}(ip_{2}) \cdot (ip_{3})\delta_{bc}$$

where in the last step we move to momentum variables by setting $\partial_{\mu} \to i p_{\mu}$. Finally

$$S_{abc}^{(3)}(p_1, p_2, p_3) = -Z' \left\{ \varphi_a \delta_{bc}(p_2 \cdot p_3) + \varphi_b \delta_{ac}(p_1 \cdot p_3) + \varphi_c \delta_{ab}(p_1 \cdot p_2) \right\}$$
(4.26)

In an analogous way we compute up to the fourth variation, which at constant field is

$$\delta^{4}S_{3} = 6 \int [Z''(\varphi \cdot \delta \varphi)^{2} + Z'(\delta \varphi)^{2}](\partial \delta \varphi \partial \delta \varphi)$$
$$= 6 \int Z''\varphi_{i}\delta \varphi_{i} \varphi_{j}\delta \varphi_{j}\partial \delta \varphi_{k}\delta \varphi_{k} + Z'\delta \varphi_{i}\delta \varphi_{i}\partial \delta \varphi_{k}\partial \delta \varphi_{k}$$

Once again, we rewrite the variation of the field, which transforms S_4 into

$$\frac{\delta^{4}S_{3}}{\delta\varphi_{1a}\delta\varphi_{2b}\delta\varphi_{3c}\delta\varphi_{4d}} = Z'' \int_{x} [\varphi_{a}\delta_{xx_{1}}\varphi_{b}\delta_{xx_{2}}\partial_{x}\delta_{xx_{3}}\delta_{kc}\partial_{x}\delta_{xx_{4}}\delta_{kd} + \cdots]
+ Z' [\delta_{ia}\delta_{xx_{1}}\delta_{ib}\delta_{xx_{2}}\partial_{x}\delta_{xx_{3}}\delta_{kc}\partial_{x}\delta_{xx_{4}}\delta_{kd}]
\rightarrow Z'' [\varphi_{a}\varphi_{b}(ip_{3}) \cdot (ip_{4})\delta_{cd}] + Z' [\delta_{ab}(ip_{3}) \cdot (ip_{4})\delta_{cd}]$$

Putting all the pieces together, we arrive at

$$\begin{split} S_{abcd}^{(4)}(p_{1},p_{2},p_{3},p_{4}) = & - Z'' \bigg\{ \varphi_{a} \varphi_{b} \delta_{cd}(p_{3} \cdot p_{4}) + \varphi_{a} \varphi_{c} \delta_{bd}(p_{2} \cdot p_{4}) \\ & + \varphi_{a} \varphi_{d} \delta_{bc}(p_{2} \cdot p_{3}) + \varphi_{b} \varphi_{c} \delta_{ad}(p_{1} \cdot p_{4}) + \varphi_{b} \varphi_{d} \delta_{ac}(p_{1} \cdot p_{3}) \\ & + \varphi_{c} \varphi_{d} \delta_{ab}(p_{1} \cdot p_{2}) \bigg\} \\ & - Z' \bigg\{ \delta_{ab} \delta_{cd}(p_{3} \cdot p_{4}) + \delta_{ac} \delta_{bd}(p_{2} \cdot p_{4}) + \delta_{ad} \delta_{bc}(p_{2} \cdot p_{3}) \\ & + \delta_{bc} \delta_{ad}(p_{1} \cdot p_{4}) + \delta_{bd} \delta_{ac}(p_{1} \cdot p_{3}) + \delta_{cd} \delta_{ab}(p_{1} \cdot p_{2}) \bigg\} \end{split}$$

We now summaries the Feynman rules by expressing the second, third and fourth variation of the action 4.17. The second variation will be used to compute the propa-

CHAPTER 4. FUNCTIONAL DIMENSIONAL REGULARIZATION FOR THE O(N) MODEL 85 gators:

$$S_{ab}^{(2)}(p_1, p_2) = U^{(1)}\delta_{ab} + U^{(2)}\varphi_a\varphi_b - (1+Z)\delta_{ab}(p_1 \cdot p_2) - \frac{1}{2}Y\varphi_a\varphi_b(p_1 \cdot p_2)$$
 (4.27)

$$S_{abc}^{(3)}(p_{1}, p_{2}, p_{3}) = U^{(2)} \left[\varphi_{a} \delta_{bc} + \varphi_{b} \delta_{ac} + \varphi_{c} \delta_{ab} \right] + U^{(3)} \varphi_{a} \varphi_{b} \varphi_{c}$$

$$- Z^{(1)} \left[\varphi_{c} \delta_{ab}(p_{1} \cdot p_{2}) + \varphi_{b} \delta_{ac}(p_{1} \cdot p_{3}) + \varphi_{a} \delta_{bc}(p_{2} \cdot p_{3}) \right]$$

$$- \frac{1}{2} Y \left[(\varphi_{a} \delta_{bc} + \varphi_{b} \delta_{ac})(p_{1} \cdot p_{2}) + (\varphi_{a} \delta_{cb} + \varphi_{c} \delta_{ab})(p_{1} \cdot p_{3}) + (\varphi_{b} \delta_{ca} + \varphi_{c} \delta_{ba})(p_{2} \cdot p_{3}) \right]$$

$$- \frac{1}{2} Y^{(1)} \left[(p_{1} \cdot p_{2}) + (p_{1} \cdot p_{3}) + (p_{2} \cdot p_{3}) \right] \varphi_{a} \varphi_{b} \varphi_{c}$$

$$(4.28)$$

CHAPTER 4. FUNCTIONAL DIMENSIONAL REGULARIZATION FOR THE O(N) MODEL 86

$$\begin{array}{lll} S_{abcd}^{(4)}(p_1,p_2,p_3,p_4) & = & U^{(2)}\left[\delta_{ad}\delta_{bc}+\delta_{ac}\delta_{bd}+\delta_{ab}\delta_{cd}\right] \\ & + & U^{(3)}\left[\varphi_a\varphi_b\delta_{cd}+\varphi_b\varphi_c\delta_{ad}+\varphi_b\varphi_d\delta_{ac}+\varphi_a\varphi_c\delta_{bd}+\varphi_a\varphi_d\delta_{bc}+\varphi_c\varphi_d\delta_{ab}\right] \\ & + & U^{(4)}\varphi_a\varphi_b\varphi_c\varphi_d \\ & - & Z^{(1)}\left[(p_1\cdot p_2)\delta_{ab}\delta_{cd}+(p_1\cdot p_3)\delta_{ac}\delta_{bd}+(p_1\cdot p_4)\delta_{ad}\delta_{bc} \\ & + & (p_2\cdot p_3)\delta_{ad}\delta_{bc}+(p_2\cdot p_4)\delta_{ac}\delta_{bd}+(p_3\cdot p_4)\delta_{ab}\delta_{cd} \\ & + & (p_2\cdot p_3)\delta_{ad}\delta_{bc}+(p_2\cdot p_4)\delta_{ac}\delta_{bd}+(p_3\cdot p_4)\delta_{ab}\delta_{cd} \\ & + & (p_2\cdot p_3)\phi_a\varphi_d\delta_{bc}+(p_1\cdot p_3)\phi_b\varphi_d\delta_{ac}+(p_1\cdot p_4)\phi_b\varphi_c\delta_{ad} \\ & + & (p_2\cdot p_3)\phi_a\varphi_d\delta_{bc}+(p_1\cdot p_2)\delta_{ac}\delta_{bd}+(p_1\cdot p_3)\delta_{ad}\delta_{bc}+(p_1\cdot p_3)\delta_{ab}\delta_{cd} \\ & + & (p_2\cdot p_3)\delta_{ad}\delta_{bc}+(p_1\cdot p_2)\delta_{ac}\delta_{bd}+(p_1\cdot p_3)\delta_{ad}\delta_{bc}+(p_1\cdot p_3)\delta_{ab}\delta_{cd} \\ & + & (p_1\cdot p_4)\delta_{ac}\delta_{bd}+(p_1\cdot p_4)\delta_{ab}\delta_{cd}+(p_2\cdot p_3)\delta_{ac}\delta_{bd}+(p_2\cdot p_3)\delta_{ab}\delta_{cd} \\ & + & (p_1\cdot p_4)\delta_{ad}\delta_{bc}+(p_2\cdot p_4)\delta_{ab}\delta_{cd}+(p_1\cdot p_2)\phi_b\varphi_c\delta_{ad}+(p_1\cdot p_2)\phi_b\varphi_d\delta_{ac} \\ & + & (p_2\cdot p_4)\delta_{ad}\delta_{bc}+(p_2\cdot p_4)\delta_{ab}\delta_{cd}+(p_1\cdot p_2)\phi_b\varphi_c\delta_{ad}+(p_1\cdot p_2)\phi_b\varphi_d\delta_{ac} \\ & + & (p_1\cdot p_2)\phi_a\varphi_b\delta_{cd}+(p_1\cdot p_2)\phi_b\varphi_c\delta_{ad}+(p_1\cdot p_2)\phi_b\varphi_d\delta_{ac} \\ & + & (p_1\cdot p_2)\phi_a\varphi_b\delta_{cd}+(p_1\cdot p_2)\phi_b\varphi_c\delta_{ad}+(p_1\cdot p_2)\phi_b\varphi_d\delta_{ac} \\ & + & (p_1\cdot p_3)\phi_b\varphi_c\delta_{ad}+(p_1\cdot p_4)\phi_a\varphi_b\delta_{cd}+(p_1\cdot p_4)\phi_b\varphi_d\delta_{ac} \\ & + & (p_1\cdot p_3)\phi_a\varphi_b\delta_{cd}+(p_1\cdot p_4)\phi_a\varphi_b\delta_{cd}+(p_1\cdot p_4)\phi_a\varphi_d\delta_{bc} \\ & + & (p_1\cdot p_4)\phi_a\varphi_c\delta_{bd}+(p_1\cdot p_4)\phi_a\varphi_b\delta_{cd}+(p_1\cdot p_4)\phi_a\varphi_b\delta_{cd} \\ & + & (p_2\cdot p_3)\phi_a\varphi_b\delta_{cd}+(p_2\cdot p_3)\phi_b\varphi_c\delta_{ad}+(p_2\cdot p_4)\phi_a\varphi_b\delta_{cd} \\ & + & (p_2\cdot p_4)\phi_b\varphi_c\delta_{ad}+(p_2\cdot p_4)\phi_b\varphi_d\delta_{ac}+(p_2\cdot p_4)\phi_a\varphi_b\delta_{cd} \\ & + & (p_2\cdot p_4)\phi_b\varphi_c\delta_{ad}+(p_3\cdot p_4)\phi_b\varphi_c\delta_{ad}+(p_3\cdot p_4)\phi_c\varphi_d\delta_{ab} \\ & + & (p_2\cdot p_4)\phi_a\varphi_b\delta_{cd}+(p_3\cdot p_4)\phi_b\varphi_c\phi_d+(p_1\cdot p_4)\phi_a\varphi_b\delta_{cd} \\ & + & (p_2\cdot p_3)\phi_a\varphi_b\varphi_c\varphi_d+(p_1\cdot p_3)\phi_a\varphi_b\varphi_c\varphi_d+(p_1\cdot p_4)\phi_a\varphi_b\varphi_c\varphi_d \\ & + & (p_2\cdot p_3)\phi_a\varphi_b\varphi_c\varphi_d+(p_1\cdot p_3)\phi_a\varphi_b\varphi_c\varphi_d+(p_1\cdot p_4)\phi_a\varphi_b\varphi_c\varphi_d \\ & + & (p_2\cdot p_3)\phi_a\varphi_b\varphi_c\varphi_d+(p_2\cdot p_4)\phi_a\varphi_b\varphi_c\varphi_d+(p_1\cdot p_3)\phi_a\varphi_b\varphi_c\varphi_d \\ & + & (p_2\cdot p_3)\phi_a\varphi_b\varphi_c\varphi_d+(p_2\cdot p_4)\phi_a\varphi_b\varphi_c\varphi_d+(p_3\cdot p_4)\phi_e\varphi_d\delta_{ab} \\ & + & ($$

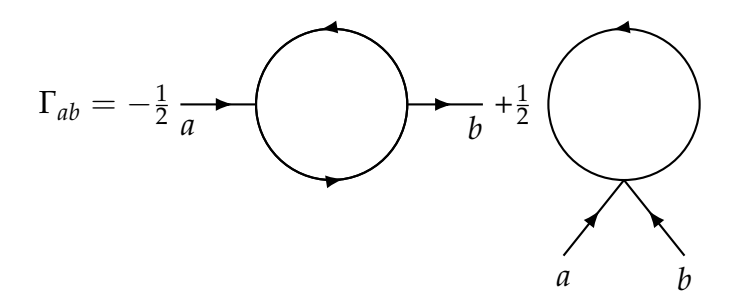


Figure 4.9: Feynman diagrams contributions to the one loop two point function.

4.2.4 Diagrams and Propagator

The propagator is the inverse of $S^{(2)}$ (see (4.27)), this computed with the aid of the projector $P_{ab} = \phi_a \phi_b / \phi^2$

$$G_{ab}(q) = G_T(q)(\delta_{ab} - P_{ab}) + G_L(q)P_{ab}$$
(4.30)

The transverse and longitudinal components are

$$G_T(q) \equiv \frac{1}{q^2 + q^2 Z_T + U'}$$
 $G_L(q) \equiv \frac{1}{q^2 + q^2 Z_L + U' + 2\rho U''}$ (4.31)

where as before $Z_T = Z$ and $Z_L = Z + \rho Y$. Diagrammatically the second derivative of the one loop effective action has two contribution as it is shown in Figure 4.9. This contribution are known as the polarization diagram and the tadpole for which we will need G(q), $S^{(3)}$ and $S^{(4)}$. The diagrams reads as

polarization =
$$\int_{q} G_{ij}(q) S_{jak}^{(3)}(q, p, -q - p) G_{kl}(q + p) S_{kbi}^{(3)}(q + p, -p, -q)$$

tadpole = $\int_{q} G_{ij}(q) S_{iabj}^{(4)}(q, p, -p, -q)$

When we write the propagator as the sum of the longitudinal and transverse part, the contribution coming from the diagrams at order $\mathcal{O}(\partial^2)$ split in two. Let start with the longitudinal part. Since we are at order 2, we are interested in terms that are proportional to the momentum square (p^2) . The left hand side of the equation is the second derivative of the effective action contracted with either the longitudinal part or the transverse part, here we take the coefficient proportional to (p^2) as we just said. As we are working on the O(N) model we work with a tensorial notation. The second

derivative of the effective action has the form

$$(\Gamma^{(2)})^{mn} = U'g^{mn} + U''\phi^m\phi^n + p^2Zg^{mn} + \frac{1}{2}p^2Y\phi^m\phi^n$$
 (4.32)

We remind the reader that the projectors are

$$(P_L)_{ab} = \frac{\phi^a \phi^b}{\Phi^2} \quad (P_T)_{ab} = g^{ab} - \frac{\phi^a \phi^b}{\Phi^2}$$
 (4.33)

The longitudinal left hand side is

$$(P_L)_{mn}(\Gamma^{(2)})^{mn} = \frac{\phi^m \phi^n}{\Phi^2} \left\{ U' g^{mn} + U'' \phi^m \phi^n + p^2 Z g^{mn} + \frac{1}{2} p^2 Y \phi^m \phi^n \right\}$$

$$= U' + p^2 Z + U'' \phi^2 + \frac{1}{2} p^2 Y^2 \phi^2$$

$$= U' + U'' \phi^2 + p^2 \left(Z + \frac{Y \phi^2}{2} \right)$$

from here we see the term we keep is

$$Z + Y\rho \tag{4.34}$$

where in the last step we made the wrote $\Phi^2 \to 2\rho$. The transverse left hand side is

$$(P_T)_{mn}(\Gamma^{(2)})^{mn} = \left(g^{mn} - \frac{\phi^m \phi^n}{\Phi^2}\right) \left\{ U'g^{mn} + U''\phi^m \phi^n + p^2 Z g^{mn} + \frac{1}{2} p^2 Y \phi^m \phi^n \right\}$$

$$= NU' + p^2 Z N + U'\phi^2 + \frac{1}{2} p^2 Y^2 \phi^2$$

$$-U' - p^2 Z - U'\phi^2 - \frac{1}{2} p^2 Y^2 \phi^2$$

$$= (N-1)(U' + p^2 Z)$$

Thus, the term we keep here is

$$(N-1)Z \tag{4.35}$$

To compute the contribution of each diagram to our beta functional – β_Z^{DR} and β_Y^{DR} – we will contract indices with the propagator to obtain two independent equations, one related to the transverse contribution and the other to the longitudinal:

$$P_{ab}\Gamma_{ab}^{(2)}(p^2) \equiv \frac{S_d}{(2\pi)^d} \int_0^\infty dq \, q^{d-1} \, \gamma_L(p,q)$$
 (4.36)

$$(\delta_{ab} - P_{ab})\Gamma_{ab}^{(2)}(p^2) \equiv \frac{S_d}{(2\pi)^d} \int_0^\infty dq \, q^{d-1} \, \gamma_T(p, q)$$
 (4.37)

where γ_L is the sum of γ_L^{pol} and γ_L^{tad} which refers to the longitudinal contribution coming from the polarization and tadpole diagram respectively and γ_T it is analogous but with the transverse contribution. Each of the last two equation (4.36) and (4.37) are split in two where we will perform the angular integration and expand in powers of the momentum p^2 :

$$\gamma_{T}|^{tad} = (P_{T})_{ab} \times \frac{1}{2}G(q^{2})_{ij}(S^{(4)})^{ijab} = \frac{1}{4}(N-1)\left\{ \left(2U'' + 4\rho U''' + q^{2}(2Z' + 2\rho Y')\right) + 2p^{2}(Z' + 2\rho Z'')\right\}G_{L} + 2\left((N+1)U'' + (p^{2} + q^{2})(Y + (N-1)Z')\right)G_{T})\right\}$$

Now we perform the angular integration of this last term and expand in terms of p^2

$$\begin{split} \frac{1}{4}(N-1) \bigg\{ \bigg(2U'' + 4\rho U''' + q^2(2Z' + 2\rho Y') + 2p^2(Z' + 2\rho Z'') \bigg) G_L \\ + \bigg(2((N+1)U'' + (p^2 + q^2)(Y + (N-1)Z')) \bigg) G_T \bigg\} \end{split}$$

Extracting the p^2 coefficient gives

$$\gamma_T|_{p^2}^{tad} = (N-1)\left\{\left(\frac{1}{2}Z' + \rho Z''\right)G_L + \frac{1}{2}\left(Y + (N-1)Z'\right)G_T\right\}$$

For the same diagram we now perform the contribution coming from the longitudinal projector

$$\begin{split} \gamma_L|^{tad} &= (P_L)_{ab} \times \frac{1}{2} G(q^2)_{ij} (S^{(4)})^{ijab} &= \frac{1}{4} \bigg\{ \bigg(6 U'' + 8 \rho^2 U'''' + 24 \rho U''' \\ &+ (p^2 + q^2) \big\{ 2 Y + 2 Z' + 4 \rho Z'' + 10 \rho Y' + 4 \rho^2 Y'' \big\} \bigg) G_L \\ &+ (N-1) \bigg(2 U'' + 2 Z' (p^2 + q^2) \\ &+ 4 \rho U''' + 2 p^2 \rho Y' + 4 \rho q^2 Z'' \bigg) G_T) \bigg\} \end{split}$$

After performing the angular integration and extracting the p^2 coefficient, we find

$$\gamma_L|_{p^2}^{tad} = \left\{ \frac{1}{2} \left(Y + Z' + 5\rho Y' + 2\rho Z'' + 2\rho^2 Y'' \right) G_L + \frac{(N-1)}{2} \left(Z' + \rho Y' \right) G_T \right\}$$

Now we want to compute the contribution to the dimensionful beta function from the polarization diagram. The procedure is the same as before:

$$\gamma_T|_{pol}^{pol} = (P_T)_{ab} \times \frac{-1}{2} G(q^2)_{jk} \Gamma_{jak}^{(3)} G(p^2 + q^2 + 2p \cdot q)_{kl} \Gamma_{lbi}^{(3)}$$
$$\gamma_L|_{pol}^{pol} = (P_L)_{ab} \times \frac{-1}{2} G(q^2)_{jk} \Gamma_{jak}^{(3)} G(p^2 + q^2 + 2p \cdot q)_{kl} \Gamma_{lbi}^{(3)}$$

The final results are

$$\begin{split} \gamma_{T}|_{p^{2}}^{pol} &= -\frac{1}{4d}(N-1)\rho \bigg\{ (2U''+q^{2}Y)G_{T}(q^{2}) \bigg((2dU''+q^{2}((8+d)Y-8Z'))G'_{L}(q^{2}) \\ &+ 2q^{2}(2U''+q^{2}Y)G''_{L} \bigg) + G_{L} \bigg(2\{ 2dU''(Y+2Z')+q^{2}((2+d)Y^{2}+2(-2+d)YZ' \\ &+ 4Z'^{2})\} G_{T} + (2U''+q^{2}Y)\{ (2dU''+q^{2}(dY+8Z'))G'_{T} + 2q^{2}(2U''+q^{2}Y)G''_{T}\} \bigg) \bigg\} \end{split}$$

and

$$\begin{split} \gamma_{L}|_{p^{2}}^{pol} &= -\frac{\rho}{d} \bigg\{ (Y + Z' + Y'\rho) \bigg(d(6U'' + 4\rho U''') + (1 + 2d)q^{2}(Y + Z' + \rho Y') \bigg) G_{L}^{2} \\ &+ \bigg(3U'' + 2\rho U''' + q^{2}(Y + Z' + \rho Y') \bigg) G_{L} \bigg(\{ (3U'' + 2\rho U''') \\ &+ (4 + d)q^{2}(Y + Z' + \rho Y') \} G_{L}' + 2q^{2}(3U'' + 2\rho U''' + q^{2}(Y + Z' + \rho Y')) G_{L}'' \bigg) \\ &+ (N - 1)G_{T} \bigg((dU''Y + q^{2}Z1(dY + Z'))G_{T} + (U'' + q^{2}Z') \{ (dU'' + (4 + d)q^{2}Z')G_{T}' + 2q^{2}(U'' + q^{2}Z')G_{T}'' \} \bigg) \bigg\} \end{split}$$

Note that $\gamma_L|_{p^2}^{pol}$, $\gamma_T|_{p^2}^{pol}$, $\gamma_L|_{p^2}^{tad}$ and $\gamma_T|_{p^2}^{tad}$ present a dependence on the longitudinal and transverse propagator as well as their derivative which are all functions of q^2 . As

computed before in (4.34) and (4.35) the left hand side of (4.36) and (4.37) are

$$P_{ab}\Gamma_{ab}^{(2)}|_{p^2} = Z + \rho Y \tag{4.38}$$

and

$$(\delta_{ab} - P_{ab})\Gamma_{ab}^{(2)}|_{p^2} = (N-1)Z \tag{4.39}$$

respectively. With this into account we are close to conclude with the computation of our beta functionals, since (4.38) and (4.39) in DR the beta functionals at each d_c come as

$$\beta_Z^{\text{DR}} + \rho \beta_Y^{\text{DR}} \equiv -\epsilon \left[\frac{S_d}{(2\pi)^d} \int_0^\infty \mathrm{d}q \, q^{d-1} \, \gamma_L(q^2) \right]_{\infty} \tag{4.40}$$

$$(N-1)\beta_Z^{\rm DR} \equiv -\epsilon \left[\frac{S_d}{(2\pi)^d} \int_0^\infty \mathrm{d}q \, q^{d-1} \, \gamma_T(q^2) \right] \tag{4.41}$$

After performing the integral in q we are left with functions that depend only on the dimension d, and now the final step is the re-summation, that is, to sum over all critical dimensions at one-loop order as our definition of beta functionals require

$$\beta_Z^{\text{FDR}}(d) = \sum_{d_c} \mu^{d-d_c} \beta_Z^{\text{DR}}(d_c)$$
 (4.42)

and

$$\beta_Y^{\text{FDR}}(d) = \sum_{d_c} \mu^{d-d_c} \beta_Y^{\text{DR}}(d_c)$$
 (4.43)

The final result of the dimension-full beta functional β_U , β_{Z_T} , β_{Z_L} are shown in the next subsection.

4.2.5 Beta Functionals

The dimensionful beta functionals have the following form:

$$\begin{split} \beta_{U} &= \ \mu^{d} \Bigg\{ (N-1)e^{-\frac{U'}{4\pi\rho^{2}(Z_{T}+1)}} + e^{-\frac{2\rho U''+U'}{4\pi\rho^{2}(Z_{L}+1)}} \Bigg\} \\ \beta_{Z_{T}} &= \ \mu^{d-2} \Bigg\{ \frac{-e^{-\frac{U'}{4\pi\rho^{2}(Z_{T}+1)}}}{4\pi\rho(Z_{T}+1)\left(U'(Z_{L}-Z_{T})-2\rho U''(Z_{T}+1)\right)} \Bigg[+8\pi\mu^{2}(Z_{T}+1)(\rho Z'_{T}+Z_{T}+1)^{2} \\ &+ (1+Z_{T})(U'(Z_{L}-Z_{T})-2\rho U''(1+Z_{T})) + (N-1)(\rho U'(Z_{L}-Z_{T})Z'_{T}-2\rho^{2}(Z_{T}+1)U''Z'_{T}) \Bigg] \\ &+ \frac{e^{-\frac{2\rho U'''+U'}{4\pi\rho^{2}(Z_{L}+1)}}}{4\pi\rho(Z_{L}+1)(U'(Z_{L}-Z_{T})-2\rho(Z_{T}+1)U'')} \Bigg[8\pi\mu^{2}(Z_{L}+1)(\rho Z'_{T}+Z_{T}+1)^{2} \\ &+ 2\rho\left(Z_{T}+1\right)U''\left(2\rho^{2}Z''_{T}+5\rho Z'_{T}+Z_{T}+1\right) - U'\left(Z_{L}-Z_{T}\right)\left(2\rho^{2}Z''_{T}+5\rho Z'_{T}+Z_{T}+1\right) \Bigg] \Bigg\} \\ \beta_{Z_{L}} &= \frac{\mu^{d-6}}{192\pi^{3}} \Bigg\{ \frac{(N-1)e^{-\frac{U'}{4\pi\rho^{2}(Z_{T}+1)}}}{\rho\left(Z_{T}+1\right)^{4}} \Bigg[-48\pi^{2}\mu^{4}(Z_{T}+1)^{2} \Big\{ Z_{T}^{2}-Z_{L}\left(2\rho Z'_{T}+Z_{T}+1\right) \\ &+ Z_{T}\left(\rho Z'_{L}+2\rho Z'_{T}+1\right) + \rho\left(Z'_{L}+\rho\left(Z'_{T}\right)^{2}\right) \Big\} - \rho^{2}\left(Z_{T}U''-U'Z'_{T}+U''\right)^{2} \\ &- 24\pi\mu^{2}\rho\left(Z_{T}+1\right)\left(-Z_{L}+\rho Z'_{T}+Z_{T}\right)\left(Z_{T}U''-U'Z'_{T}+U''\right) \Bigg] \\ &+ \frac{e^{-\frac{2\rho U''+U'}{4\pi\rho^{2}(Z_{L}+1)}}}{(Z_{L}+1)^{4}} \Bigg[-48\pi^{2}\mu^{4}\left(Z_{L}+1\right)^{2}\left(-3\rho\left(Z'_{L}\right)^{2}+2\rho\left(Z_{L}+1\right)Z''_{L}+\left(Z_{L}+1\right)Z'_{L}\right) \\ &+ 24\pi\mu^{2}\rho\left(Z_{L}+1\right)Z'_{L}\left(2\rho U^{(3)}\left(Z_{L}+1\right) + U''\left(-2\rho Z'_{L}+3Z_{L}+3\right) - U'Z'_{L}\right)^{2} \Bigg] \Bigg\} \end{split}$$

These equations presented here for the first time are the main result of this thesis and will be published soon [87].

Definitions and equations of Strict, Light, Strict-Light

In this subsection, we present the structure of the dimensionful beta functionals in their strict, light, and strict-light forms. These approximations are derived from the original beta functionals.

Let us first consider the case we will refer to as *strict*, as formulated in [39]. This truncation consists of discarding terms of order p^4 and higher in momenta when

working with the derivative expansion at order 2. The discarded terms can be observed, for instance, in the polarization diagram. It is important to note that these terms involve the third derivative of the Γ function, which in turn produces contributions of the form $p \cdot q$ and terms of order $\propto p^2$. Since in the derivative expansion at order two we consider terms proportional to p^2 , it does not seem incorrect to retain terms of this order on the right-hand side of the equation, in contrast to the *full* case, where all contributions are included regardless of their order in momenta. In the case of $\Gamma^{(3)}$, the terms proportional to p^2 are $\{Z', Y, Y'\}$. Thus, the strict case is computed by setting terms proportional to $\{Z'^2, YZ', Y'Z', Y'Z', YY', Y'^2\}$ to zero. This last step must be done before expanding the propagator and only applies for the products of vertices.

The light case consists of setting Z_L and Z_T to zero in the propagator (4.31) to alleviate the complexity of the beta function, and the strict-light case is simply a combination of the two. The only reason we perform these approximations is to simplify the computations. The explicit form of these equations are shown in Appendix C.

4.2.6 Fixed Points and Critical Exponents

At this point we are free to use any basis we like, whether the (U, Z, Y) or the (U, T, L) basis. Now we will present the analysis of the fixed point for the (U, T, L) basis. This means that we will work with the β_U , β_{Z_T} , β_{Z_L} functions and their respective flow equations. The relation between the dimensionful and dimension-less beta functionals is

$$\beta_{u} = -du + (d - 2 + \eta)\rho u' + \beta_{U}$$

$$\beta_{z_{L}} = \eta(1 + Z_{L}) + (d - 2 + \eta)\rho Z'_{L} + \beta_{Z_{L}}$$

$$\beta_{z_{T}} = \eta(1 + Z_{T}) + (d - 2 + \eta)\rho Z'_{T} + \beta_{Z_{T}}$$
(4.44)

Among the several ways to solve the flow equation (4.44) we choose to write U, Z_T, Z_L as an expansion of the field ρ as

$$u(\rho) = \sum_{k=1}^{n} \frac{\lambda_{2k}}{k!} \rho^{k}, \qquad z_{L}(\rho) = \sum_{k=1}^{n-2} \frac{\zeta_{2k}}{k!} \rho^{k}, \qquad z_{T}(\rho) = \sum_{k=1}^{n-2} \frac{\psi_{2k}}{k!} \rho^{k}$$
(4.45)

This manner requires to implement a truncation number n for which we will have $N_U + N_{Z_T} + N_{Z_L} = n + 2(n-2) = 3n - 4$ coupled differential equations to solve. We proceed to solve this equation step by step, starting for n = 2 were the coupling are

 λ_2 and λ_4 since for this truncation z_L and z_T start at n=3.

With this choice, we can easily compute the anomalous dimension η from the equation for β_{z_T} by setting $\rho \to 0$ and imposing the normalization condition $z_T(0) = 0$. Then

$$\eta \to -\beta_{Z_T}$$

We found a simple expression for η which holds for any truncation with n > 3

$$\eta = \frac{e^{-\frac{\lambda_2}{4\pi}}}{4\pi} [(N-1)\psi_2 + \zeta_2]$$
 (4.46)

This same expression for η can also be computed from β_{z_L} .

At the fixed point the dimensionless beta functions are zero, then in order to solve the equations for n=2 we have two equations for λ_2 and λ_4 which can be solved exactly and has two solution, $\lambda_2^*=0$, $\lambda_4^*=0$ which is the Gaussian fixed point and

$$\lambda_2^* = rac{2\pi(d-4)(N+2)}{N+8} \qquad \lambda_4^* = -rac{16\pi^2(d-4)e^{rac{(d-4)(N+2)}{2(N+8)}}}{N+8}$$

which is the Wilson-Fished fixed point. The next step is to set n=3 which is the first time a coupling coming from Z_L and Z_T appears. To solve this we implement the *FindRoot* of Mathematica which requires to give an anzats for which we took the previous solution of the fixed point plus a random guess for the new coupling. We then repeat the procedure until we verify the convergence of the critical exponent ν and ω which are computed from the stability matrix whereas the critical exponent η is computed from (4.46). To verify the accuracy of the fixed point we also checked their convergence.

4.2.7 Results

Below, we present the results obtained for the critical exponents ν , ω , and η , first for the universality classes in dimension 3 with N=0,1,2,3,4, and then for large values of N, specifically for N=10,20,100. These results are compared with raw data and final estimate [45] and the state of the art for the expansion around zero. Subsequently, we present the results for the same critical exponents and the anomalous dimension, but expanding the fields at the minimum of the potential.

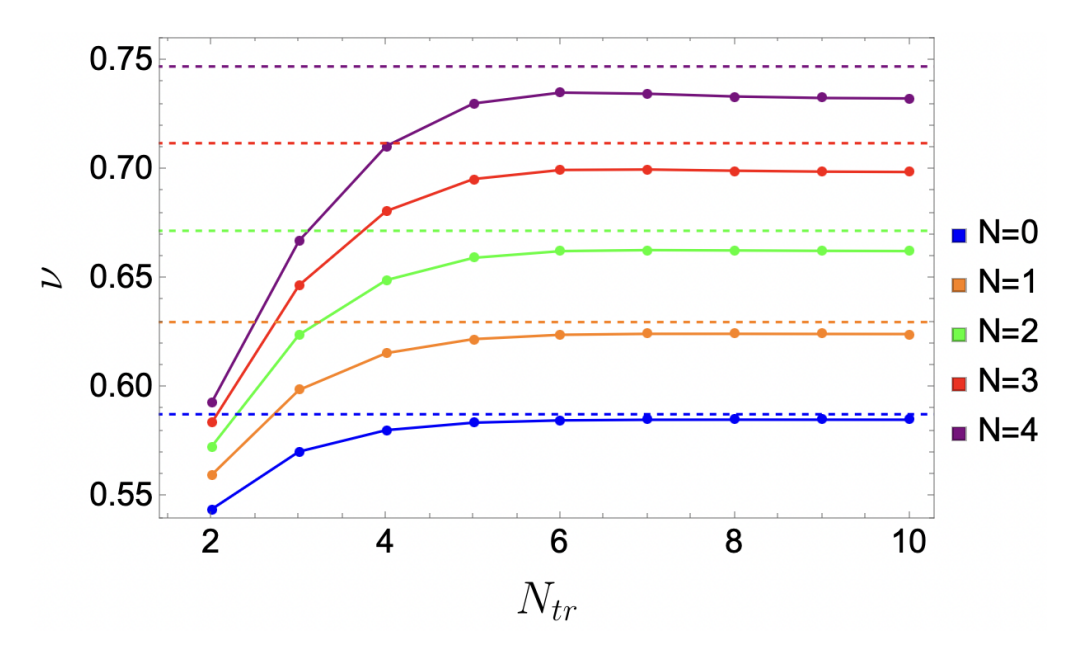


Figure 4.10: Convergence of the critical exponent ν in the DE FDR- $\mathcal{O}(\partial^2)$ around zero applied to O(N) models. Comparison is made with state-of-the-art estimates (CB) dashed lines.

Expansion around zero

For the expansion around zero we perform the truncation up to $N_{tr} = 10$ and did not proceed further since it was computationally challenging. As shown in Figure 4.10 the convergence of the critical exponent ν is well defined for all N. These values are comparable to those found in the literature, especially with NPRG-DE2, but they are not as accurate as in the case of our LPA.

For the ω there is also a slower but still clear convergence (see Figure 4.11) except for the N=4 from which we expect to converge faster with the expansion around the minima and extract from here the definitive value.

Finally, the result for the anomalous dimension showing in Figure 4.12 is remarkable for a first approximation (recall that the LPA predict a $\eta=0$ for all cases) and the final value of convergence goes in the same direction as the conformal bootstrap. Moreover, when compared with the raw data [45] in Figure 4.17 the first values of N are closer to the curve NPRG-DE4 than to the NPRG-DE2. All the results presented graphically above are summarized in the following Tables 4.7 and 4.6.

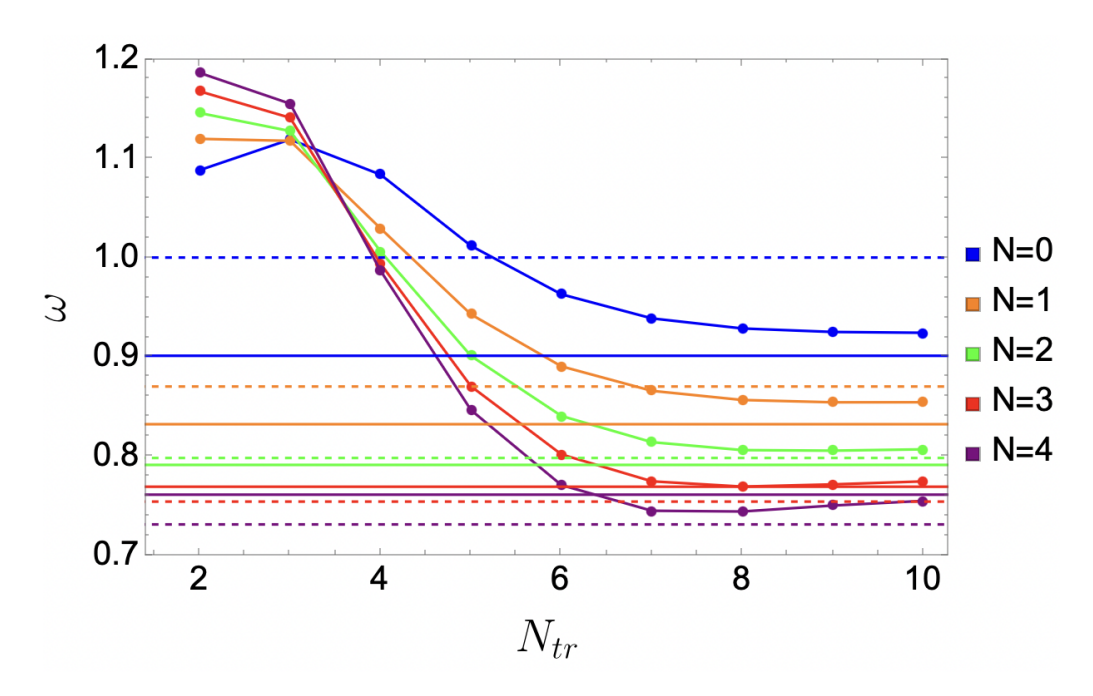


Figure 4.11: Convergence of the critical exponent ω in the DE FDR- $\mathcal{O}(\partial^2)$ around zero applied to O(N) models. Comparison is made with final estimate DE2 (dashed) and DE4 (continuous).

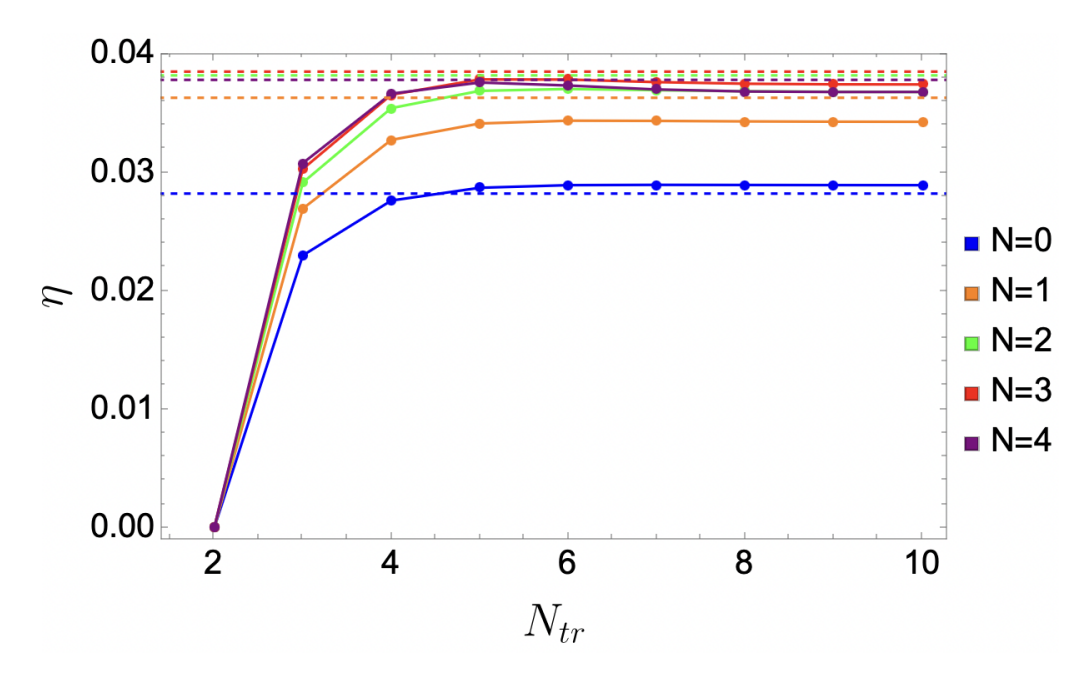


Figure 4.12: Convergence of the critical exponent η in the DE FDR- $\mathcal{O}(\partial^2)$ around zero applied to O(N) models. Comparison is made with state-of-the-art estimates.

N	ν_8	1/9	ν_{10}	ω_8	ω_9	ω_{10}	η_8	η_9	η_{10}
0	0.585112	0.585105	0.585093	0.928509	0.924993	0.924168	0.0289248	0.0289149	0.0289095
1	0.624511	0.624452	0.624409	0.856422	0.854084	0.854148	0.0342960	0.0342711	0.0342602
2	0.662770	0.662585	0.662484	0.805907	0.805351	0.806696	0.0368416	0.0367998	0.0367854
3	0.699356	0.698951	0.698777	0.769127	0.771378	0.774381	0.0374752	0.0374236	0.0374127
4	0.733434	0.732743	0.732527	0.744027	0.750043	0.754732	0.0368234	0.0367793	0.0367819
5	0.764184	0.763238	0.763078	0.729813	0.740074	0.745875	0.0353670	0.0353528	0.0353767

Table 4.5: Convergence of critical exponents for expansion around zero.

N	ν	ω	η
10	0.866059	0.779504	0.0258998
20	0.93793	0.845266	0.0147138
100	0.9884	0.971913	0.00312589

Table 4.6: Final values of critical exponents for expansion around zero for large *N*.

Expansion around minima

For the expansion around the minima at the DE2 we follow the same approach as in 4.1.3, where the beta function of the minima and the coupling are computed as it was explained before in equation (4.16) and (4.15). The flow equation (4.44) still stands and we aim to solve it but this time we make a slightly different choice on the potential U and on the wave-function-renormalization.

$$u(\rho) = \sum_{k=2}^{n} \frac{\lambda_k}{k!} (\rho - \lambda_1)^k, \quad z_L(\rho) = \sum_{k=1}^{n-2} \frac{\zeta_k}{k!} (\rho - \lambda_1)^k, \quad z_T(\rho) = \sum_{k=0}^{n-2} \frac{\psi_k}{k!} (\rho - \lambda_1)^k (4.47)$$

The importance of performing this approximation lies in clarifying some final results for the critical exponents, such as the case of ω for N=4, where the convergence does not appear to be complete when we make the approximation around zero.

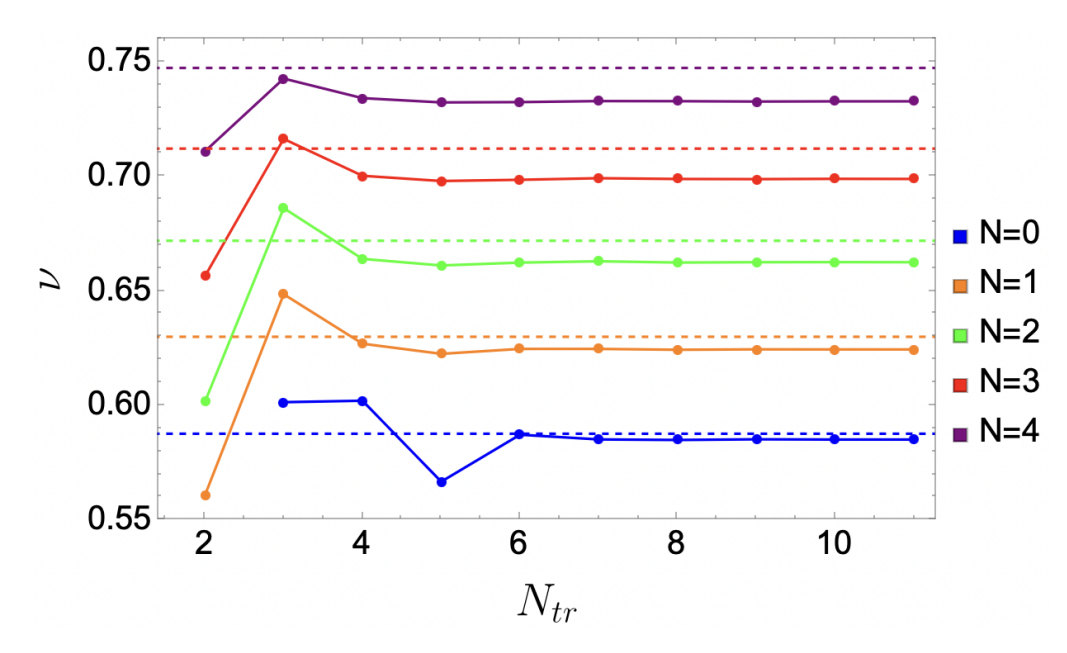


Figure 4.13: Convergence of the critical exponent ν in the DE FDR- $\mathcal{O}(\partial^2)$ around the minima applied to O(N) models. Comparison is made with state-of-the-art estimates (CB).

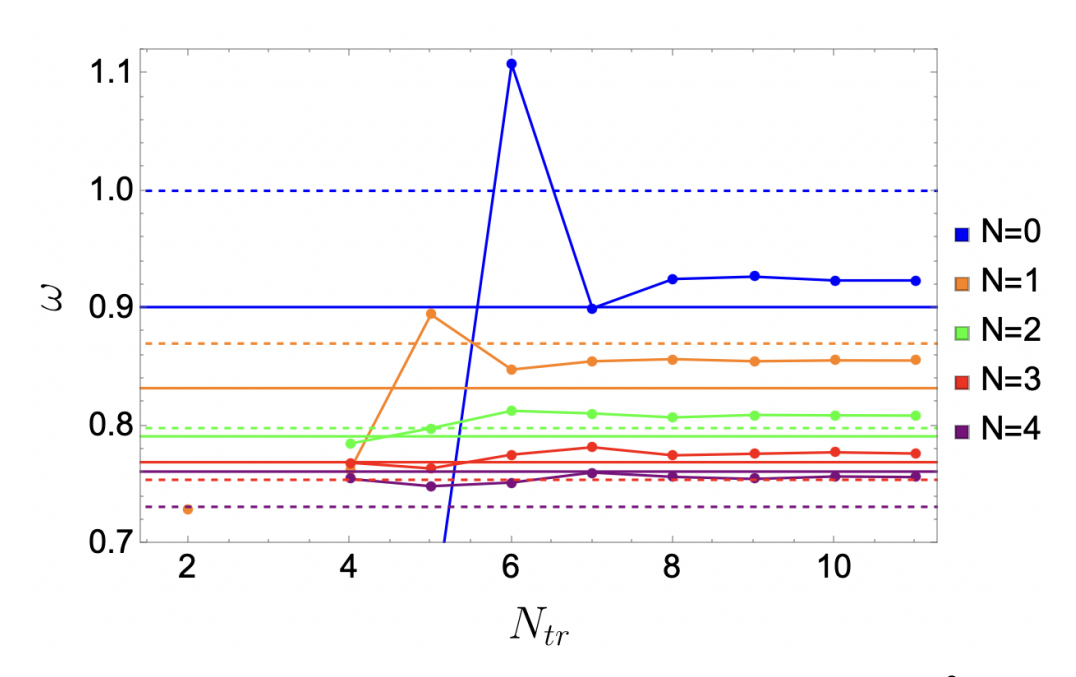


Figure 4.14: Convergence of the critical exponent ω in the DE FDR- $\mathcal{O}(\partial^2)$ around the minima applied to O(N) models. Comparison is made with DE2 (dashed) and DE4 (continuous).

Unlike for the case around zero, we see that in Figure 4.14 the convergence of the ω at N=4 is much more remarkable which gives us a more accurate value.

N	ν ₉	ν_{10}	ν_{11}	ω_9	ω_{10}	ω_{11}	η_9	η_{10}	η_{11}
0	0.585165	0.585062	0.585062	0.926907	0.923685	0.923714	0.0290550	0.0288722	0.0288725
1	0.624416	0.624379	0.624375	0.85491	0.855627	0.855519	0.0342329	0.0342569	0.0342576
2	0.662438	0.662476	0.662429	0.809206	0.808869	0.80865	0.0367847	0.0367760	0.0367896
3	0.698685	0.698812	0.698762	0.776165	0.777389	0.776385	0.0374435	0.0374098	0.0374238
4	0.73254	0.732627	0.732638	0.75474	0.756824	0.756326	0.036824	0.0367987	0.0367997
5	0.763333	0.763335	0.763372	0.744275	0.745229	0.745725	0.0354129	0.0354071	0.0354008
10	0.866366	0.866366	0.866365	0.7698	0.76974	0.769722	0.0258475	0.0258479	0.0258480
20	0.93654	0.93654	0.93654	0.858735	0.858736	0.858736	0.0147698	0.0147698	0.0147698
100	0.988442	0.988442	0.988442	0.970606	0.970606	0.970606	0.00311808	0.00311808	0.00311808

Table 4.7: Convergence of critical exponents for expansion around the minima.

4.2.8 Comparison with State-of-the-Art of the critical exponents

To conclude this chapter we want to show the curves for the critical exponents η , ν and ω as a function of N overlapped with the state-of-the-art data, that is, CB and the NPRG up to the fourth derivative in the DE. Additionally we add the large-N.

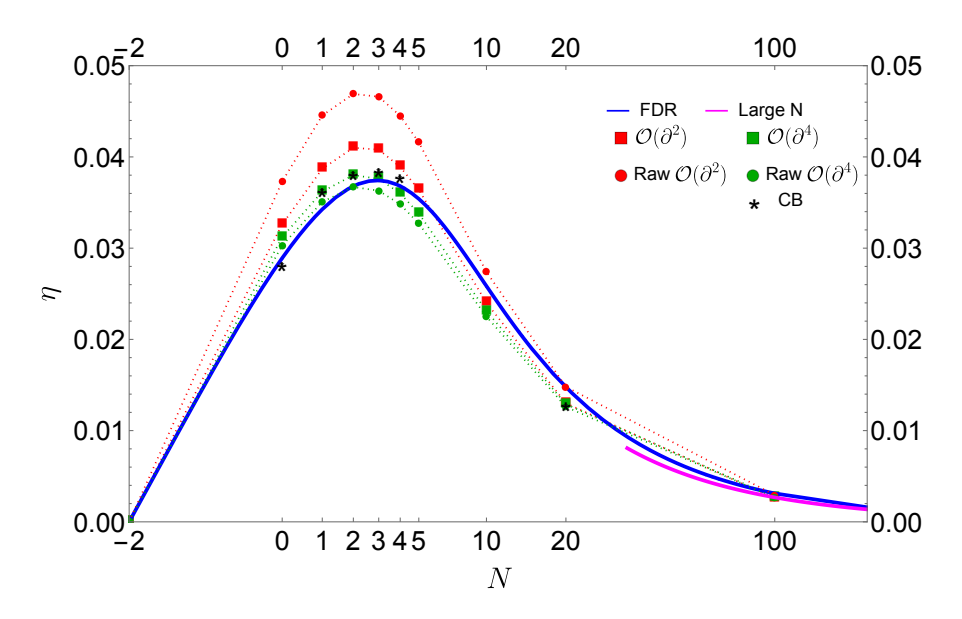


Figure 4.15: Estimate of the critical exponent η as a function of N in d=3 at order NPRG-DE2 (red-square final and red-dot raw), order NPRG-DE4 (green-square final and green-dot) and at order NPDR-DE2 blue n=11, large-N magenta and conformal bootstrap black stars.

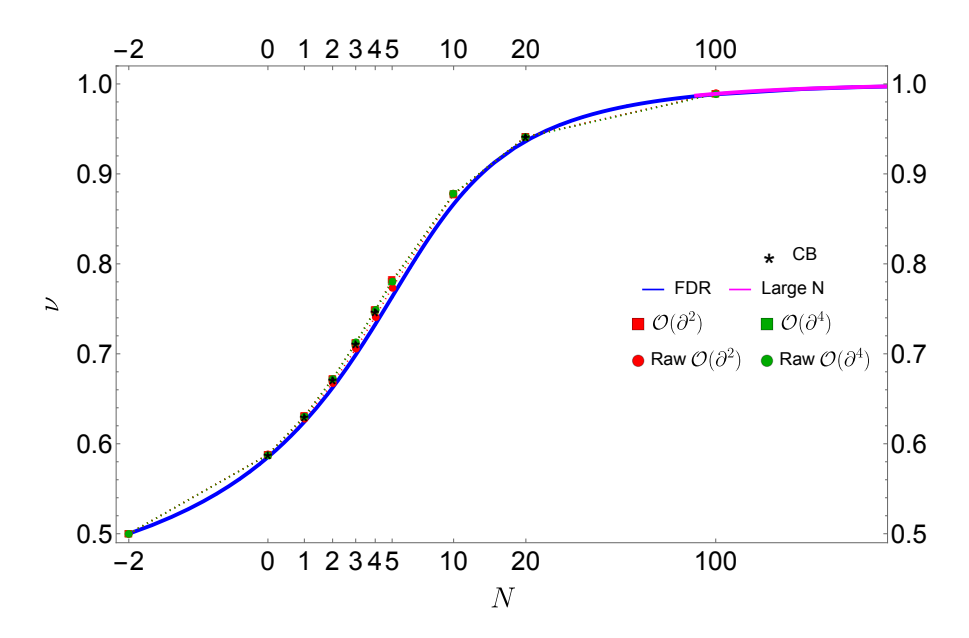


Figure 4.16: Estimate of the critical exponent ν as a function of N in d=3 at order NPRG-DE2 (red square final and red-dotted raw), order NPRG-DE4 (green-square final and green-dotted raw) and at order NPDR-DE2 blue n=11, large-N magenta and conformal bootstrap black stars.

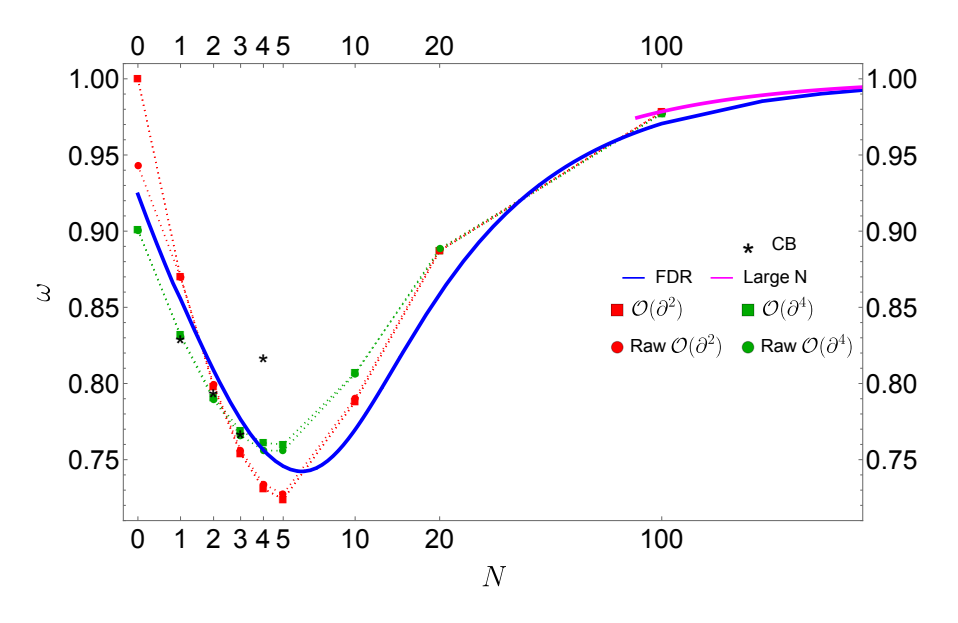


Figure 4.17: Estimate of the critical exponent ω as a function of N in d=3 at order NPRG-DE2 (red-square final and red-dotted raw), order NPRG-DE4 (green-square final and green-dotted raw) and at order NPDR-DE2 blue n=11, large-N magenta and conformal bootstrap black stars.

CHAPTER 4. FUNCTIONAL DIMENSIONAL REGULARIZATION FOR THE O(N) MODEL 101

		ν	ω	η
NPRG				
	LPA	0.65103	0.6533	0
	$\mathcal{O}(\partial^2)$	0.62752	0.8707	0.04551
	$\mathcal{O}(\partial^4)$	0.63057	0.8321	0.03357
FDR				
	LPA	0.6259	0.7622	0
	$\mathcal{O}(\partial^2)$	0.6244	0.8555	0.0342
СВ		0.6299	0.8295	0.03629

		ν	ω	η
NPRG				
	LPA	0.7106	0.6716	0
	$\mathcal{O}(\partial^2)$	0.6663	0.7972	0.0480
	$\mathcal{O}(\partial^4)$	0.6732	0.7934	0.0350
FDR				
	LPA	0.6689	0.7457	0
	$\mathcal{O}(\partial^2)$	0.6624	0.8086	0.0367
CB		0.6717	0.794(8)	0.0381

Final results for the N=1 universality class for different methods

Final results for the N=2 universality class for different methods

Table 4.8: Comparison of the critical exponent with the state-of-the-art. The NPRG results (raw) are taken from [45], and CB values from Tables 2.4 and 2.5

		ν	ω	η
NPRG				
	LPA	0.7639	0.7026	0
	$\mathcal{O}(\partial^2)$	0.7039	0.7516	0.0476
	$\mathcal{O}(\partial^4)$	0.7136	0.7729	0.0347
FDR				
	LPA	0.7103	0.7345	0
	$\mathcal{O}(\partial^2)$	0.6987	0.7763	0.0374
СВ		0.71168	0.7668	0.0385

		ν	ω	η
NPRG				
	LPA	0.8071	0.7383	0
	$\mathcal{O}(\partial^2)$	0.7396	0.7274	0.0455
	$\mathcal{O}(\partial^4)$	0.7500	0.7649	0.0332
FDR				
	LPA	0.7485	0.7296	0
	$\mathcal{O}(\partial^2)$	0.7326	0.7563	0.03679
СВ		0.7472	0.817	0.0378

Final results for the N=3 universality class for different methods

Final results for the N=4 universality class for different methods

Table 4.9: Comparison of the critical exponent with the state-of-the-art. The NPRG results (raw) are taken from [45], and CB values from Tables 2.6 and 2.7

CHAPTER 4. FUNCTIONAL DIMENSIONAL REGULARIZATION FOR THE O(N) MODEL 102

		ν	ω	η
NPRG				
	LPA	0.8402	0.7721	0
	$\mathcal{O}(\partial^2)$	0.7722	0.7199	0.0425
	$\mathcal{O}(\partial^4)$	0.7815	0.7648	0.0313
FDR				
	LPA	0.7825	0.7313	0
	$\mathcal{O}(\partial^2)$	0.7633	0.7457	0.0354
6-loop		0.766		0.034

		ν	ω	η
NPRG				
	LPA	0.5926	0.6635	0
	$\mathcal{O}(\partial^2)$	0.5878	1.0489	0.0388
	$\mathcal{O}(\partial^4)$	0.5875	0.9005	0.0292
FDR				
	LPA	0.5827	0.7818	0
	$\mathcal{O}(\partial^2)$	0.5850	0.9237	0.0288
СВ		0.5876		0.0282

Table 4.10: Final results for the N=5 universality class for different methods

Table 4.11: Final results for the N=0 universality class for different methods

Table 4.12: Comparison of the critical exponent with the state-of-the-art. The NPRG results (raw) are taken from [45], six-loop and CB values from Tables 2.3 and 2.8

In summary, the calculation of critical exponents using our method aligns closely with the predictions found in the literature. Our approach is notable for its rapid convergence of critical exponents, providing a better estimation of the values of ω compared to the LPA level, and offering greater accuracy in the anomalous dimension compared to the calculation obtained through NPRG at the second derivative order.

Chapter 5

Conclusions and Perspectives

In this thesis, we develop a new regularization scheme called *Functional Dimensional Regularization* (FDR). Our main motivation stems from the traditional use of dimensional regularization, in the $\overline{\rm MS}$ scheme, which we show can be extended beyond the ε -expansion. To this end, we define a well-behaved functional RG flow by subtracting all $1/\varepsilon$ -poles that appear in perturbation theory. The final result, applicable to arbitrary dimension, is obtained by computing in each critical dimension the perturbative RG functions which are then summed together to obtain the FDR result. Among the virtues of this new scheme stand out its simplicity and rapid convergence when computing critical exponents as well as the unnecessary use of a mass cut-off.

Initially, in Chapter 3, we calculate the beta functions at the lowest order of the derivative expansion (LPA) and compare them with the standard method within the framework of NPRG and the FPRG in the ε -expansion up to order ε^2 . For the Ising universality class we compared our results against the NPRG noticing that using our scheme the critical exponents shows a better approximation compared to the usual method. In particular, we observe that the critical exponent ν closely approximates the currently most accepted value (the conformal bootstrap), which is surprising given that this is the lowest order in the derivative expansion approximation. Another surprising result when computing this critical exponent becomes apparent upon comparing it with the outcome from FPRG at two-loop order, given that our calculation only involves a one-loop approach. Additionally, the critical exponent ω also improves compared to the standard method, although this time the result is not as close to the most accepted value by the community. We calculated the critical exponents at this order for different universality classes derived from the O(N) model, and in all cases, the convergence exhibits the same characteristics: a very accurate ν

and an ω better than those known in the literature at this order.

The main original contribution exposed in this thesis is the analysis of the second order of the derivative expansion developed in Chapter 4. We derive the equations following the general prescription of FDR and applying them to O(N) universality classes using a field expansion as anzats. As expected, we observe an improvement in the results for the critical exponent ω , and for the first time we calculate the values for the critical exponent η . Notably, in the case of the self-avoiding walk (SAW) universality class, our FDR-based approach yields a value for η that is closer to the most accepted value (CB) than the equivalent calculation from the NPRG at fourth order in the derivative expansion. For other universality classes – Ising, XY, Heisenberg, and N=4 – our prediction for η displays accuracy comparable to or surpassing the results obtained with NPRG at second order, and in some cases even matches the raw values at fourth order. Conversely, the results for the critical exponent ν exhibit a slight deterioration compared to the zeroth-order (LPA) calculation. Nonetheless, the precision with which ω is obtained, as it closely approaches, for some N, higher-order NPRG estimates, which themselves are extremely close to the best-established values in the literature. In other words, our second-order calculation comes notably close to matching the fourth-order results from the traditional non-perturbative approach. The latter has important implications, given that the equations for the beta functions at order two fit on a half A4 sheet, while the equations for the NPRG order fourth derivative can extend to dozens of pages. This gives us an idea of the magnitude of the simplification in numerical calculations and execution time which enables us to generate a nearly continuous curve of critical exponents as a function of the parameter *N*, providing definitive proof that this method is effective.

The results above motivates us to test further the properties of the FDR from where we see two different paths that can be taken. On the one hand, the natural approach would be to go one order further in the derivative expansion (by adding higher dimensional operators) and analyze whether the results improve compared to the previous order and contrast them with those of the NPRG. Otherwise, another path would be to expand the calculation by one loop order and calculate the flow at two loop. As a possible direction for future work, this new regularization scheme – currently applied to the O(N) model in d=3 – could be extended to d=2; moreover, it can be applied to many other multi-field theories with more general symmetries, such as the clock, Potts and $O(N) \times O(2)$ models. Finally FDR can be extended to and many other areas of physics, like gauges theory, high energy physics and gravity.

Bibliography

- [1] M. B. Hindmarsh, M. Lüben, J. Lumma and M. Pauly, *Phase transitions in the early universe*, SciPost Phys. Lect. Notes **24** (2021), 1 doi:10.21468/SciPostPhysLectNotes.24 [arXiv:2008.09136 [astro-ph.CO]].
- [2] H. Georgi and S. L. Glashow, *Unity of All Elementary Particle Forces*, Phys. Rev. Lett. **32** (1974), 438-441 doi:10.1103/PhysRevLett.32.438
- [3] S. Weinberg, *Gauge and Global Symmetries at High Temperature*, Phys. Rev. D **9** (1974), 3357-3378 doi:10.1103/PhysRevD.9.3357
- [4] K. G. Wilson and M. E. Fisher, *Critical exponents in 3.99 dimensions*, Phys. Rev. Lett. **28** (1972), 240-243 doi:10.1103/PhysRevLett.28.240
- [5] Jones, J. E. (1924). *On the determination of molecular fields.—II. From the equation of state of a gas.* Proceedings of the Royal Society of London. Series A, Containing Papers of a Mathematical and Physical Character, 106(738), 463-477.
- [6] Van der Waals, J. D. (1873). Over de Continuiteit van den Gas-en Vloeistoftoestand (Vol. 1). Sijthoff.
- [7] R. K. Pathria, *Statistical Mechanics*, Butterworth-Heinemann, 1996, ISBN 978-0-08-054171-6
- [8] Curie, P. (1895). *Propriétés magnétiques des corps a diverses températures* (No. 4). Gauthier-Villars et fils.
- [9] M. Le Bellac, Quantum and statistical field theory
- [10] Ernst Ising. *Beitrag zur Theorie des Ferromagnetismus*. Zeitschrift fur Physik, 31(1):253–258, feb 1925.
- [11] Lenz, W. (1920). Beitrag zum Verständnis der magnetischen Erscheinungen in festen Körpern. Z. Phys., 21, 613-615.

[12] Lars Onsager. Crystal Statistics. I. A Two-Dimensional Model with an Order-Disorder Transition. En: Phys. Rev. 65 (3-4 feb. de 1944)

- [13] R. Peierls. *On Ising's model of ferromagnetism*. En: Mathematical Proceedings of the Cambridge Philosophical Society 32.3 (1936)
- [14] Kadanoff, L. P. (1966). *Scaling laws for Ising models near Tc*, Physics Physique Fizika, 2(6), 263.
- [15] K. G. Wilson, Renormalization group and critical phenomena. 1. Renormalization group and the Kadanoff scaling picture, Phys. Rev. B 4 (1971), 3174-3183 doi:10.1103/PhysRevB.4.3174
- [16] J. J. Binney, N. J. Dowrick, A. J. Fisher and M. E. J. Newman, *The Theory of critical phenomena: An Introduction to the renormalization group*
- [17] A. Franklin, *On the Renormalization Group Explanation of Universality*, Phil. Sci. **85** (2018) no.2, 225-248 doi:10.1086/696812
- [18] Batterman, R. W. (2019). *Universality and RG explanations*. Perspectives on Science, 27(1), 26-47.
- [19] G. Von Gersdorff and C. Wetterich, *Nonperturbative renormalization flow and essential scaling for the Kosterlitz-Thouless transition*, Phys. Rev. B **64** (2001), 054513 doi:10.1103/PhysRevB.64.054513 [arXiv:hep-th/0008114 [hep-th]].
- [20] M. Campostrini, M. Hasenbusch, A. Pelissetto and E. Vicari, *The Critical exponents of the superfluid transition in He-4*, Phys. Rev. B **74** (2006), 144506 doi:10.1103/PhysRevB.74.144506 [arXiv:cond-mat/0605083 [cond-mat]].
- [21] A. Pelissetto and E. Vicari, *Critical phenomena and renormalization group theory*, Phys. Rept. **368** (2002), 549-727 doi:10.1016/S0370-1573(02)00219-3 [arXiv:cond-mat/0012164 [cond-mat]].
- [22] M. Campostrini, M. Hasenbusch, A. Pelissetto, P. Rossi and E. Vicari, *Critical exponents and equation of state of the three-dimensional Heisenberg universality class*, Phys. Rev. B **65** (2002), 144520 doi:10.1103/PhysRevB.65.144520 [arXiv:cond-mat/0110336 [cond-mat]].
- [23] P. G. de Gennes, Exponents for the excluded volume problem as derived by the Wilson method, Phys. Lett. A **38** (1972), 339-340 doi:10.1016/0375-9601(72)90149-1

[24] Havlin, S., & Ben-Avraham, D. (1982). *New approach to self-avoiding walks as a critical phenomenon*. Journal of Physics A: Mathematical and General, 15(6), L321.

- [25] K. J. Wiese and A. A. Fedorenko, *Field Theories for Loop-Erased Random Walks*, Nucl. Phys. B **946** (2019), 114696 doi:10.1016/j.nuclphysb.2019.114696 [arXiv:1802.08830 [cond-mat.stat-mech]].
- [26] Wiese, K. J., Fedorenko, A. A. (2019). *Depinning transition of charge-density waves:* $mapping\ onto\ O\ (n)\ symmetric\ \phi^4\ theory\ with\ n \to -2\ and\ loop-erased\ random\ walks.$ Physical Review Letters, 123(19), 197601.
- [27] G. Mussardo, Statistical field theory: an introduction to exactly solved models in statistical physics, Oxford Univ. Press, 2010,
- [28] M. Campostrini, A. Pelissetto, P. Rossi and E. Vicari, 25th order high temperature expansion results for three-dimensional Ising like systems on the simple cubic lattice, Phys. Rev. E **65** (2002), 066127 doi:10.1103/PhysRevE.65.066127 [arXiv:cond-mat/0201180 [cond-mat]].
- [29] Clisby, N. (2017). Scale-free Monte Carlo method for calculating the critical exponent gamma of self-avoiding walks. Journal of Physics A: Mathematical and Theoretical, 50(26), 264003.
- [30] S. El-Showk, M. F. Paulos, D. Poland, S. Rychkov, D. Simmons-Duffin and A. Vichi, *Solving the 3D Ising Model with the Conformal Bootstrap*, Phys. Rev. D **86** (2012), 025022 doi:10.1103/PhysRevD.86.025022 [arXiv:1203.6064 [hep-th]].
- [31] F. Kos, D. Poland and D. Simmons-Duffin, *Bootstrapping Mixed Correlators in the 3D Ising Model*, JHEP **11** (2014), 109 doi:10.1007/JHEP11(2014)109 [arXiv:1406.4858 [hep-th]].
- [32] F. Kos, D. Poland, D. Simmons-Duffin and A. Vichi, *Bootstrapping the O(N) Archipelago*, JHEP **11** (2015), 106 doi:10.1007/JHEP11(2015)106 [arXiv:1504.07997 [hep-th]].
- [33] F. Kos, D. Poland, D. Simmons-Duffin and A. Vichi, *Precision Islands in the Ising and O(N) Models*, JHEP **08** (2016), 036 doi:10.1007/JHEP08(2016)036 [arXiv:1603.04436 [hep-th]].
- [34] A. Castedo Echeverri, B. von Harling and M. Serone, *The Effective Bootstrap*, JHEP **09** (2016), 097 doi:10.1007/JHEP09(2016)097 [arXiv:1606.02771 [hep-th]].

[35] D. Simmons-Duffin, *The Lightcone Bootstrap and the Spectrum of the 3d Ising CFT*, JHEP **03** (2017), 086 doi:10.1007/JHEP03(2017)086 [arXiv:1612.08471 [hep-th]].

- [36] J. Henriksson, *The critical O(N) CFT: Methods and conformal data*, Phys. Rept. **1002** (2023), 1-72 doi:10.1016/j.physrep.2022.12.002 [arXiv:2201.09520 [hep-th]].
- [37] Clisby, N. and Dünweg, B. (2016). *High-precision estimate of the hydrodynamic radius for self-avoiding walks*. Physical Review E, 94(5), 052102.
- [38] H. Shimada and S. Hikami, *Fractal dimensions of self-avoiding walks and Ising high-temperature graphs in 3D conformal bootstrap*, J. Statist. Phys. **165** (2016), 1006 doi:10.1007/s10955-016-1658-x [arXiv:1509.04039 [cond-mat.stat-mech]].
- [39] G. De Polsi, I. Balog, M. Tissier and N. Wschebor, *Precision calculation of critical exponents in the* O(N) *universality classes with the nonperturbative renormalization group*, Phys. Rev. E **101** (2020) no.4, 042113 doi:10.1103/PhysRevE.101.042113 [arXiv:2001.07525 [cond-mat.stat-mech]].
- [40] M. V. Kompaniets and E. Panzer, *Minimally subtracted six loop renormalization of O(n)-symmetric* ϕ^4 *theory and critical exponents*, Phys. Rev. D **96** (2017) no.3, 036016 doi:10.1103/PhysRevD.96.036016 [arXiv:1705.06483 [hep-th]].
- [41] R. Guida and J. Zinn-Justin, *Critical exponents of the N vector model*, J. Phys. A **31** (1998), 8103-8121 doi:10.1088/0305-4470/31/40/006 [arXiv:cond-mat/9803240 [cond-mat]].
- [42] D. J. Broadhurst, J. A. Gracey and D. Kreimer, *Beyond the triangle and uniqueness relations: Nonzeta counterterms at large N from positive knots*, Z. Phys. C **75** (1997), 559-574 doi:10.1007/s002880050500 [arXiv:hep-th/9607174 [hep-th]].
- [43] Y. Okabe and M. Oku, 1/n Expansion Up to Order $/n^2$. 3. Critical Exponents gamma and nu for d=3, Prog. Theor. Phys. **60** (1978), 1287-1297 doi:10.1143/PTP.60.1287
- [44] A. N. Vasiliev, Y. M. Pismak and Y. R. Khonkonen, 1/N expansion: Calculation of the exponent v in the order $1/n^3$ by the conformal bootstrap method, Theor. Math. Phys. **50** (1982), 127-134 doi:10.1007/BF01015292
- [45] G. De Polsi Astapenco, *Critical phenomena: non-perturbative renormalization group and conformal invariance*, Tesis de doctorado, Universidad de la República (Uruguay), Facultad de Ciencias PEDECIBA (2020).

[46] Hasenbusch, M., 2010. Finite size scaling study of lattice models in the three-dimensional Ising universality class. Physical Review B, 82(17), p.174433.

- [47] M. Hasenbusch, *Restoring isotropy in a three-dimensional lattice model: The Ising universality class,* Phys. Rev. B **104** (2021) no.1, 014426 doi:10.1103/PhysRevB.104.014426 [arXiv:2105.09781 [cond-mat.stat-mech]].
- [48] M. Reehorst, *Rigorous bounds on irrelevant operators in the 3d Ising model CFT* JHEP **09** (2022), 177 doi:10.1007/JHEP09(2022)177 [arXiv:2111.12093 [hep-th]].
- [49] Hasenbusch, M., 2019. *Monte Carlo study of an improved clock model in three dimensions*. Physical Review B, 100(22), p.224517. arXiv:1910.05916 [cond-mat.stat-mech]]
- [50] S. M. Chester, W. Landry, J. Liu, D. Poland, D. Simmons-Duffin, N. Su and A. Vichi, *Carving out OPE space and precise O(2) model critical exponents*, JHEP **06** (2020), 142 doi:10.1007/JHEP06(2020)142 [arXiv:1912.03324 [hep-th]].
- [51] Hasenbusch, M. and Vicari, E., 2011. *Anisotropic perturbations in three-dimensional O (N)-symmetric vector models.*, Physical Review B, 84(12), p.125136. [arXiv:1108.0491v1 [cond-mat.stat-mech]]
- [52] M. Hasenbusch, *Eliminating leading corrections to scaling in the three-dimensional O(N) symmetric phi**4 model: N=3 and N=4*, J. Phys. A **34** (2001), 8221-8236 doi:10.1088/0305-4470/34/40/302 [arXiv:cond-mat/0010463 [cond-mat]].
- [53] Hasenbusch, M. (2020). *Monte Carlo study of a generalized icosahedral model on the simple cubic lattice*. Physical Review B, 102(2), 024406.
- [54] S. M. Chester, W. Landry, J. Liu, D. Poland, D. Simmons-Duffin, N. Su and A. Vichi, *Bootstrapping Heisenberg magnets and their cubic instability*, Phys. Rev. D **104** (2021) no.10, 105013 doi:10.1103/PhysRevD.104.105013 [arXiv:2011.14647 [hep-th]].
- [55] Y. Deng, *Bulk and surface phase transitions in the three-dimensional O(4) spin model*, Phys. Rev. E **73** (2006), 056116 doi:10.1103/PhysRevE.73.056116
- [56] S. A. Antonenko and A. I. Sokolov, *Critical exponents for 3-D O(n) symmetric model with n* > 3, Phys. Rev. E **51** (1995), 1894-1898 doi:10.1103/PhysRevE.51.1894 [arXiv:hep-th/9803264 [hep-th]].

[57] M. E. Peskin and D. V. Schroeder, An Introduction to quantum field theory, Addison-Wesley, 1995, ISBN 978-0-201-50397-5, 978-0-429-50355-9, 978-0-429-49417-8 doi:10.1201/9780429503559

- [58] M. D. Schwartz, *Quantum Field Theory and the Standard Model*, Cambridge University Press, 2014, ISBN 978-1-107-03473-0, 978-1-107-03473-0
- [59] J. Zinn-Justin, *Quantum field theory and critical phenomena*, Int. Ser. Monogr. Phys. **113** (2002), 1-1054
- [60] C. G. Bollini and J. J. Giambiagi, *Dimensional Renormalization: The Number of Dimensions as a Regularizing Parameter*, Nuovo Cim. B **12** (1972), 20-26 doi:10.1007/BF02895558.
- [61] A. Codello, M. Safari, G. P. Vacca and O. Zanusso, *Functional perturbative RG and CFT data in the e-expansion*, Eur. Phys. J. C **78** (2018) no.1, 30 doi:10.1140/epjc/s10052-017-5505-2 [arXiv:1705.05558 [hep-th]].
- [62] J. Polchinski, *Renormalization and Effective Lagrangians*, Nucl. Phys. B **231** (1984), 269-295 doi:10.1016/0550-3213(84)90287-6
- [63] C. Wetterich, *Average Action and the Renormalization Group Equations*, Nucl. Phys. B **352** (1991), 529-584 doi:10.1016/0550-3213(91)90099-J
- [64] C. Wetterich, *The Average action for scalar fields near phase transitions*, Z. Phys. C 57 (1993), 451-470 doi:10.1007/BF01474340
- [65] J. Berges, N. Tetradis and C. Wetterich, *Nonperturbative renormalization flow in quantum field theory and statistical physics*, Phys. Rept. **363** (2002), 223-386 doi:10.1016/S0370-1573(01)00098-9 [arXiv:hep-ph/0005122 [hep-ph]].
- [66] T. R. Morris, The Exact renormalization group and approximate solutions, Int. J. Mod. Phys. A 9 (1994), 2411-2450 doi:10.1142/S0217751X94000972 [arXiv:hep-ph/9308265 [hep-ph]].
- [67] C. Wetterich, *Exact evolution equation for the effective potential*, Phys. Lett. B **301** (1993), 90-94 doi:10.1016/0370-2693(93)90726-X [arXiv:1710.05815 [hep-th]].
- [68] N. Dupuis, L. Canet, A. Eichhorn, W. Metzner, J. M. Pawlowski, M. Tissier and N. Wschebor, *The nonperturbative functional renormalization group and its applications*, Phys. Rept. **910** (2021), 1-114 doi:10.1016/j.physrep.2021.01.001 [arXiv:2006.04853 [cond-mat.stat-mech]].

[69] B. Delamotte, *An Introduction to the nonperturbative renormalization group*, Lect. Notes Phys. **852** (2012), 49-132 doi:10.1007/978-3-642-27320-9_2 [arXiv:cond-mat/0702365 [cond-mat.stat-mech]].

- [70] P. Beretta and A. Codello, Functional Dimensional Regularization, [In preparation]
- [71] K. G. Wilson and J. B. Kogut, *The Renormalization group and the epsilon expansion*, Phys. Rept. **12** (1974), 75-199 doi:10.1016/0370-1573(74)90023-4
- [72] S. B. Liao, On connection between momentum cutoff and the proper time regularizations, Phys. Rev. D **53** (1996), 2020-2036 doi:10.1103/PhysRevD.53.2020 [arXiv:hep-th/9501124 [hep-th]].
- [73] A. Bonanno and D. Zappala, *Towards an accurate determination of the critical exponents with the renormalization group flow equations*, Phys. Lett. B **504** (2001), 181-187 doi:10.1016/S0370-2693(01)00273-8 [arXiv:hep-th/0010095 [hep-th]].
- [74] D. Zappala, *Perturbative and nonperturbative aspects of the proper time renormalization group*, Phys. Rev. D **66** (2002), 105020 doi:10.1103/PhysRevD.66.105020 [arXiv:hep-th/0202167 [hep-th]].
- [75] D. F. Litim and J. M. Pawlowski, *Predictive power of renormalization group flows: A Comparison*, Phys. Lett. B **516** (2001), 197-207 doi:10.1016/S0370-2693(01)00922-4 [arXiv:hep-th/0107020 [hep-th]].
- [76] S. Abel and L. Heurtier, *Exact Schwinger Proper Time Renormalisation*, [arXiv:2311.12102 [hep-th]].
- [77] M. Mazza and D. Zappala, *Proper time regulator and renormalization group flow*, Phys. Rev. D **64** (2001), 105013 doi:10.1103/PhysRevD.64.105013 [arXiv:hep-th/0106230 [hep-th]].
- [78] D. F. Litim, *Critical exponents from optimized renormalization group flows*, Nucl. Phys. B **631** (2002), 128-158 doi:10.1016/S0550-3213(02)00186-4 [arXiv:hep-th/0203006 [hep-th]].
- [79] N. Tetradis and D. F. Litim, *Analytical solutions of exact renormalization group equations*, Nucl. Phys. B **464** (1996), 492-511 doi:10.1016/0550-3213(95)00642-7 [arXiv:hep-th/9512073 [hep-th]].

[80] D. F. Litim, *Optimized renormalization group flows*, Phys. Rev. D **64** (2001), 105007 doi:10.1103/PhysRevD.64.105007 [arXiv:hep-th/0103195 [hep-th]].

- [81] D. F. Litim, *Derivative expansion and renormalization group flows*, JHEP **11** (2001), 059 doi:10.1088/1126-6708/2001/11/059 [arXiv:hep-th/0111159 [hep-th]].
- [82] N. Tetradis and C. Wetterich, Critical exponents from effective average action, Nucl. Phys. B 422 (1994), 541-592 doi:10.1016/0550-3213(94)90446-4 [arXiv:hep-ph/9308214 [hep-ph]].
- [83] A. Codello and G. D'Odorico, *O*(*N*)-*Universality* Classes and the Mermin-Wagner Theorem, Phys. Rev. Lett. 110 (2013),141601 doi:10.1103/PhysRevLett.110.141601 [arXiv:1210.4037 [hep-th]].
- [84] L. Canet, B. Delamotte, D. Mouhanna and J. Vidal, *Optimization of the derivative expansion in the nonperturbative renormalization group*, Phys. Rev. D **67** (2003), 065004 doi:10.1103/PhysRevD.67.065004 [arXiv:hep-th/0211055 [hep-th]].
- [85] L. Canet, B. Delamotte, D. Mouhanna and J. Vidal, *Nonperturbative renormalization group approach to the Ising model: A Derivative expansion at order partial**4*, Phys. Rev. B **68** (2003), 064421 doi:10.1103/PhysRevB.68.064421 [arXiv:hep-th/0302227 [hep-th]].
- [86] T. R. Morris and M. D. Turner, *Derivative expansion of the renormalization group in O(N) scalar field theory*, Nucl. Phys. B **509** (1998), 637-661 doi:10.1016/S0550-3213(97)00640-8 [arXiv:hep-th/9704202 [hep-th]]
- [87] P. Beretta and A. Codello, Functional Dimensional Regularization for O(N) Models, [In preparation].

A Derivation of the Wetterich's equation

We want to derive an equation that describe the evolution of Γ_k , to do so it is standard to work with the variable $t \equiv log(k/\Lambda)$, thus $k\partial_k(\cdot) = \partial_t$. We need to use the following relation which is nothing but the chain rule

$$\left|\partial_t(\cdot)\right|_{\phi} = \left|\partial_t(\cdot)\right|_J - \int_x \partial_t(\phi)_J \left(rac{\delta(\cdot)}{\delta\phi(x)}
ight)_J$$

With this the evolution for Γ_k is

$$\left[\left(\partial_t \Gamma_k[\phi]\right)_{|\phi} = \left(\partial_t \Gamma_k[\phi]\right)_{|J} - \int_x \partial_t (\phi)_J \left(\frac{\delta \Gamma_k}{\delta \phi(x)}\right)_J \left(\frac{\delta \Gamma_k}{\delta \phi(x)}\right)_J$$

Applying the time derivative to the Legendre Transform (3.29) we see that

$$\begin{aligned} \partial_t \Gamma_k[\phi]_{|_J} &= & - & \partial_t W_k[J]_{|_J} + \int_x J(x) \partial_t \phi(x)_{|_J} \\ &- & \int_{x,y} \partial_t \phi(x)_{|_J} R_k(|x-y|) \phi(y) - \frac{1}{2} \int_{x,y} \phi(x) R_k(|x-y|) \phi(y) \end{aligned}$$

To solve we need $\partial_t W_k$.

$$\begin{split} e^{W_k[J]} \partial_t W_k[J]|_J &= \partial_t (e^{W_k[J]})_{|_J} \\ &= \int \mathcal{D} \varphi e^{S[\varphi] + \int_x J(x) \varphi(x) - \frac{1}{2} \int_{x,y} \varphi(x) R_k(|x-y|) \varphi(y)} \times \\ &\left[-\frac{1}{2} \int_{x,y} \varphi(x) \partial_t R_k(|x-y|) \varphi(y) \right] \end{split}$$

Recall that $Z_k[J] = e^{W_k[J]}$, and dividing the last expression by $Z_k[J]$

$$\begin{split} \partial_t W_k[J]_{|J} &= -\frac{1}{2} \int_{x,y} \partial_t R_k(|x-y|) \left\langle \varphi(x) \varphi(y) \right\rangle_{J,k} \\ &= -\frac{1}{2} \int_{x,y} \partial_t R_k(|x-y|) \left[\frac{\delta \left\langle \varphi(x) \right\rangle_{J,k}}{\delta J(y)} + \left\langle \varphi(x) \right\rangle_{J,k} \left\langle \varphi(y) \right\rangle_{J,k} \right] \\ &= -\frac{1}{2} \int_{x,y} \partial_t R_k(|x-y|) \left[\frac{\delta^2 W_k[J]}{\delta J(x) \delta J(y)} + \varphi(x) \varphi(y) \right] \end{split}$$

Putting all this together and using the equation of state $\frac{\delta \Gamma_k}{\delta \phi} = J - \int_{\mathcal{Y}} R_k(x-y) \phi_k(y)$ we arrive at

$$\partial_t \Gamma_k[\phi]_{|\phi} = \frac{1}{2} \int_{x,y} \partial_t R_k(|x-y|) \frac{\delta^2 W_k[J]}{\delta J(x) \delta J(y)}$$
(A.1)

We want to work only with Γ_k , can we express $\frac{\delta^2 W_k[J]}{\delta J(x)\delta J(y)}$ in terms of Γ_k ? Recall that $J(y) = \frac{\delta \Gamma_k}{\delta \phi(y)} + \int_v R_k(|y-v|\phi(v))$ and note that

$$\frac{\delta\phi(x)}{\delta\phi(z)} = \delta(x-z) = \frac{\delta^2 W_k[J]}{\delta\phi(z)\delta J(x)} = \int_y \frac{\delta^2 W_k[J]}{\delta J(x)\delta J(y)} \frac{\delta J(y)}{\delta\phi(z)}
= \int_y \frac{\delta^2 W_k[J]}{\delta J(x)\delta J(y)} \cdot \left(\frac{\delta^2 \Gamma_k}{\delta\phi(y)\delta\phi(z)} + R_k(|y-z|)\right)$$

Then the full propagator G(x, y) is

$$G(x,y) \equiv \frac{\delta^2 W_k[J]}{\delta J(x)\delta J(y)} = \left(\frac{\delta^2 \Gamma_k}{\delta \phi(y)\delta \phi(z)} + R_k(|y-z|)\right)^{-1}$$

Finally the evolution of Γ_k reads

$$\partial_t \Gamma_k[\phi]_{|\phi} = \frac{1}{2} \int_{x,y} \partial_t R_k(|x-y|) G(x,y) \tag{A.2}$$

B The Feynman rules for the derivative expansion at order two

In the subsection 4.2.3 we derived the Feynman Rules for the term involving the wave-function renormalization. Apart from the term involving $Z(\rho)$ there is another

one which has the form $\frac{1}{4}Y(\rho)\partial_{\mu}\rho\partial^{\mu}\rho$ which we named as S_4 .

$$S_4 = \int \frac{1}{4} Y(\rho) \partial_{\mu} \rho \partial^{\mu} \rho \tag{B.1}$$

Since the polarization and the tadpole diagrams are computed with the third and fourth variation respectively, we need to calculate $\delta^3 S_4$ and $\delta^4 S_4$. The first two variations are

$$\delta S_4 = \int \frac{1}{4} Y'(\rho) (\varphi \cdot \delta \varphi) (\partial \rho)^2 + \frac{1}{2} Y(\rho) \partial \delta \rho \cdot \partial \rho$$

$$\delta^2 S_4 = \int \frac{1}{4} Y''(\rho) (\delta \rho)^2 (\partial \rho)^2 + \frac{1}{4} Y'(\rho) (\delta \varphi)^2 (\partial \rho)^2$$

$$+ Y'(\rho) \delta \rho (\partial \rho \cdot \partial \delta \rho) + \frac{1}{2} Y(\rho) (\partial \delta \rho)^2 + \frac{1}{2} (\partial \rho \cdot \delta \delta^2 \rho)$$

We can easily change from variable ρ to φ by plugging

$$\delta\rho = \varphi \cdot \delta\varphi$$
$$\delta^2\rho = (\delta\varphi)^2$$
$$\delta^3\rho = 0$$

$$\begin{split} \frac{\delta^2 S_4}{\delta \varphi_{1a} \delta \varphi_{2b}} &= \frac{1}{2} Y \int_x \varphi_i (\partial_x \delta_{xx_1} \delta_{ia} \varphi_j ((\partial_x \delta_{xx_2} \delta_{jb})) \\ &\to \frac{1}{2} Y \varphi_a \varphi_b (ip_1) \cdot (ip_2) = -\frac{1}{2} Y \varphi_a \varphi_b (p_1 \cdot p_2) \end{split}$$

The third and fourth variation of this term has the following form

$$\delta^{3}S_{4} = \int \left\{ \frac{3}{2}Y''(\rho)(\delta\rho)^{2}(\partial \cdot \partial \delta\rho) + \frac{3}{2}Y'(\rho)(\delta^{2}\rho)(\partial \cdot \partial \delta\rho) \right\}$$

$$\frac{3}{2}Y'(\rho)\delta\rho(\partial \delta\rho)^{2} + \frac{3}{2}Y'(\rho)(\partial \delta\rho \cdot \partial \delta^{2}\rho) + \frac{3}{2}Y'(\rho)\delta\rho(\partial \rho \cdot \partial \delta^{2}\rho) \right\}$$
(B.2)
$$(B.3)$$

Which at constant field is

$$\delta^{3}S_{4} = \int \left\{ \frac{3}{2} Y'(\rho) \delta \rho (\partial \delta \rho)^{2} + \frac{3}{2} Y'(\rho) (\partial \delta \rho \cdot \partial \delta^{2} \rho) \right\}$$
 (B.4)

$$\begin{split} \frac{\delta^3 S_4}{\delta \varphi_{1a} \delta \varphi_{2b} \delta \varphi_{3c}} &= \int \left\{ \frac{3}{2} Y' \varphi_a \delta_{xx_1} \varphi_b \partial_x \delta_{xx_2} \varphi_c \partial_x \delta_{xx_3} + \frac{1}{2} Y \varphi_a \partial_x \delta_{xx_1} \delta_{jb} \delta_{xx_2} \delta_{jc} \partial_x \delta_{xx_3} \right. \\ &\quad + \text{combinations} \right\} \\ &\quad \to -\frac{1}{2} Y' \varphi_a \varphi_b \varphi_c (p_2 \cdot p_3 + p_1 \cdot p_2 + p_3 \cdot p_1) \\ &\quad -\frac{Y}{2} [\varphi_a \delta_{bc} (p_1 \cdot p_2 + p_1 \cdot p_3) + \varphi_b \delta_{ca} (p_2 \cdot p_3 + p_2 \cdot p_1) \\ &\quad + \varphi_c \delta_{ab} (p_3 \cdot p_1 + p_3 \cdot p_2)] \end{split}$$

$$\delta^4 S_4 = \int 3Y''(\rho)(\delta\rho)^2(\partial\delta\rho)^2 + 3Y'(\rho)(\delta^2\rho)(\partial\delta\rho)^2 + 6Y'(\rho)\delta\rho(\partial\delta\rho \cdot \partial\delta^2\rho) + \frac{3}{2}Y(\rho)(\partial\delta^2\rho)^2$$

This last equation is at constant field.

Let's split this last equation and see individually term by term. Starting with the term $3Y''(\delta\rho)^2(\partial\delta\rho)^2$.

$$3Y''(\delta\rho)^2(\partial\delta\rho)^2 = 3Y''(\varphi \cdot \delta\varphi)^2(\partial(\varphi \cdot \delta\varphi))^2 = 3Y''(\varphi \cdot \delta\varphi)^2(\varphi \cdot \partial\delta\varphi)^2$$
$$= 3Y''(\varphi_i \cdot \delta\varphi_i)^2(\varphi_j \cdot \partial\delta\varphi_j)^2 = (\varphi_i \cdot \delta\varphi_i)(\varphi_j \cdot \delta\varphi_j)(\varphi_k \cdot \partial\delta\varphi_k)(\varphi_l \cdot \partial\delta\varphi_l)$$

$$\frac{\delta^4 S_4}{\delta \varphi_{1a} \delta \varphi_{2b} \delta \varphi_{3c} \delta \varphi_{4d}} = Y'' \int \varphi_a \delta_{xx_1} \varphi_b \delta_{xx_2} \varphi_c \partial_x \varphi_d \partial_x \delta_{xx_1} + \cdots
= -Y'' \varphi_a \varphi_b \varphi_c \varphi_d (p_3 \cdot p_4 + p_1 \cdot p_2 + p_1 \cdot p_3 + p_1 \cdot p_4 + p_2 \cdot p_3 + p_2 \cdot p_4)$$

The next term is

$$\int \frac{6}{2} Y'(\delta^{2} \rho) (\partial \delta \rho)^{2} = \int \frac{6}{2} Y'(\delta \varphi \cdot \delta \varphi) (\varphi \cdot \partial \delta \varphi)^{2} = \int \frac{6}{2} Y'(\delta \varphi_{i} \cdot \delta \varphi_{i}) (\varphi_{j} \cdot \partial \delta \varphi_{j}) (\varphi_{k} \cdot \partial \delta \varphi_{k})
\rightarrow \frac{Y'}{2} (\delta_{xx_{1}} \delta_{xx_{2}} \delta_{ab}) (\varphi_{c} \partial_{x} \delta_{xx_{3}} \varphi_{d} \partial_{x} \delta_{xx_{4}}) + \cdots
= -\frac{Y'}{2} (\delta_{ab} \varphi_{c} \varphi_{d} (p_{3} \cdot p_{4}) + \delta_{ac} \varphi_{b} \varphi_{d} (p_{2} \cdot p_{4}) + \delta_{ad} \varphi_{c} \varphi_{b} (p_{3} \cdot p_{2}) +
\delta_{cb} \varphi_{a} \varphi_{d} (p_{1} \cdot p_{4}) + \delta_{bd} \varphi_{a} \varphi_{c} (p_{1} \cdot p_{3}) + \delta_{cd} \varphi_{a} \varphi_{b} (p_{1} \cdot p_{2}))$$

The next term is

$$\int 6Y' \delta \rho (\partial \delta \rho \cdot \partial \delta^{2} \rho) = \int 6Y' (\varphi \cdot \delta \varphi) (\varphi \partial \delta \varphi 2\delta \varphi \partial \delta \varphi) = \int 12Y' (\varphi_{i} \cdot \delta \varphi_{i}) (\varphi_{j} \cdot \partial \delta \varphi_{j}) (\delta \varphi_{k} \cdot \partial \delta \varphi_{k})
\quad \rightarrow \frac{Y'}{2} \varphi_{a} \delta_{xx_{1}} \varphi_{b} \partial_{x} \delta_{xx_{2}} \delta_{xx_{3}} \partial_{x} \delta_{xx_{4}} \delta_{cd} + \cdots
= -\frac{Y'}{2} (\varphi_{a} \varphi_{b} \delta_{cd} p_{2} \cdot p_{4} + \varphi_{a} \varphi_{c} \delta_{bd} p_{3} \cdot p_{4} + \varphi_{a} \varphi_{c} \delta_{bd} p_{2} \cdot p_{3}
+ \varphi_{a} \varphi_{b} \delta_{dc} p_{2} \cdot p_{3} + \varphi_{a} \varphi_{d} \delta_{bc} p_{3} \cdot p_{4} + \varphi_{a} \varphi_{d} \delta_{cb} p_{2} \cdot p_{4}
+ \varphi_{b} \varphi_{a} \delta_{cd} p_{1} \cdot p_{4} + \varphi_{b} \varphi_{a} \delta_{dc} p_{1} \cdot p_{3} + \varphi_{b} \varphi_{c} \delta_{ad} p_{3} \cdot p_{4}
+ \varphi_{b} \varphi_{c} \delta_{da} p_{1} \cdot p_{3} + \varphi_{b} \varphi_{d} \delta_{ac} p_{3} \cdot p_{4} + \varphi_{b} \varphi_{d} \delta_{ca} p_{1} \cdot p_{4}
+ \varphi_{c} \varphi_{a} \delta_{bd} p_{1} \cdot p_{4} + \varphi_{c} \varphi_{a} \delta_{db} p_{1} \cdot p_{2} + \varphi_{c} \varphi_{b} \delta_{ad} p_{2} \cdot p_{4}
+ \varphi_{c} \varphi_{b} \delta_{da} p_{1} \cdot p_{2} + \varphi_{c} \varphi_{d} \delta_{ab} p_{2} \cdot p_{4} + \varphi_{c} \varphi_{d} \delta_{ba} p_{1} \cdot p_{4}
+ \varphi_{d} \varphi_{a} \delta_{bc} p_{1} \cdot p_{3} + \varphi_{d} \varphi_{a} \delta_{cb} p_{1} \cdot p_{2} + \varphi_{d} \varphi_{b} \delta_{ac} p_{2} \cdot p_{3}
+ \varphi_{d} \varphi_{b} \delta_{ca} p_{1} \cdot p_{2} + \varphi_{d} \varphi_{c} \delta_{ab} p_{2} \cdot p_{3} + \varphi_{d} \varphi_{c} \delta_{ba} p_{1} \cdot p_{3}$$

Next is

$$\int \frac{3}{2} Y(\partial \delta^{2} \rho)^{2} = \int \frac{12}{2} Y(\delta \varphi \cdot \partial \delta \varphi)^{2} = \int \frac{12}{2} Y(\delta \varphi_{i} \cdot \partial \delta \varphi_{i}) (\delta \varphi_{j} \cdot \partial \delta \varphi_{j})
\rightarrow \frac{12}{2} Y(\delta_{xx_{1}} \partial_{x} \delta_{xx_{2}} \delta_{ab}) (\delta_{xx_{3}} \partial_{x} \delta_{xx_{4}} \delta_{c} d)
\rightarrow -\frac{Y}{2} (\delta_{ab} \delta_{cd} (p_{2} \cdot p_{4} + p_{1} \cdot p_{3} + p_{1} \cdot p_{4} + p_{2} \cdot p_{3})
+ \delta_{ac} \delta_{bd} (p_{1} \cdot p_{2} + p_{1} \cdot p_{4} + p_{3} \cdot p_{2} + p_{3} \cdot p_{4})
+ \delta_{ad} \delta_{bc} (p_{1} \cdot p_{2} + p_{1} \cdot p_{3} + p_{4} \cdot p_{2} + p_{4} \cdot p_{3}))$$

We now summarize the contribution coming from S_4 by collecting all terms computed individually

$$S_{3,abc}^{(3)}(p_{1},p_{2},p_{3}) = -\frac{1}{2}Y[(\varphi_{a}\delta_{bc} + \varphi_{b}\delta_{ac})(p_{1} \cdot p_{2}) + (\varphi_{a}\delta_{cb} + \varphi_{c}\delta_{ab})(p_{1} \cdot p_{3}) + (\varphi_{b}\delta_{ca} + \varphi_{c}\delta_{ba})(p_{2} \cdot p_{3})]$$

$$- \frac{1}{2}Y^{(1)}[(p_{1} \cdot p_{2}) + (p_{1} \cdot p_{3}) + (p_{2} \cdot p_{3})]\varphi_{a}\varphi_{b}\varphi_{c}$$
(B.5)
(B.6)

$$S_{4,abcd}^{(4)}(p_{1},p_{2},p_{3},p_{4}) = -\frac{1}{2}Y[(p_{1} \cdot p_{2})\delta_{ad}\delta_{bc} + (p_{1} \cdot p_{2})\delta_{ac}\delta_{bd} + (p_{1} \cdot p_{3})\delta_{ad}\delta_{bc} + (p_{1} \cdot p_{3})\delta_{ab}\delta_{cd} + (p_{1} \cdot p_{3})\delta_{ad}\delta_{bc} + (p_{1} \cdot p_{3})\delta_{ab}\delta_{cd} + (p_{1} \cdot p_{3})\delta_{ad}\delta_{bc} + (p_{2} \cdot p_{3})\delta_{ac}\delta_{bd} + (p_{2} \cdot p_{3})\delta_{ab}\delta_{cd} + (p_{2} \cdot p_{3})\delta_{ac}\delta_{bd} + (p_{2} \cdot p_{3})\delta_{ac}\delta_{bd} + (p_{2} \cdot p_{3})\delta_{ac}\delta_{bd} + (p_{2} \cdot p_{3})\delta_{ac}\delta_{bd} + (p_{3} \cdot p_{4})\delta_{ad}\delta_{bc} + (p_{3} \cdot p_{4})\delta_{ac}\delta_{bd}]$$

$$- \frac{1}{2}Y^{(1)}[(p_{1} \cdot p_{2})\varphi_{a}\varphi_{b}\delta_{cd} + (p_{1} \cdot p_{2})\varphi_{b}\varphi_{c}\delta_{ad} + (p_{1} \cdot p_{2})\varphi_{b}\varphi_{d}\delta_{ac} + (p_{1} \cdot p_{2})\varphi_{a}\varphi_{d}\delta_{bc} + (p_{1} \cdot p_{3})\varphi_{a}\varphi_{b}\delta_{cd} + (p_{2} \cdot p_{3})\varphi_{b}\varphi_{c}\delta_{ad} + (p_{2} \cdot p_{3})\varphi_{a}\varphi_{b}\delta_{cd} + (p_{2} \cdot p_{3})\varphi_{a}\varphi_{b}\delta_{cd} + (p_{2} \cdot p_{3})\varphi_{a}\varphi_{b}\delta_{cd} + (p_{2} \cdot p_{3})\varphi_{a}\varphi_{b}\delta_{cd} + (p_{2} \cdot p_{3})\varphi_{a}\varphi_{b}\varphi_{c}\varphi_{d} + (p_{2} \cdot p_{3})\varphi_{a}\varphi_{b}\varphi_{c}\varphi_{d} + (p_{1} \cdot p_{3})\varphi$$

C Strict, Light and Strict-light beta functions

In this appendix we show the explicit form of the beta functions in each case, strict, light and strict-light as explained on 4.2.5

$$\begin{split} \beta_U &= \mu^d (N-1) e^{-\frac{U'}{4\pi\mu^2(Z_T+1)}} + \mu^d e^{-\frac{2\rho U''+U'}{4\pi\mu^2(Z_L+1)}} \\ \beta_{Z_T}^{strict} &= \frac{\mu^{d-2}}{16\pi\rho^4(U'')^3} \bigg\{ e^{-\frac{U'}{4\pi\mu^2}} \bigg[4\pi\mu^2 \Big(U'(Z_L-Z_T) - 2\rho U''(-Z_L+\rho Z_T'+Z_T+1) \Big)^2 \\ &- \rho U'' \Big(4\rho^2 (U'')^2 \Big\{ \rho Z_T'(N-1) + (Z_T-Z_L) + 1 \Big\} + (U')^2 (Z_L-Z_T)^2 \\ &+ 4\rho U'U''((Z_L-Z_T)^2 - (Z_L-Z_T)) \Big) \bigg] \\ &- e^{-\frac{2\rho U''+U'}{4\pi\mu^2}} \bigg[4\pi\mu^2 (U'(Z_L-Z_T) - 2\rho U''(-Z_L+\rho Z_T'+Z_T+1))^2 \\ &+ \rho U'' \Big\{ (U')^2 (Z_L-Z_T)^2 + 4\rho U' U''(Z_L-Z_T) (Z_L-2\rho Z_T'-Z_T-1) \\ &+ 4\rho^2 (U'')^2 (-2Z_L(2\rho Z_T'+Z_T+1) + Z_L^2 + 2\rho^2 Z_T'' + 5\rho Z_T' + Z_T(4\rho Z_T'+2) + Z_T^2 + 1) \Big\} \bigg] \bigg\} \\ \beta_{Z_L}^{strict} &= -\frac{\mu^{d-6}}{192\pi^3\rho} \bigg\{ (N-1) e^{-\frac{U'}{4\pi\mu^2}} \bigg[24\pi\mu^2 (Z_T-Z_L) (2\pi\mu^2 + \rho Z_T'(4\pi\mu^2 - U') + \rho U'') \\ &+ \rho \Big\{ 48\pi^2 \mu^4 Z_L' + \rho ((Z_T')^2 (48\pi^2 \mu^4 - 24\pi\mu^2 U' + (U')^2) + 2U'' Z_T' (12\pi\mu^2 - U') + (U'')^2) \Big\} \bigg] \\ &+ \rho e^{-\frac{2\rho U''+U'}{4\pi\mu^2}} \bigg[-48\pi^2 \mu^4 (3\rho (Z_L')^2 - 2\rho Z_L'' - Z_L') + 24\pi\mu^2 \rho Z_L' \Big\{ U'' (2\rho Z_L' - 3) \\ &+ U' Z_L' - 2\rho u^{(3)} \Big\} + \rho (U''(2\rho Z_L' - 3) + U' Z_L' - 2\rho U^{(3)})^2 \bigg] \bigg\} \end{split}$$

$$\begin{split} \beta_{U} &= \mu^{d} \Bigg\{ (N-1)e^{-\frac{iJ'}{4\pi \mu^{2}}} + e^{-\frac{2\rho U''+U'}{4\pi \mu^{2}}} \Bigg\} \\ \beta_{Z_{T}}^{light} &= \frac{\mu^{d-2}}{4\pi \rho (U'(Z_{L}-Z_{T})-2\rho(Z_{T}+1)U'')^{3}} \Bigg\{ -\frac{e^{-\frac{iJ'}{4\pi \mu^{2}}}}{Z_{T}+1} \Bigg[(U')^{3}(Z_{L}-Z_{T})^{3} \times \\ &\times (Z_{L}-Z_{T}+(N-1)\rho Z_{T}') - 2\rho(Z_{L}-Z_{T})^{2}(Z_{T}+1)(U')^{2} \Big\{ U''(3Z_{L}+3\rho Z_{T}'(N-1)-Z_{T}+2) \Big\} + 8\rho^{2}(Z_{T}+1)^{3}(U'')^{2} \Big\{ -4\pi \mu^{2}(Z_{L}+1) \times \\ &(Z_{L}-2\rho Z_{T}'-2Z_{T}-1) - \rho U''((N-1)\rho Z_{T}'+Z_{T}+1) \Big\} - 4\rho(Z_{L}-Z_{T}) \times \\ &(Z_{T}+1)^{2} U'U'' \Big\{ 8\pi \mu^{2}(Z_{L}+1)(\rho Z_{T}'+Z_{T}+1) - \rho U''(2Z_{L}+3\rho Z_{T}'(N-1)+Z_{T}+3) \Big\} \Bigg] \\ &+ \frac{\rho e^{-\frac{2\rho U''+U''}{4\pi \mu^{2}}}}{1+Z_{L}} \Bigg[-(Z_{L}-Z_{T})^{3}(U')^{3}(2\rho Z_{T}''+Z_{T}') \\ &+ 2(U')^{2} U''(Z_{L}-Z_{T})^{2} \Big\{ \rho(4Z_{L}+3Z_{T}+7)Z_{T}'+2(Z_{L}+1)(Z_{T}+1)+6\rho^{2}(Z_{T}+1)Z_{T}'' \Big\} \\ &+ 8\rho(Z_{T}+1)^{2}(U'')^{2} \Big\{ -4\pi \mu^{2}(Z_{L}+1)^{2}(Z_{L}-2\rho Z_{T}'-2Z_{T}-1) \\ &+ \rho U''(-((1+Z_{L})(Z_{L}-2Z_{T}-1))+\rho(5+4Z_{L}+Z_{T})Z_{T}'+2\rho^{2}(1+Z_{T})Z_{T}'') \Big\} \\ &+ 4(Z_{T}+1)U'U''(Z_{L}-Z_{T}) \Big(-8\pi \mu^{2}(Z_{L}+1)^{2}(\rho Z_{T}'+Z_{T}+1) \\ &+ \rho U'' \Big\{ (1+Z_{L})(Z_{L}-4Z_{T}-3)-\rho(3Z_{T}+8Z_{L}+11)Z_{T}'-6\rho^{2}(1+Z_{T})Z_{T}'' \Big\} \Big) \Big] \Big\} \\ \beta_{Z_{L}}^{light} &= -\frac{\mu^{d-6}}{192\pi^{3}\rho} \Big\{ -\frac{(N-1)e^{-\frac{U''}{4\pi \mu^{2}}}}{(1+Z_{T})^{3}} \Big[-48\pi^{2}\mu^{4}(Z_{T}+1)^{2}(\rho Z_{L}'-Z_{L}+Z_{T}) \\ &-24\pi \mu^{2}\rho(Z_{T}+1)U''(-Z_{L}+\rho Z_{T}'+Z_{T}) - \rho^{2}U''((Z_{T}+1)U''-2U'Z_{T}') \Big] \\ &+ \rho \frac{e^{-\frac{2\rho U''+U'}{4\pi \mu^{2}}}}{(1+Z_{L})^{3}} \Big[48\pi^{2}\mu^{4}(Z_{L}+1)^{2}(2\rho Z_{L}''+Z_{L}') - 24\pi \mu^{2}\rho(Z_{L}+1)Z_{L}'(2\rho U^{(3)}+3U'') \\ &+ \rho(2\rho U^{(3)}+3U'')(2\rho U^{(3)}(Z_{L}+1)+U''(-4\rho Z_{L}'+3Z_{L}+3) - 2U'Z_{L}') \Big] \Big\} \end{aligned}$$

$$\begin{split} \beta_{U} &= \mu^{d} \Bigg\{ (N-1)e^{-\frac{U'}{4\pi\mu^{2}}} + e^{-\frac{2\rho U'' + U'}{4\pi\mu^{2}}} \Bigg\} \\ \beta_{Z_{T}}^{Strict-light} &= -\frac{\mu^{d-2}}{4\pi\rho^{3}(U'')^{2}} \Bigg\{ e^{-\frac{U'}{4\pi\mu^{2}}} \Bigg[(Z_{L} - Z_{T})(\rho U''(8\pi\mu^{2} - \rho U'') + U'(4\pi\mu^{2} - \rho U'')) \\ &+ \rho U''(-4\pi\mu^{2} + \rho Z_{T}'((N-1)\rho U'' - 8\pi\mu^{2}) + \rho U'') \Bigg] \\ &+ e^{-\frac{2\rho U'' + U'}{4\pi\mu^{2}}} \Bigg[(Z_{T} - Z_{L})(4\pi\mu^{2} + \rho U'')(2\rho U'' + U') \\ &+ \rho U''(4\pi\mu^{2} + \rho Z_{T}'(8\pi\mu^{2} + 5\rho U'') + U''(\rho + 2\rho^{3}Z_{T}'')) \Bigg] \Bigg\} \\ \beta_{Z_{L}}^{Strict-light} &= -\frac{\mu^{d-6}}{192\pi^{3}\rho} \Bigg\{ (N-1)e^{-\frac{U'}{4\pi\mu^{2}}} \Bigg[24\pi\mu^{2}(2\pi\mu^{2} + \rho U'')(Z_{T} - Z_{L}) \\ &+ \rho (48\pi^{2}\mu^{4}Z_{L}' + \rho U''(Z_{T}'(24\pi\mu^{2} - 2U') + U'')) \Bigg] \\ &- \rho e^{-\frac{2\rho U'' + U'}{4\pi\mu^{2}}} \Bigg[-\rho \Big\{ 96\pi^{2}\mu^{4}Z_{L}'' + 9(U'')^{2} + 4\rho^{2}(u^{(3)})^{2} + 12\rho U^{(3)}U'' \Big\} \\ &+ Z_{L}' \Big\{ 12\rho^{2}(U'')^{2} - 48\pi^{2}\mu^{4} + 4\rho^{2}u^{(3)}(12\pi\mu^{2} + U') \\ &+ U''(72\pi\mu^{2}\rho + 8\rho^{3}U^{(3)} + 6\rho U') \Big\} \Bigg] \Bigg\} \end{split}$$